ADDIS ABABA UNIVERSITY

ADDIS ABABA INSTITUTE OF TECHNOLOGY

SCHOOL OF GRADUATE STUDIES

Impact Analysis of Sisal Fiber Reinforced Epoxy Resin Composite Material for Automotive Applications

A Thesis Submitted to the Graduate School of Addis Ababa University in Partial Fulfillment of the Requirements for the Degree of Masters of Science

In

Mechanical Engineering (Mechanical Design)

By: Habtamu Dagne

Advisor: Dr. Daniel Tilahun

Co-Advisor: Mulugeta H/Mariam

March, 2017

Addis Ababa University

Addis Ababa Institute of Technology

School of Mechanical and Industrial Engineering

Impact Analysis of Sisal Fiber Reinforced Epoxy Resin Composite Material for Automotive Applications

By

Habtamu Dagne

Submitted in accordance with the requirements for the degree

MASTER OF SCIENCE(M.Sc.)

Approved By Board of Directors

Daniel Tilahun (Dr.)	_____	_____
Advisor	Signature	Date
Mulugeta H/Mariam	_____	_____
Co Advisor	Signature	Date
_____	_____	_____
Internal Examiner	Signature	Date
_____	_____	_____
External Examiner	Signature	Date
_____	_____	_____
Chairman of the School	Signature	Date

Addis Ababa University

School of Graduates

This is to certify that the thesis prepared by **Habtamu Dagne**, entitled: "**Impact analysis of sisal fiber reinforced epoxy resin composite material for Automotive applications**", do here by declare this thesis is my original work and that it has not been submitted partially, or in full for a degree in any university/institution, which compiles with the regulations of the university and meets the accepted standards with respect to originality and quality.

Signature: _____

*Date:*_____

Advisor: Daniel Tilahun (Dr.) Signature:_____ Date:_____

Co Advisor: Mulugeta H/Mariam Signature: _____ Date: _____

Head of School: _____ Signature: _____Date:_____

ABSTRACT

Impact analysis of sisal fiber reinforced Epoxy resin composite material for Automotive Applications

Habtamu Dagne

Addis Ababa University, 2017

The main goal of this study is to investigate the impact analysis of sisal fiber reinforced epoxy resin composite material for automotive applications using Abaqus/CEA 6.13 software based on ASTM D-7136 standard. For this simulation a $[0]_4$ unidirectional sisal/epoxy composite laminate with overall thickness of 2.16 mm was used, and 0.5kg, 1kg, 2kg and 3kg of impactor mass with 1 m/s, 2 m/s and 3 m/s of velocities were used in order to deal their effects on the composite laminate. Generally, in order to get the Abaqus/Explicit software in put data's, first the sisal fiber was extracted manually from the sisal plants and treated with 8% of NaOH. Then the testing specimens was manufactured using volume fraction of 60% matrix and 40% of sisal fibers using vacuum bagging assisted hand lay-up technique (VBAHT) , and finally the tensile, compression and in-plane shear test was conducted based on their ASTM standards. The impact simulation results showed that when the impactor mass and velocity increases, the contact forces of the composite plate was increase up to 1kg of the impactor with 3m/s. Apart from that, the reaction forces of the composite plate was decreased and perforation of the plate was takes place for 2kg and 3kg of impactor mass. From all force-time history graph, the highest reaction force of 656.69 N occurred at 1kg of impactor for 3m/s. Furthermore it is found that the sisal fiber reinforced epoxy resin composite material has a good energy absorption capacity (up to 4.5 J) in the transverse direction and can have a potential to be used for different automotive application.

***Keywords**: composites, sisal, epoxy, impactor, VBAHT, ASTM, Abaqus/CEA 6.13*

ACKNOWLEDGEMENT

First I would like to thanks my Advisor Dr. Daniel Tilahun and Co. Advisor Mr.Muluguta H/Mariam (PhD candidate) for their great effort in terms of supervision, support, dedication and patience from the every start and every detailed process until accomplishment of my research.

Also special thanks to Mr. Birhanu and Mr. Serkalem (Dejen Aviation Industry, unmanned air vehicle department) and all Dejen Aviation Industry, Unmanned air vehicle department Staff for guiding, and providing all the necessary materials & equipment for manufacturing of the sisal fibre reinforced epoxy resin composite materials.

Many thanks are also extend to all AAiT Mechanical Engineering workshop staffs, especially for Mr.Tollosa and Mr. Yohannes for facilitating the material testing equipment's and their valuable guidance during the material properties test.

Finally, I would like to thanks and give my appreciation to all of my family members and my friends those who were supporting and motivating me for the achievement of this study.

TABLE OF CONTENTS

CHAPTER SIX: CONCLUSION AND RECOMMENDATION

LIST OF TABLE

LIST OF FIGURES

NOMENCLATURE

E_1	Longitudinal young's modulus
E_2	Transverse young's modulus
X_t	Longitudinal ultimate tensile strength
Y_t	Transverse ultimate tensile strength
L_0	Original gage length of the specimen
ΔL	Change in gage length (L-L_0)
P^{1max}	Maximum load before failure for longitudinal tensile testing specimen
P^{2max}	Maximum load before failure for transverse tensile testing specimen
σ_i	Tensile stress at i^{th} data point,
ε_i	Tensile strain at i^{th} data point.
$[C]$	Stiffness matrix
[S]	Compliance matrix
$[Q]$	Reduced stiffness matrix
$[T]$	Transformation matrix
$[A]$	Extensional stiffness matrix for the laminate (N/m)
$[B]$	Coupling stiffness matrix for the laminate (N)
$[D]$	Bending stiffness matrix for the laminate (Nm)
N_x	Normal force resultant in the x direction (per unit width)
N_y	Normal shear resultant in the y direction (per unit width)
N_{xy}	Shear force resultant (per unit width)
M_x	Bending moment resultant in the yz plane (per unit width)
M_y	Bending moment resultant in the xz plane (per unit width)

M_{xy}	Twisting moment (torsion) resultant (per unit width)
h	Lamina(ply) thickness (mm)
V_m	Volume of matrix (cm^3)
ρ_f	Density of fiber (gm/cm^3)
M_M	Matrix mass fraction
ρ_m	Density of matrix (gm/cm^3)
M_F	Fiber mass fraction
V_F	Fiber volume fraction
M_f	Mass of fiber(gm)
E_i	Impact energy (J)
V_i	Velocity of the impactor (m/s^2)

LIST OF ABBREVIATIONS AND ACRONYMS

ASTM	American society of testing materials
BVID	Barely visible impact damage
CAD	Computer aided Design
CFM	Displacement in cubic feet per minute
CLT	Classical Laminate Theory
DAVI	Dejen Aviation
FEA	Finite element analysis
FEM	Finite element method
HSNMTCRT	Hashin matrix tension criteria
HSNMCCRT	Hashin matrix compression criteria
HSNFTCRT	Hashin fibre tension criteria
HSNTCCRT	Hashin fibre compression criteria
ms	Millisecond
S.D	Standard deviation
SEM	Scanning electron microscopy
SEA	Specific energy absorption
SNNPRS	Southern Nations, Nationalities and Peoples region
Sisal/epoxy	Sisal fibre reinforced epoxy resin
VBAHT	Vacuum bagging Assisted Hand Lay-up technique
UTM	Universal testing machine
VUMAT	User subroutine to define material behavior
UMAT	User subroutine to define a material's mechanical behavior

CHAPTER ONE

INTRODUCTION

1.1. Background of the study

In recent decades the use of composite materials has become increasingly common in different automotive industries because of their superior specific properties; such as high strength and stiffness to weight ratio, design flexibility, improves corrosion and environmental resistance, improved fatigue life, potential reduction of fabrication process and life time costs, and etc. Such Composite materials are being considered to make lighter, strengthen, safe and more fuel-efficient vehicles. For example a Carbon –fiber composites has a weight about one fifth as much as steel, but are as good or better in terms of stiffness and strength. They also do not rust or corrode like conventional materials, and they could significantly improve vehicle fuel economy by reducing vehicle weight by as much as 60% [4].

However most of the composite material types that used in these automotive industries are the synthetic composite material types and it has some drawbacks including high production cost and green house emission during production period. Due to this, various academic and industrial researchers are conducting researches on environmentally friendly, sustainable materials to replace this conventional materials [23, 32].

Based on different literatures, natural fibers are received more attention to be used in automotive structural application in recent years both for external and internal components such as seat backs, underbodies, door trim panels, interior parts and etc [3, 31,48]. Comparing to synthetic fibers, natural fibers have more advantages such as low cost, low weight, renewable resources, low energy production and etc. For example the natural fiber such as sisal fibers have density about 1.33 g/cm^3 and cost between \$0.27~\$1.12/kg. In comparison, synthetic fiber such glass fiber's density is about 2.6 g/cm^3 and the cost is around between \$1.30~\$2.00/kg [18]. Also the uses of this natural fiber reduces weight by 10% and lowers the energy needed for production by 80% when compared to glass-reinforced components. So it is very attractive for different automotive industry to use the natural fibres to replace synthetic fibres. According to literatures, Mercedes-Benz used epoxy/jute fibre composite to manufacture door panels in its E-class vehicles and also

Toyota automotive company used kenaf fibres to reinforce PLA matrix, making parts for its vehicles. Also many researchers have done their work on natural fibres composites (jute fibres, hemp fibres, bamboo fibres, sisal fibres and etc.) and their applications in automotive industry [12, 18, 40, 48].

However, such both types of composite materials have common serious limitations. One of the most significant amongst these is their response to impact loading from the foreign objects during life time application. Such Composites structure can be susceptible to damage under this transverse impacts. Due to this, impact damage is a major issue in the design of a composite structures, as it may reduce strength and stiffness significantly with and without any visible damage at the surface and leads to the catastrophic damage depending on the types of impact [1, 2, 9, 18].

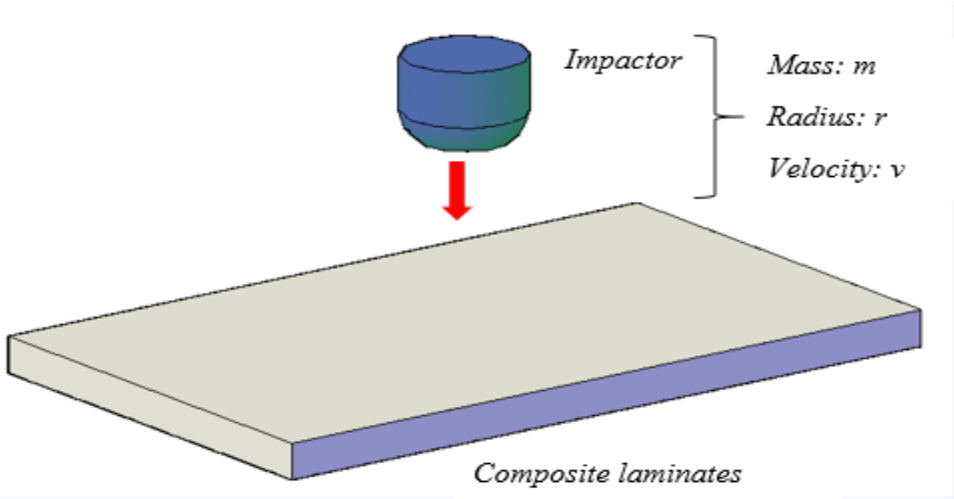

Figure 1.1. A basic model of composite transverse impact problem [7].

The impact response of the composite structures are depends on various factor including the impactor mass and stiffness, impactor geometry, impactor velocity, composite layup, composite thickness, composite mechanical property and etc. [14]. From this different factor, the impact velocity is one of the fundamental quantities in impact dynamics because collisions at different velocities can lead to different dynamic responses and damage in the target. Generally the researchers [33] are classified the impact analysis into two main categories based on the impactor velocity, such as low and high impact velocity analysis.

Low velocity impact can be defined as events which can be treated as quasi-static, the upper limit of which can vary from 1-20 m/s depending on different factors including the composites stiffness, composite material properties and the impactor's mass and stiffness [38]. The impact damage in composite material is generally different from metallic structure. In metallic structure due to the ductile nature of the material, large amounts of the energy may be absorbed and the most dominant failure mode is excessive plastic deformations. At yield stress the material may flow for every large strain (up to 20 percent) at constant yield before work hardening. In contrast, composites can fail in a wide variety of modes and contain barely visible impact damage (BVID) which nevertheless severely reduces the structural integrity of the component. Most composites are brittle and so can only absorb energy in elastic deformation and through damage mechanisms, and not via plastic deformation. In composite materials, a fiber usually fails at a small value of the axial strain but can support large axial loads because of the high value of Young's modulus. The matrix can undergo large deformations before failure but cannot support significant normal and shear stresses. Low velocity impact events represent a serious design concern for use of laminated composites for in-service applications as for example, dropping of tools during maintenance, bird strike, contact of a composite leaf spring in a car to runaway stones on a gravel road, and etc. [38, 39].

During this impact events, as shown in figure 1.2 the various damage such as matrix cracks, delamination's, fiber fractures, fiber-matrix debonding, fiber pull out and penetration can occurs. These damages causes considerable reduction in structural stiffness, leading to growth of the damage and final fracture. Therefore, the impact response of the composite materials has been an important area of research for a long period of time.

Generally the impact design problem is approached in two ways; experimental approach and simulation approach. The experimental approach is generally requires the manufactured composite material and impactor specimens. Also it requires several measurements of the impact behavior of the studied materials under different sample geometry and loading conditions. However such approach was time consuming and costly. On the other hands, the simulation approach is mainly related to the simulation of these impact phenomena by using finite element methods and it requires powerful hardware and software computers [19]. These simulation approach are commonly used by many industries and research centers due to cost and time reduction capability

when compared to experimental approach. In a modern design for impact analysis of structures a wide range of software packages are used. Among them ABAQUS, LS-DYNA, ANSYS, and PRO/ENGINEER are most commonly used [11].

In experimental testing approach different impact testing techniques was used by different researchers for composite materials. For example for low velocity impact; drop weight, izod and charpy impact test is commonly used. Actually, the impact test fixture should be designed to simulate the loading conditions to which a composite components is subjected in an operational service and then reproduce the failure modes and mechanisms, which are likely to occur. However, due to a lack of experimental standards, a wide variety of different testing techniques is presently being employed in order to assess the dynamic response of the composite materials making direct comparison difficult [19].

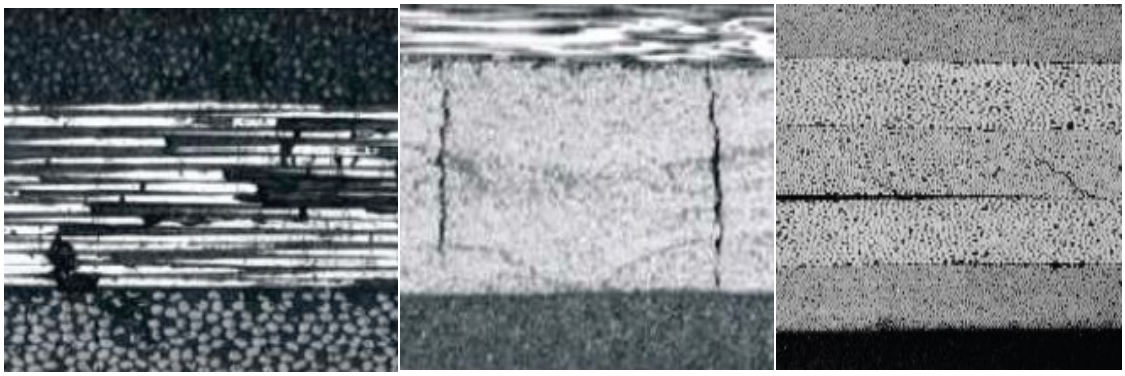

A. Fiber fracture *B. Transverse matrix crack* *C. Delamination*

Figure 1.2. Damage mechanisms in laminated composites [11].

In numerical simulation approach, the ability to accurately predict the behavior of composite materials during impact event requires the use of material models that represent multiple physical mechanisms. There are many failure modes in composite materials, including fiber compressive and tensile failure, matrix compressive and tensile failure, delamination and others. Several researchers have proposed models which attempt to capture varying degrees of these mechanisms, such as the Tsai-Wu, Tsai-Hill, Yamada-Sun, Hart-Smith, Hashin and Puck failure criteria, as well as many others. The model that will work best for a given real world problem depends on a number of factors, including structural loading, boundary conditions and impact velocity [4].

In this study the low velocity impact analysis of sisal fiber reinforced epoxy resin composite materials for automotive application was done using Abaqus/CEA 6.13 software based on ASTM D-7136 standards. For this simulation a $[0]_4$ unidirectional sisal/epoxy composite laminate with overall thickness of 2.16 mm was used.

Generally, in order to get the Abaqus/CEA 6.13 software in put data's, first the sisal fibre was extracted manually from the sisal plants and treated with 8% of NaOH. Then the testing specimens was manufactured using volume fraction of 60% matrix (epoxy with hardener) and 40% of sisal fibres, and finally the tensile, compression and in-plane shear test was conducted based on ASTM standards.

1.2. Theoretical background

1.2.1. Composite materials

Composite material is defined as it is a structural material that consists of two or more materials which together produce desirable properties that cannot be achieved with any of constitute alone [34,35]. Such composite materials has two main phases; the reinforcing and matrix phase. The reinforcing phase material may be in the form of fibers, particles, or flakes and it is continuous or discountinuous. The matrix phase materials are generally continuous and its serves to distribute the fibers and also to transmit the load to the reinforcing phase material. Reinforcing materials are strong and low densities while the matrix material is usually a ductile or tough.

Generally composite materials are broadly classified in to two main groups such as Natural fibre composites and Synthetic fibre composites [34, 36]. Natural composites are a composites that the fiber are found naturally (i.e. sisal, bamboo etc.) and synthetic composites are a man-made composites that produced by combining two or more materials in definite proportions under controlled condition (i.e. carbon, glass, etc.).

According to [34] composite materials are classified and related to constituents as shown in figure 1.3.

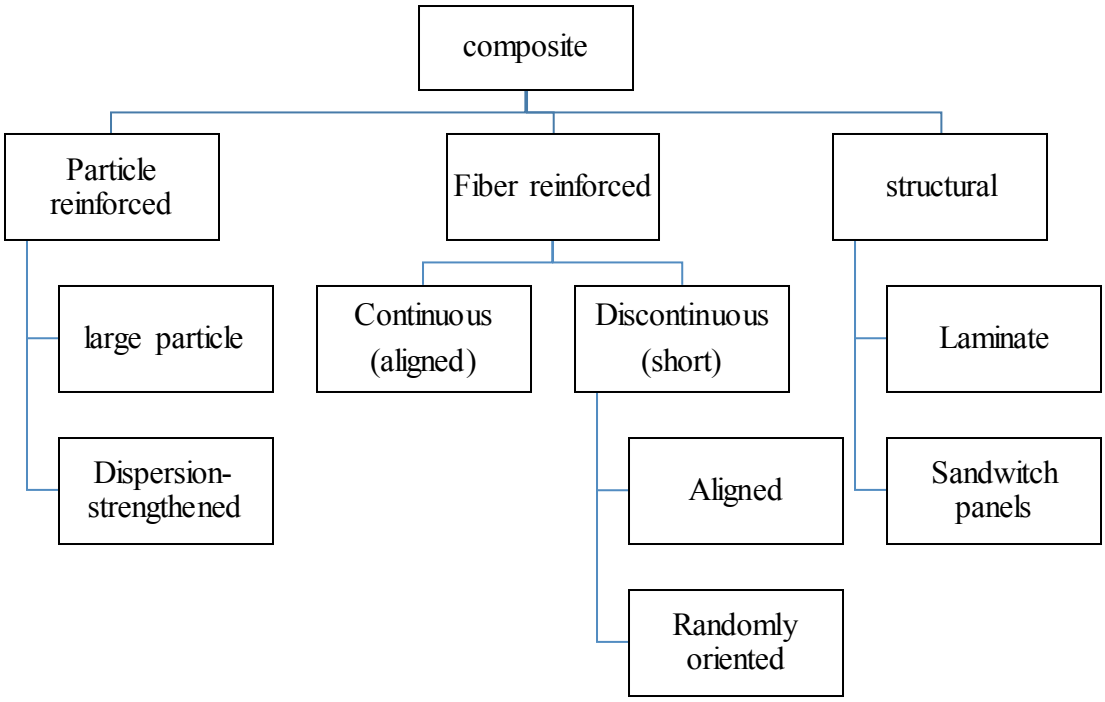

Figure 1.3. Composite material classifications [34].

1.2.1.1. Fiber reinforced composites

Fiber-reinforced composite materials are mainly consist of fibers reinforcing and a matrix materials. A fiber has high strength and modulus, and a matrix is generally acts as a binder for the fiber. In this form, both fibers and matrix retain their physical and chemical identities, yet they produce a combination of properties that cannot be achieved with either of the constituents acting alone. In general, fibers are the principal load-carrying members, while the surrounding matrix keeps them in the desired location and orientation, acts as a load transfer medium between them, and protects them from environmental damages due to elevated temperatures, humidity and etc. [34].

Manufacturing of a fiber reinforced composite material was started with the incorporation of a large number of fibers into a thin layer of matrix to form a lamina (ply). The thickness of a lamina is usually in the range of 0.1-1 mm [34, 36, 41]. As shown in below figure 1.4 the laminas are constructed either by continuous (long) or discontinuous (short) fibers.

The continuous fibers are arranged either in a unidirectional orientation (i.e. all fibers in one direction), in a bidirectional orientation (i.e., fibers in two direction, usually perpendicular each

other), or in a multidirectional orientation (i.e. fiber in more than two direction). For a lamina containing unidirectional fibers, the composite material has the highest strength and modulus in the longitudinal direction of the fibers. However, in the transvers direction, its strength and modulus are very low. For a lamina containing bidirectional fibers, the strength and modulus can be varied using different amounts of fibers in the longitudinal and transverse directions. For a balanced lamina, these properties are the same in both directions.

The thickness required to support a given load or to maintain a given deflection in a fiber reinforced composite structure is obtained by stacking several laminas in a specified sequence and then consolidating them to form a laminate. Various laminas in a laminate may contain fibers either all in one direction or in different directions.

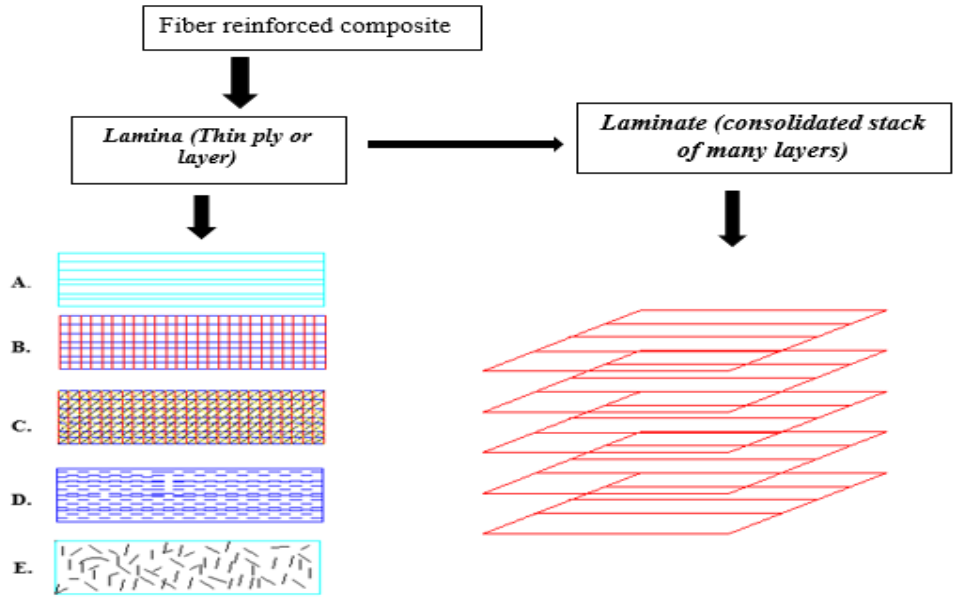

Figure 1.4. Basic building block in fibre reinforced composites [41].

A. *Unidirectional continuous fibers*
B. *Bidirectional continuous fibers*
C. *Multidirectional continuous fibers*
D. *Unidirectional discontinuous fibers*
E. *Random discontinuous fibers*

1.2.2. Natural fiber and natural fiber reinforced composites

In polymer composites, the reinforcing phase can either be fibrous or non-fibrous (particulates) in nature and if the fibers are derived from natural resources like plants or some other living species, they are called natural fibers [32].

Over the recent years, the natural fiber composites have received more attention, both from the academic world and various industries because of their advantageous properties when compared with the synthetic fibres (glass, carbon, etc.).Their low density, neutral to CO_2, recyclable, biodegradable, renewability, availability and price as well as satisfactory mechanical properties make them an attractive ecological alternatives to synthetic fibers that used for manufacturing of composite materials [32].

Natural fibers are generally categorized into three main groups based on their origin such as plant or vegetable fibers (i.e. sisal, bamboo, hemp, flax, etc.), animal/protein fibers (i.e. hair, wool, silk, chitin, etc.) and mineral fibers (i.e. asbestos, wollastonite, etc.). From this main groups, plant fibers are commonly used as reinforcement for polymers because of their good mechanical properties and renewability.

Different types and examples of natural fibers/plant fibers and matrix material are classified according to their origin are presented in Figure 1.5. From this classification sisal, flax, hemp, bamboo and kenaf fibers are commonly used as a reinforcement in a composite materials due to their properties and availability.

1.2.2.1. Sisal fiber

Sisal fiber is a types of plant fiber that obtained from the leaves of the plant Agave sisalana, which was originated from Mexico and is now mainly cultivated in East Africa, Brazil, Haiti, India and Indonesia [21]. The composition of sisal fiber is 60-80% cellulose, 5-20% lignin and 20% moisture content. Sisal (agave sisalana) can be extracted from its leaves by retting and mechanical extraction methods. The fiber extracted is dried under the sun until it turns white in color and then it is made ready for knotting. Fiber is separated to various sizes and knotting is done on the other side from long continuous stands [28].

Sisal fiber has numerous advantage including high specific properties, low density, less abrasive behavior to the processing equipment, good dimensional stability and harmlessness. Sisal fiber is

a low cost eco-friendly product and is abundantly available, easy to transport and has superior drivability. It is widely being used traditionally as a natural choice for ropes, carpets, clothing and other reinforcement materials. Due to sisal low density combined with relatively stiff and strong behavior, the specific properties of sisal fibre can compare to those of glass and some other fibres as shown in table 1.1 [30,57].

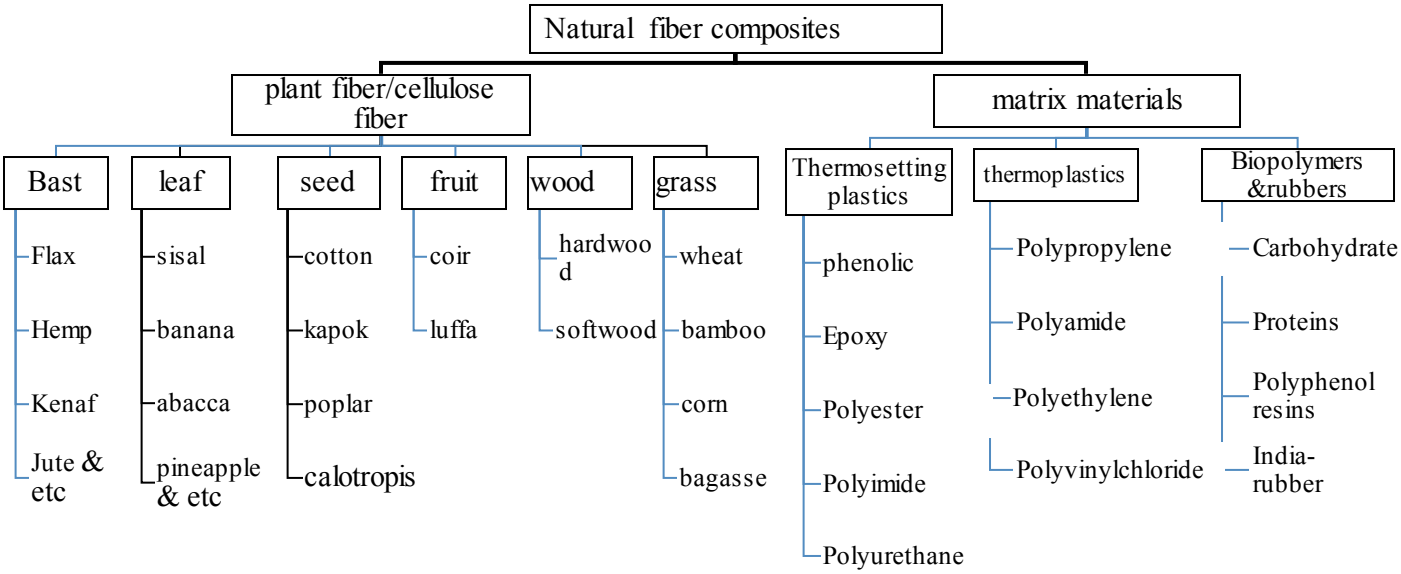

Figure 1.5. Commonly used natural fibers and polymer composites.

1.2.2.1.1. Production of Sisal plants in Ethiopia

Most part of the country is semi-arid and it accounts for about 71% of the entire 1.115 million Km^2 land area and 46% of the arable land [42]. These implies that there is a fertile ground and tremendous potential especially in SNNPRS, Oromia, Amhara and Tigray regional state to produce Agave sisal both on small-scale basis and on large scale basis. However the cultivation and production process of Agave sisal plant in organized manner is quite minimal. It can only cultivated, harvested and collected by local peoples (farmers), and used it for local purposes only.

Fiber	*Density (g/cm^3)*	*Tensile strength (Mpa)*	*Young's modulus (GPa)*	*Elongation at break (%)*	*Specific tensile strength ($Mpa/g.cm^{-3}$)*	*Specific young's modulus ($GPa/g.cm^{-3}$)*
Sisal	1.3-1.45	468-700	9.4-38.0	3.7	323 - 441	6-15
Flax	1.5	345-1100	27.6	2.7-3.2	230-773	18
Ramie	1.5	400-938	61.4-128	1.2-3.8	267-625	41-85
Jute	1.3-1.45	393-773	13-26.5	1.16-1.5	286-562	9-19
Coir	1.15	131-175	4-6	15-40	114-152	3-5
E-glass	2.5	2000-3500	70	2.5	800-1400	28
S-glass	2.5	4570	86	2.8	1828	34

Table 1.1. Properties of sisal fiber in comparison with other natural and synthetic fibers [30, 57].

1.2.3. The application of natural fibers in the automotive industry

As mentioned in previous section, the automotive industry gives a long list of presumed benefits of natural fibre composites. For example According to the literature [30] the uses of the natural fiber for automotive industries in different countries are dramatically increasing in the last decade. The main reason includes its low density (which may lead to weight reduction of 10 to 30%), good mechanical properties, favorable processing properties, favorable accident performance, high stability, favorable Eco-balance for part production, favorable Eco-balance during vehicle operation due to weight savings, occupational health benefits compared to synthetic fibers during production, price advantages both for the fibres and the applied technologies and etc.

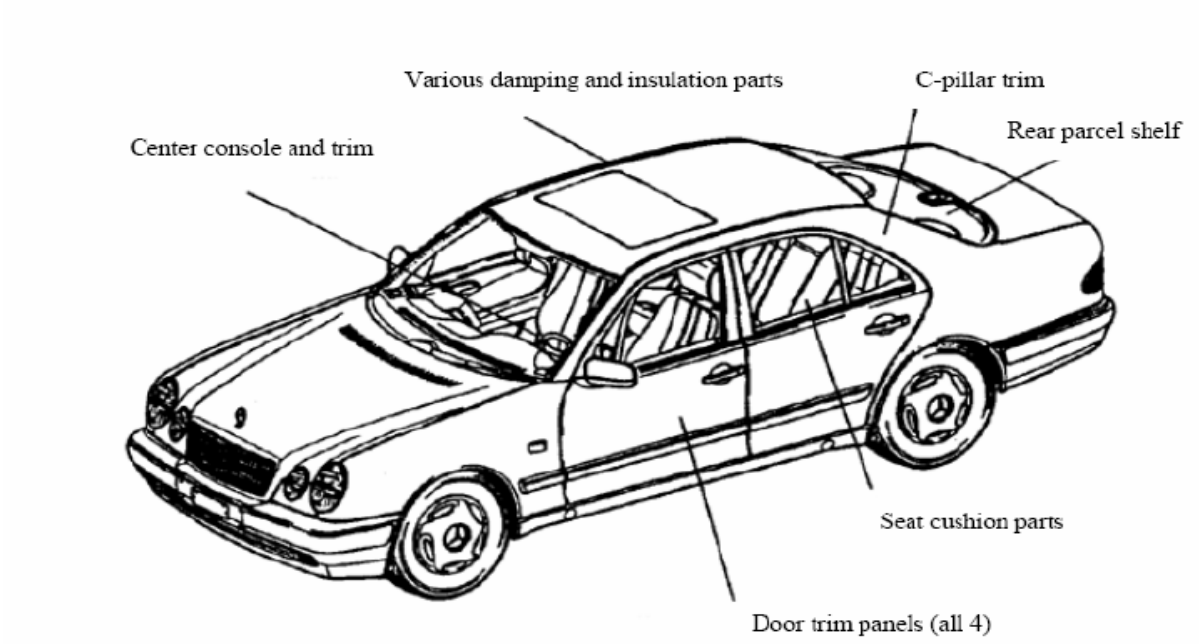

Figure 1.6. Plant fibre applications in the current Mercedes-Benz R-class [30].

However due to high moisture absorption property, most of the automotive companies are limited the uses these natural composite material for interior automotive part applications. According to the literatures [40], the present state of technology allows for the use of about 5-10 kg natural fibers per automobile. Below table1.2 shows the typical weight of natural fibers being incorporated for the automotive components in well- established applications.

Besides the advantages mentioned above, the natural fiber composites possess also some disadvantages including high moisture absorption properties and poor compatibility. The poor compatibility between a hydrophobic polymer matrix and the hydrophilic fibers leads to the formation of weak interfaces, which results in poor mechanical properties of the composites. Also the high moisture absorption by the fiber in the composite materials could lead to swelling and dimensional instability and to a loss of mechanical properties due to the degradation of the fibres and the interface between the fibre and Matrix [37].

Therefore, in order to improve the adhesion between the matrix and the fibres, a third component, called compatibiliser has to be used for matrix modification or the fibres have to be surface modified before the preparation of the composites [25, 29, 37]. Several studies have shown the

influence of various types of chemical modifications on the performance of natural fibres and fibre reinforced composites. The different surface chemical modifications of natural fibres such as alkali treatment, silane treatment, isocyanate treatment, latex coating, permanganate treatment, acetylation, monomer grafting under UV radiation, etc. have achieved various levels of success in improving fibre strength and fibre/matrix adhesion in natural fibre composites[17, 30, 32, 37].

Automotive components	***Typical weight of natural fibers (Kg)***
Seatbacks	1.6 – 2.0
Headrests	~2.5
Front door-liners	1.2-1.8
Rear door-liners	0.8-1.5
Parcel shelves	< 2.0
Boot-liners	1.5-2.5
Sunroof interior shield	< 0.4
Noise, vibration and harshness materials	>0.5

Table 1.2. Typical weight of natural fiber being incorporated in automotive components [40].

1.2.4. Impact condition and tests in automotive structures

With the development of automotive industry, the safety of the car has increasingly become an important research field of modern automobile development design. Also the energy absorption capability of a composite material is important in developing improved human safety in an automotive crash [48-52].

The ability to absorb impact energy and be survivable for the passengers is called the "crashworthiness" of the structure in vehicle. There are two important safety concepts in automotive industry to consider, crashworthiness, and penetration resistance. Crashworthiness is defined as the potential of absorption of energy through controlled failure modes and mechanisms that provides a gradual decay in the load profile during allowing projectile or fragment penetration [51].

The current legislation in design of the automobiles requires that, in the case of impact at speeds up to 15.5m/s (35mph) with a solid, immovable object, the occupants of the passenger compartment should not experience a resulting force that produce a net deceleration greater than 20gm. Subjection of the occupant to decelerations greater than 20 gm can cause serious internal injury, particularly brain damage [52].

The current trend of materials in car industry is towards replacing metal parts more and more by polymer composites in order to improve the fuel economy and reduce the weight of the vehicles. Also the use of composite materials as energy absorber is important in developing improved human safety in automotive crash. The behavior of composite failure in compression is the opposite of metals. Most composite are generally characterized by a brittle rather than ductile response to load. While metals structures collapse under crush or impact by buckling and/or folding in accordion(concertina) type fashion involving extensive plastic deformation, composite fail through a sequence of fracture mechanisms involving fibre fracture, matrix crazing and cracking, fibre-matrix de-bonding, delamination and interplay separation. The actual mechanisms and sequence of damage are highly dependent on the geometry of the structure, lamina orientation, and type of trigger and crash speed, all of which can be suitability designed to develop high energy absorbing mechanisms. Also the energy absorption in this composite materials is dependent on many parameters such as fiber type, matrix type, fiber architecture, specimen geometry and fiber volume fraction. Changes in these parameters can cause subsequent changes in the specific energy absorption (SEA) of composite materials up to a factor of two [52].

According to the literatures data survey [33], from different types of impact on automotive car structures, 60.6% were frontal impacts (that includes car to car impacts and the majority of impact against fixed object and non-motorists), 25.7% were side impacts (both left and right, and some impacts against fixed objects such as ole), 6.2% were rear impacts (that include car to car impacts and some impacts against non-motorists).

There are three main categories of impact (crash) tests in automotive, component tests, sled tests and full-scale barrier impacts. The complexity of the test associated variables increase from components to full- scale tests. This may cause a decline in test repeatability- a reality that may not be realized from the mathematical models. The component test determines the dynamic and/or

quasi-static response to loading of an isolated component. These component test are crucial in identifying the crush mode and energy absorption capacity. Understanding their performance is also essential to the development of prototype substructures and mathematical models [33, 50].

In a sled test, engineers use a vehicle buck representing the passenger compartment with all or some of its interior components such as the seat, instrument panel, steering system, seat belts, and air bags. Mechanical surrogates of humans (an-thropomorphic test devices-"dummies") or cadaver subjects are seated in the buck to simulate a driver and/or passenger and subjected to dynamic loads, similar to a vehicle deceleration-time pulse, to evaluate the occupant response in a frontal impact or side impact. The primary objective of a sled test is evaluation of the restraints. This is accomplished by high-speed photography of the dummy kinematics. In addition, various sensors located in the dummy and the restraints monitor the forces and moments to help determine the impact severity and the effectiveness of the restraint system in reducing loads transferred to the occupants.

The typical full-scale barrier involves collision of a guided vehicle, propelled into a barrier at a predetermined initial velocity and angles. Typically, a barrier test use a complete vehicle. To evaluate individual substructures, a sled test can be equally effective, especially in evaluation of the restraint systems. [33, 50].

1.2.5. Impact damage on composite materials

The impact responses of the laminated composite structures have been studied extensively over the years since the impact damage caused by foreign objects can reduce the load carrying capacity of the laminate composites significantly.

Impacts are classified in to different categories according to different literatures. Most of the literature's [11, 23, 33] are generally categorized this impacts in to low and high velocity, but there is not a clear and definite transition between those categories. However, a pure difference in the form of damage developed after each impact event exists.

An impact phenomenon is considered as low velocity impact if the contact period of the impactor is longer than the time period of the lowest mode of vibration of the structure. Apart from that, the

support condition is critical since the stress waves generated during the impact will have enough time to reach the edges of the structure and causing full vibration response. Conversely, high velocity impact is involved with smaller contact period of the impactor on the structure than the time period of the lowest vibration mode. The response of the structure is localized on the impacted area and it is usually not dependent on the support conditions [24]. Also the damage is much localized due to the high velocity impact, since the incident energy is dissipated in a very small volume; high velocity impact is characterized by penetration induced fiber breakage. During low velocity impacts, damage is initiated by matrix cracks which create delamination at interfaces between plies with different orientations [39]. Composites materials have shown to be very vulnerable especially to out of plane impact, which causes barely visible impact damage (BVID) and contributes to the loss in structure compressive strength and major reason for catastrophic damage and failures. BVID is a hidden menace and the residual strength in compression may be only 30 % of the undamaged value [11]. However, there is also a threshold velocity which distinguishes low and high velocity impact. As implied by some researcher 20m/s is a transition velocity between two different types of impact damage and it allows a definition of high and low velocity impacts.

The damage of composite laminates due to impact usually consists of several modes such as matrix cracking, delamination, fiber and matrix debonding, and fiber breakage, etc. Among these damage modes, delamination is the most important mode because it contributes the most to the reduction in post-impact residual compressive strength [2].

1.2.5.1. Mode of failure in low velocity impact

The heterogeneous and anisotropy nature of the laminated composite material contributes to different modes of failure. In most cases, these include;

a. Matrix failure that occurs parallel to the fibers due to tension, compression and shear.
b. Debonding and/or delamination between the plies as a result of interlaminar stresses
c. Fiber breakage and buckling ; and
d. Penetration. The interaction between failure modes influences damage mode initiation and propagation [33].

A. Matrix damage

Matrix damage is the first type of failure that induced by a transverse low- velocity impact. Usually, this takes the form of matrix cracking, debonding between the fibre and the matrix, and delamination initiation. Barley visible or minimal damage occurs at low impact energy levels (1 J to 5 J).

Matrix cracks are occurs due to property mismatching between the fibre and the matrix, and are usually oriented in planes parallel to the fibre direction in unidirectional fiber composites [15, 33].

B. Delamination

A delamination is a separation of plies which progress in the resin rich area between the plies. Delamination is a result of the bending stiffness mismatch between adjacent layers, i.e. the different fiber orientations between the layers. The greater the mismatch (0/90 is the worst-case fibre orientation), the greater the delamination area will be [15]. This will affect the material's properties, stacking sequence and laminate thickness. Delamination caused by the transverse impact occurs after a threshold energy has been reached, delamination develop in the presence of a matrix crack. Both bending cracks and shear cracks could initiate delamination, but the delamination induced by shear cracks is unstable and the bending crack induced delamination grows in a stable manner and proportional to the applied load [15, 33].

C. Fiber failure

This damage mode generally occurs later than matrix cracking and delamination in the fracture process. Fiber failure occurs just below the striker due to locally high stresses, and indentation effects (mainly governed by shear forces) and on the non-impacted face due to high bending stresses. Fibre failure is a precursor to the catastrophic penetration mode [15, 33].

D. Penetration

Penetration is a macroscopic mode of failure and occurs when the fiber failure reaches a critical extent, enabling the impactor to completely penetrate the material. The impact energy penetration threshold rises rapidly with specimen thickness. The major forms of energy absorption during laminate penetration are; shear –out (shear plug), delamination and elastic flexure. On these mechanisms, 'shear-out' accounts for 50-60% depending on the plate thickness, various factors

including tow size, fiber sizing, and orientation. , matrix type and interface have an influence on the penetration process [15, 33].

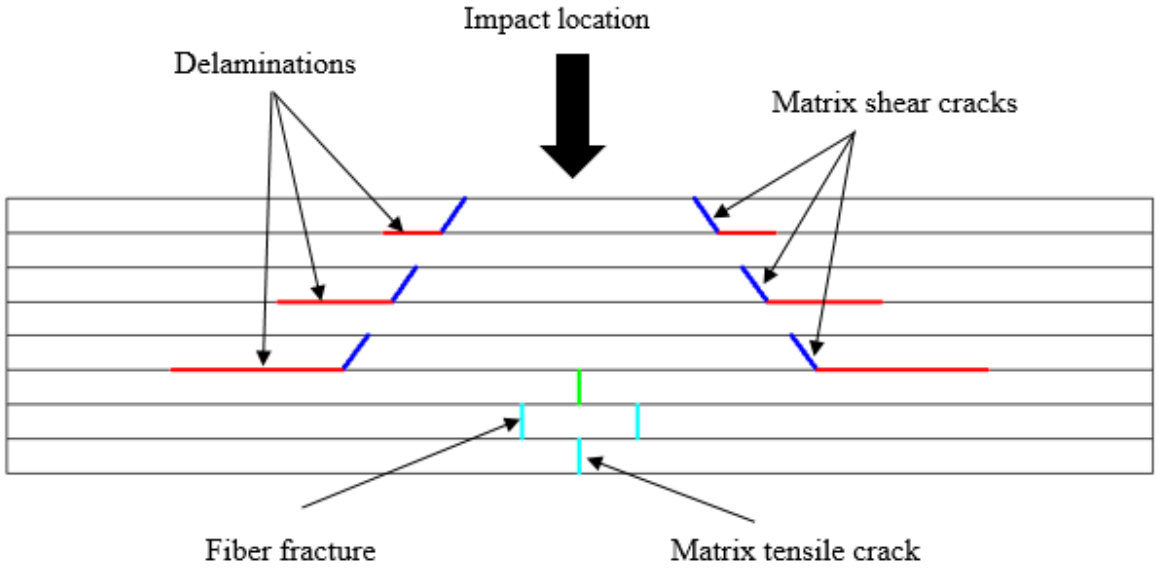

Figure 1.7. Cross-sectional view showing typical damage modes caused by an impact event.

1.3. Literature review

The purpose of this literature review is to provide background information on the issues to be considered in this study and to emphasize the relevance of the present study. This section includes reviews of available research reports about previous work related to natural fiber composite, impact analysis of composite material and impact analysis on the automotive structures. At the end of the literature survey, the knowledge gap in the earlier investigations/studies are presented.

1.3.1. Natural fiber and properties of natural fiber reinforced composite

Mwaikambo. L.Y [2006] presented the research review on the history, properties and application of plant fibers. The aim of the researcher is to briefly describe and discuss the historical use of plant fibers (fruit fiber, leaf fiber, Bast stem fiber and seed fibers), methods of extraction and/or separation, physical and mechanical properties, and to discuss the future end uses of these natural fibres. The final conclusion of the researcher shows that; there is a strong relationship between the

fine structure of the plant fibres and their mechanical properties, Plant fibres are an alternative resource to synthetic fibres as reinforcement for polymeric materials for the manufacture of cheap, renewable and environmentally friendly composites, and finally the author recommended that the researches must be continue on the natural fibre property optimization in order to compete with the well-established glass and carbon fibre reinforcement.

Enrico Mangino, Joe Carruthers et al. [2007] were presented the future use of structural composite materials in the automotive industry. In their paper they reported the findings of a recent European initiative that examine the future uses of composite materials in the automotive sectors. The principal technical challenges that must be overcome in ten keys(repair, design, crashworthiness, manufacturing, light weighting, joining, recycling, modeling, fire safety and new material concept) area relating to composite usage are reviewed. They also show that the uses of the natural fibre in automotive industry are increased in recent years. Furthermore, recommendation for future research priorities to overcome these challenges are presented by the authors.

Vieira, L.M.G., Santos, J.C et al. [2012] investigate the effects of chemical treatment and fibers orientations in the flexural strength of sisal fiber composites that's made up of five unidirectional layers oriented such as 0°/0°/0°/0°/0° and 0°/90°/0°/90°/0°. The researchers are first uses the mercerization process by immersing the washed and cleaned sisal fiber in 10% of NaOH for 1 hour at room temperature, and then immersing it in 97% acetic anhydride (plus two drops of concentrated sulfuric acid per 50 mL of acetic anhydride) for 5 min at room temperature. After this two process, the authors are fabricated the unidirectional sisal fibers composite lamina by using hand layup procedure meanwhile the sisal fibers were fixed in the metallic frame structure in order to voiding the presence of the stress concentration due to the misalignment or disorder of the fibers. Then after seven day of curing time, each lamina was cut off from the frame and assembled it layer by layer according to their desired set order. Finally after seven day of curing time of the composite, the flexural test was conducted by the researcher based on ASTM-D790 standards. From this investigation researchers are finally concluded that the chemical treatment was able to enhance the interface adhesion, and the composites that fabricated as 0°/90°/0°/90°/0° showed a lower flexural strength compared to those composites laminated at 0°.

M.Sakthivel and S.Ramesh [2013] conducted a research on the mechanical properties of natural fiber (banana, coir, sisal) polymer composites. The researchers are focused on the fabrication of polymer matrix composites by the help of various structures of patterns and calculating its material characterstics such as flextural modulus, flextural rigidity, hardness number and percentage of gain water conducting tests like flexural test, hardness test, water absorption test, impact test and density test. The researchers are first cleaned the discontinuous natural fiber by distilled water, then the cleaned natural fibers are dried in the sun light and finally the dried natural fibres are cleaned by chemical cleaning process using the mixture of 80% of NaOH and 20% of distilled water in the natural fiber preparation stage in order to improve the interfacial bonding of the natural fibre composites, then they fabricate the natural fibre composite using 70% epoxy resin hardener mixture and 30% of natural fibre using hand laminating process and finally they make the mechanical property tests.. From the final results and comparison, the researchers conclude that polymer banana reinforced natural composite is the best natural composites among the various combination and it can be used for the manufacturing of automotive seat shell among the other fiber combination. However the researchers did not briefly explain the standards that used for those material property tests.

M.K.Gupta and R.K.Srivastava [2014] conducted a research on the tensile and flexural properties of sisal fibre reinforced epoxy composite by using both unidirectional and mat form of fibres. The researchers are prepared the composite by using Hand lay-up method with 15, 20, 25 and 30 wt % of sisal fibres into the mixture of epoxy resin AY-105 and hardener with ratio of 10:1 by weight. From the testing results, the authors concluded that the tensile and flexural properties of sisal fibre epoxy composite both in unidirectional and in the mat form are maximum at 30 wt%, and also composite in unidirectional orientation of fibres gives better tensile ,flexural and adhesion properties in comparison to the mat form.

Sudhir. A Madhukiran et.al [2014] were conducted a research on the tensile and flexural properties of Sisal/jute hybrid natural fiber composites. The aim of the researcher is to describe the development and characterization of this new set of hybrid natural fiber composites. In order to prepare the composites and carried out the tensile and flextural test, the authors first extracted the natural fibers by using retting and combing process manually. Then they reinforced sisal/jute fibers of 0/40, 10/30, 20/20, 30/10, 40/0 weight fraction ratios with epoxy resin in matrix by using hand layup techniques. From the testing results ,they finally concluded that the jute/sisal(20/20)

weight fraction hybrid composite samples have maximum tensile and flexural strenghth, and also addition of sisal fiber in jute/epoxy composite up to 50% weight fraction results increasing the material properties.

Rafi Ali Alqahtani [2014] conducted a research paper on the flexural properties of a continuous sisal fiber/epoxy composites using ASTM D790-07 standards. On this paper the researcher fabricate and study the flexural behavior of sisal reinforced epoxy composites using experimental method. The composites were fabricated using hand layup techniques by considering treated and untreated sisal fibres and 6% of NaOH chemical treatment was used owing to improve the interfacial adhesion of the fibres with the matrix. The researcher uses scanning electron microscopy (SEM) to study the morphology of the failure surface of the composite after flexural tests and the result revealed that untreated fibres did not improve the composite's flexural strength due to a poor interfacial adhesion of the fibre with the matrix, which is consistent with the morphology study, i.e. debonding, detachment, and fibre pull out were observed on the fractured surfaces. However, 6% NaOH treated sisal fibres significantly improved the composite's flexural strength and modulus by about 76% and 162%, respectively compared to pure epoxy. Therefore the author finally conclude that 6% NaOH alkali treatment is an effective chemical treatment in improving interfacial adhesion between sisal fibres and the epoxy and flexural experiment results are in agreement with morphology study results that the sisal fibre is in better interfacial adhesion with epoxy resin. However, in the fabrication process the researcher does not present proper techniques in order to align the direction of the sisal fibre with the specimen/ moulds direction because this is the key process to control a specimen's mechanical property.

1.3.2. Impact analysis of composite materials

Serge Abrate [2001] proposed a research on the modeling of impact on composite structures. In this paper the researcher presented a brief overview of mathematical models that used for the analysis of the dynamics of impacts between a foreign object and a composite structure. The author was studied the various mathematical models available for analyzing the impact including energy balance model, spring mass model, complete model, and model for impact on infinite plate and presented an approach for selecting an appropriate model for each particular case using some examples as a demonstration. From his research the author finally concluded that: If bending waves travel from the impact point to the edge of the plate and back many times during the

predicted contact duration, we have a boundary controlled impact and a spring mass model or energy balance approach might be adequate because in that case, the plate behaves in a quasi-static manner, If the deformation never reaches the edge of the plate, we have a wave controlled impact and the approximate solution provides very good results. For intermediate cases, the infinite plate model might be adequate initially but reflected waves will affect the contact force history. Then, a complete model taking into account the full dynamic behavior of the plate and the boundary condition will be necessary. Examples demonstrating this procedure also show that in many cases a simple model can provide accurate predictions of the contact force history.

Zhidong Guan and Chihdar Yang [2002] presented the paper on the low-velocity impact and damage process of composite laminate. In their paper several important issues regarding to the damage simulation of composite laminate due to low velocity impact including contact law, damping initiation and the corresponding change of stiffness and damping were investigated. The researchers was modified the Hertzian contact law in order to accommodate the serious damage in the plate and they applied the continuum damage mechanics to account for the change of mechanical properties of damaged materials. The researchers uses a FORTAN finite element program using twenty-noded solid elements with layered structure to analyze the transient dynamic response of composite laminates. The damage in the forms of matrix cracking, delamination, and fiber breakage were analyzed. Finally conclude that the results that gained from the model including the force history and delamination areas are comparable well with the experiments. The researchers showed that the impact induced delamination is the most important damage mode because the level of impact energy to initiate delamination is low and the post-impact compressive strength is dramatically reduced due to delamination. However the author was not given a brief finite element simulation analysis.

Ramazan Karakuz, Emre Erbil and Mehmet Aktas [2010] are conducted the research on the damage prediction in glass/epoxy laminates subjected to low velocity impact loading using both numerical simulation and experimental laboratory analysis. The experimental laboratory test was done by using Fractovis plus impact testing machine using 20 J of impact energy. In their paper the impact behavior of unidirectional laminated glass/epoxy composite plates with $[0/\pm\theta/90]$s fiber orientation is investigated numerically equal energy of 40J, equal velocity 2m/s and equal

impactor mass 5kg. In order to examine the stacking effect, they chose five different $\pm\theta$ fiber directions (15° , 30°, 45 ° , 60° and 75°).Three different plate thicknesses at 2.9 mm, 5.8 mm, and 8.7 mm are also selected to survey the thickness effect on impact behavior of glass/epoxy composite plates. A transient finite element code 3D IMPACT is used for numerical analyses in order to calculate the stress and contact forces according to composite plate during impact events. It can also be used for predicting the threshold of impact damage and initiation using choi and chang failure/damage criteria. In this code an eight- point brick element and the direct gauss quadrature integration scheme are used by authors through the element thickness to account for the change in material properties from layer to layer. The Newmark scheme is also adopted to perform time integration step by step. In addition a contact law incorporated with the newton Raphson method is applied to calculate the contact forces during impact. Finally the researchers are compared the numerical results with the experimental study and it conclude that they are in good agreement with the experimental results.

R.C. Batra, G.Gopinath and J.Q.Zheng [2012] are investigated the damage and failure in low energy impact of fiber- reinforced polymeric composite laminates. The researchers analyzed the damage initiation, damage progression, and failure during 3-dimensional elasto-plastic deformation of a fiber reinforced polymeric laminated composites impacted by a low speed rigid sphere, and compare computed results with experimental findings available in the literatures. They assumed that the damage is initiated when one of the Hashin's failure criteria is satisfied and modeled its evolution by using an empirical relation proposed by Matzenmiller, Lubliner and Taylor. They solved the transient nonlinear problems using finite element method (FEM). The main contribution of this work includes considering the damage in 3-D rather than plane stress deformations of a laminated structure and elasto-plastic deformations of the composite. This has been accomplished by developing a user defined subroutine and implementing in the FE software ABAQUS. From strains supplied by ABAQUS the material subroutine uses a micromechanics approach based on the method of cells and values of material parameters of constituents to calculate average stress in an FE, and checks for Hashin's failure criteria. If the damage has initiated in the material, the subroutine evaluates the damage developed, computes resulting stress, and provides them to ABAQUS. The delamination failure mode is simulated by using the cohesive zone model available in ABAQUS. Finally they compared the ABAQUS results with the experimental ones that available in the literatures and concluded that: the computed time histories

of the axial load acting on the impactor are found to agree well with the experimental results, and various damage and failure modes are agreed qualitatively with those observed in tests.

Dragan Kreculji and Bosko Rasuo [2013] are conducted the research on the review of impact damages modeling in laminated composite aircraft structures. In this paper the researchers are presented a brief review on the area of the impact damages modeling of laminated composite aircraft structure including the impact damages in composite laminates, finite element modeling of impact laminates, multi scale modeling of damage, numerical simulation of impact on composite laminated structures and failure criteria of laminated composite structures that made by many researchers. The researcher's shows that the impact damage in laminated composite structures are very complex but matrix cracking, fiber failure and delamination are the most common failure mechanism and the ability to predict the initiation and growth of the damage is crucial for predicting performance and developing reliable and safe designs of composites. They finally concluded that the two dimensional or three dimensional Tsai-Wu, Change-Change and Hashin failure criteria's are the most commonly used criteria's in order to predict the level or degree of damage, fracture and failure of the composite structures ; and ABAQUS and LS-DYNA is the most frequently used commercial software's in the impact damage analysis of composite laminates.

Sunith Babu L. and H.K Shivanand [2014] are investigated the impact analysis of the laminated composite on glass fiber and carbon fiber. The main aim of the researchers is to present and discuss/analyze the experimental results obtained during a low velocity impact testing campaign conducted on E-glass/epoxy and carbon fiber epoxy matrix laminate plates under impact of steel projectile from an energy viewpoint by means of two parameters such as; the saturation impact energy and the damage degree of a plate specimen subjected to drop-dart test according to the ASTM D3029 and ASTM D7137 standards. The imapact test were carried out using an instrumented drop weight testing machine. The researchers are conducted the drop dart test by selecting different levels of the dart kinetic energy at impact by modification of the drop weight height of the impactor. Thus, impact velocities are different in one test from the other hand and consequently, the material of the plates is submitted to different deformation rate. For this analysis or investigation, the researchers area used the cross-ply laminates [0-90] and the time history of the impactor of the impact process such as the load, energy, velocity for both laminates is

determined for the target asquare plate of 2mm thickness and deflection due to an impact force acting at the center. The researchers are finally concluded that carbon fiber reinforced plastic has less impact strength than the glass fiber reinforced plastic laminates. In this paper the effects of the projectile velocities and a laminate sequences on composite plate behavior are also discussed, but the authors are not discussed the failure mechanism of this two composite materials breifly .

S.N.A. Safri, M.T.H.Sultan et.al [2014] are presented a review on the low velocity and high velocity impact test on composite materials. On this paper the authors are briefly reviewed/discussed about damage in composite materials, low-velocity impact test(izod and charpy impact test, drop weight test) , high-velocity impact test(powder gun test, gas gun test), factor influencing impact characteristics (effect of projectile mass and shape, effect of projectile velocity), failure modes in impact test(matrix cracking, delamination, fibre failure), structural health monitoring(SHM) and finally they made conclusion. The authors show that the izod , charpy and drop weight impact testing machine are commonly used in experimentally low velocity impact test analysis, however the reseachers are not present the review on the numerical simulation of impact analysis.

M.T.H. Sultan, F.Mustapha et.al [2014] presented a review of impact damage on composite structures. The authors briefly discussed and reviewed the damage in composite material, impact in composite material, classification of impact, impact response, high velocity impact, energy absorption and impact force of composites, and mode of failure of the composite structures. They also discussed the parameters that affect the performance of composite materials under low and high velocity impact tests such as the fiber properties, the specimen thickness, the projectile mass and shape, and the projectile velocity. The researchers show that izod impact test, charpy impact test and drop weight impact test is the most commonly used low velocity impact testing machines. The review showed that the main function of izod and charpy impact test is to test the impact toughness of the material and to compare the composites with different layups, including woven and unidirectional laminates. However the main function of the drop weight impact is to analyze the impact behavior of composite materials. From their review the researchers concluded that the damage of composite structure caused by impact events is one of the most critical behaviors that inhibits more widespread application of composite material and it is important to study and understand the damage mechanism in order to produce effective design for composite structures.

Ravi kumar.M and Keerthiprasad.K.S [2014] investigate the interlaminar low-velocity impact resistance of hemp and E-glass hybrid composite laminates experimentally using instrumented drop weight impact testing machine. For this study the researchers are manufactured the two different composite laminates using hand lay-up techniques. The dimensions of the hybrid composite laminates was 60 x 60 mm^2 with typical thickness of 3.6mm and the impact velocities are in the region 3-7 m/s, with an impactor mass between 5-10 kg. From this investigation, the authors are finally concluded that the hybrid hemp and E-glass fabric reinforced epoxy composites have very good impact strength up to 22.95 J of energy as just matrix cracking is observed at this energy level and further increase in energy has resulted in back face split up and finally perforation was taking place.

Rakesh Reghunath, Mahadevan Lakshmanan et.al. [2014] are conducted a research on low velocity impact analysis on glass fiber reinforced composites with varied volume fraction. This paper presented an experimental study to assess the impact response of bidirectional woven type of glass fiber reinforced composite material with varied volume fractions and hence to find out the optimal volume fraction which gives better impact resistance. The specimens are prepared using vacuum bagging process and the volume fraction is estimated by resin burn off method. For getting information regarding surface topography of the impacted specimen, scanning electron microscopy is conducted. The study is done by slightly varying the velocities and it is found that a volume fraction is 43-44% gives a better impact resistance which it is observed that matrix cracking, fiber breakage, debonding and fiber pull out are the major modes of failure during the impact, which reduces the structural strength and stability of the structure.

The other researchers **Azzam Ahmad and Li Wei [2015]** presented a brief review of research progress in dynamic and static response of composite structures subjected to low velocity impact and quasi-static load. This review paper focused on mathematical, experimental and numerical studies that done by many researchers recently for low-velocity impact damage. The researcher's viewed that for simulations of drop weight low-velocity impact damage, many researchers has used software's programs in order to predict the failure modes in composite structures such as ABAQUS/Explicit. Ls-Dyna, and MSC. Dytran, DYNA3D, and 3DIMPACT have been commonly used. The researchers are finally conclude the review with detailed discussion on the damage mechanisms and failure criteria for composite structures subjected to impact loads.

1.3.3. Impact analysis on automotive structures

George C. Jacob et.al [2004] conducted a research on the Crashworthiness of Automotive Composite Material Systems. The main goal of the researchers are to compare the crashworthiness capacity of a chopped carbon fiber reinforced in an epoxy resin system (CCF) with that of other fiber resin system such as graphite /epoxy cross-ply laminate (CP#1 and CP#2), graphite/epoxy triaxial braids with $0/+30^0/-30^0$ fiber orientation (O), and glass/polyurethane continuous strand mat (SSM) based on their specific energy absorption (SEA). The quasi-static progressive crush tests were then performed on these composite plate to identify and quantify their energy- absorbing mechanisms. An attempt was made to understand in great detail the effect of various material (fiber volume fraction. Fiber length, fiber tow size) and test (specimen width, loading rate, profile radius, constraint condition) parameters on their energy absorption capability by varying these parameters during testing. The quantity of these material systems needed to ensure passenger safety in a midsize car traveling at various velocities was calculated and compared. It was verified whether the CCF composite crushed at 5mm/min loading rate met both the criteria that need to be satisfied before a material is deemed highly crashworthy: a high magnitude of energy absorption and a safe allowable rate of this energy absorption. Finally from the result, the authors concluded that the SEA of the chopped carbon fiber composite material was the highest compared to that of all the other composite investigated, and 4.27 Kg of it would need to be placed at specific place in the car to ensure passenger safety in the event of a crash of 15.5m/s (35mph).

Pradeep Kumar Uddandapu [2013] presented a research on the impact analysis of car Bumper by varying speeds using materials Carbon fiber-reinforced poly-ether-IMIDE PEI and ABS plastic by Finite element Analysis Solid Work software. The author is first use Pro/Engineer software in order to modeling the 3D bumper and then used Solid Work in order to make the FEA impact analysis using different speed such as 48 km/hr and 75km/hr based on the Federal motor vehicle safety standards. The main aim of the researcher is to analyze and study the structure and material employed for car bumper in one of the car manufacturer. In this paper, the researcher is briefly discussed the most important variables such as, materials, structures, shapes and impact conditions for analysis of the bumper beam in order to improve the crashworthiness during collisions. Finally by observing the impact analysis results like stress, displacement and strain, the author concluded

that the Carbon fiber-reinforced poly-ether-IMIDE PEI and ABS plastic materials have a potential to replace the conventional steel bumpers.

Haining Chen, Hao Chen et.al [2014] are conducted a research on Analysis of vehicle seat and research on structure optimization in front and rear impact. The researchers are used the Hyper Mesh and LS-DYNA software to establish a dummy- seat finite element simulation model. The head, chest and neck injury of the dummy were analyzed respectively during the frontal and rear impact for both original and modified seats. From the simulation results, the authors concluded that the optimized seat was improved the occupant protection performance by reducing occupant damage parameters when compared to the original seat.

1.3.4. Research gap in previous investigation

- Many researchers has been done on the different types of natural fibers for fabricating the polymer composite, however a very less has been reported on the reinforcing potential of sisal fiber in spite of its several advantages over others. Also most of the literature's are fabricates the chopped or discontinuous and a very little literatures are found in manufacturing the continuous laminated sisal fiber reinforced composites for automotive applications.
- There is a lack of researches on the full mechanical characterization properties of the sisal fiber composites especially for unidirectional sisal epoxy laminate.
- On the impact analysis of composite material, many research have been done using the synthetic or man-made composites as a reinforcement. However it is hard to get using natural fibre especially using sisal fibre.

All the above literate's are deals all about the impact analysis and material properties of composite materials (natural and synthetic fiber composites). From the above literatures review and research gap it is possible to conclude that the impact analysis of the composite materials for automotive application are still the demanding research areas and there is still a lack of the simulation and experimental impact analysis of the composite materials when they strike by the transverse impact load especially for natural fiber composites. Also there is a lack of research on the manufacturing

and mechanical property characterization of the unidirectional sisal /epoxy laminate composite materials.

1.4. Statement of the problem

The uses of the natural composite materials for automotive application are radically increased in the recent decades due to their advantageous properties when compared with the synthetic composite materials. Beside this advantageous properties, this natural fibers has some disadvantages as synthetic fibers. One of the most amongst this is their susceptibility response to the transverse impact damage during the impact event. This impact damage is a major issue in the design of laminated composite, as it may reduce strength and stiffness significantly with and without any visible damage at the surface depending on the types of impact.

The various damage such as matrix cracks, delamination's, fiber fracture, fiber-matrix debonding, fiber pull out and penetration can occurs during transverse impact event. These damages causes considerable reduction in structural stiffness, leading to growth of the damage, catastrophic damage and final fracture. Based on the literatures, there is still demands on the need to understand and analyze the impact damage mechanisms of the composite materials for automotive application especially for the natural fiber composite materials, and also there is a lack of research on the full mechanical characterization of the natural fiber composites.

Therefore this paper was proposed in order to fill this research gap by investigating the impact analysis of sisal fiber reinforced epoxy resin composite material for automotive applications using Abaqus/CEA 6.13 software.

1.5. Objective of the study

The general objectives of this thesis is to investigate the impact analysis of the sisal fibre reinforced epoxy resin composite materials for automotive application using Abaqus/CEA 6.13 software based on ASTM D-7136 standard, and the fabrication , mechanical property characterization of this natural fiber in order to get the input data's for Abaqus software.

The specific objectives of these thesis are:

- Extraction of the sisal fiber from sisal plants.
- Chemical treatment of sisal fibres to improve its interfacial adhesion and stiffness.
- Manufacturing of sisal/epoxy composite materials.
- Conducting experimental test to characterize the unidirectional sisal/epoxy composite material properties.
- Determination of modulus of elasticity for the proposed materials.
- To analysis the damage mechanisms of the composite structure subjected to impact loads Using Abaqus/CEA
- To predict the time history of the impact process such as the load, energy, velocity and deflection using Abaqus/CEA.
- To predict the energy absorption capacity of the sisal/epoxy laminate using Abaqus/CEA.

1.6. Scope of the study

In this study the impact analysis of sisal fiber reinforced epoxy resin composite material for automotive application was presented using Abaqus software by varies the velocity and mass of the impactor based on based on ASTM D7136. In order to get the software input data's, the sisal fiber reinforced epoxy resin composite material was manufactured and the experimental material characterization test was done using universal testing machine. Also a two dimensional Hashin failure criteria was used in the simulation in order to predict and evaluate the transverse impact damage.

1.7. Limitation of the study

The composite materials may face different impact damage that caused by foreign object from different direction during their lifetime application. However, this study was limited only on the foreign impact damage from the transverse direction. Also due to the unavailability of the drop weight impact testing machine, and due to the lack of the published experimental paper on the transverse impact analysis of sisal fiber reinforced epoxy resin composite material, the validation of the finite element simulation results wasn't presented on this study.

1.8. Organization of the Thesis

This study is organized in six chapters. Chapter one, it outlines the background, the general idea of the researches and the literature review from previous studies. Also this chapter includes the statement of the problems, the scopes of the study, the limitation and the objectives of the study.

Chapter two deal with mathematical formulation. In this chapter the finite element constitute modeling, the classical laminate theory, the damage and failure in the fibre-reinforced composite material, and etc were discussed.

Chapter three deal with experimental determination of composite material properties. Here the full fiber extraction, composite fabrication, experimental testing process and its result was briefly discussed and presented.

In chapter four, Finite element impact simulation and procedure using Abaqus software was briefly discussed and presented. Also Results from the impact simulation using Abaqus software are presented and discussed briefly in chapter five. Finally the conclusion and recommendations are presented in chapter six.

CHAPTER TWO

MATHEMATICAL FORMULATION

2.1. Constitutive modeling

2.1.1 Composite Materials

In nature most of composite materials are anisotropic and heterogeneous. These two characteristics applied to the composite materials since the material properties are different in all directions and locations in the body. It differs from any common isotropic material, for example, steel which has identical material properties in any direction and location in the body. Hence, the difficulty in analyzing the stress-strain relationship of composite materials becomes greater. However, it is still acceptable assuming that the stress-strain relationship of composite material behaves linearly and elastically and follows Hooke's law. The relationship for three dimensional bodies in a 1-2-3 orthogonal Cartesian coordinate system is given as follows [34, 36]:

$$\begin{bmatrix}\sigma_1\\ \sigma_2\\ \sigma_3\\ \tau_{23}\\ \tau_{31}\\ \tau_{12}\end{bmatrix}=\begin{bmatrix}C_{11} & C_{12} & C_{13} & C_{14} & C_{15} & C_{16}\\ C_{21} & C_{22} & C_{23} & C_{24} & C_{25} & C_{26}\\ C_{31} & C_{32} & C_{33} & C_{34} & C_{35} & C_{36}\\ C_{41} & C_{42} & C_{43} & C_{44} & C_{45} & C_{46}\\ C_{51} & C_{52} & C_{53} & C_{54} & C_{55} & C_{56}\\ C_{61} & C_{62} & C_{63} & C_{64} & C_{65} & C_{66}\end{bmatrix}\begin{bmatrix}\varepsilon_1\\ \varepsilon_2\\ \varepsilon_3\\ \gamma_{23}\\ \gamma_{31}\\ \gamma_{12}\end{bmatrix} \tag{2.1}$$

Where 6 x 6 $[C]$ matrix is called stiffness matrix and this stiffness matrix has 36 constants. However, due to symmetry of stiffness matrix, the constants can be reduced to 21 constants.

$$\begin{bmatrix}\sigma_1\\ \sigma_2\\ \sigma_3\\ \tau_{23}\\ \tau_{31}\\ \tau_{12}\end{bmatrix}=\begin{bmatrix}C_{11} & C_{12} & C_{13} & C_{14} & C_{15} & C_{16}\\ & C_{22} & C_{23} & C_{24} & C_{25} & C_{26}\\ & & C_{33} & C_{34} & C_{35} & C_{36}\\ & sym & & C_{44} & C_{45} & C_{46}\\ & & & & C_{55} & C_{56}\\ & & & & & C_{66}\end{bmatrix}\begin{bmatrix}\varepsilon_1\\ \varepsilon_2\\ \varepsilon_3\\ \gamma_{23}\\ \gamma_{31}\\ \gamma_{12}\end{bmatrix} \tag{2.2}$$

As mentioned earlier, composite material is an anisotropic material. Thus, in order to determine its stress- strain relationship, all 21 constants must be obtained. However, many composite material possess material symmetry in nature. Material symmetry is defined as the material and its mirror image about the plane of symmetry are identical. In that case, the elastic properties are similar in directions of symmetry due to a symmetry present in the internal structure. Consequently, this symmetry leads to reducing the number of the independent elastic constants by zeroing out or relating some of the constants within the 6 x 6 stiffness matrix.

2.1.2. Orthotropic material (orthogonally anisotropic material)

A material is considered as an orthotropic material if there are three mutually perpendicular directions and has only three mutually perpendicular planes of material symmetry. Generally, composite materials are considered as an orthotropic material since there are three mutually perpendicular plane of property symmetry at a point in the body. The directions orthogonal to the plane of material symmetry in an orthotropic material define the principal material direction and it has been illustrated in figure 2.1.

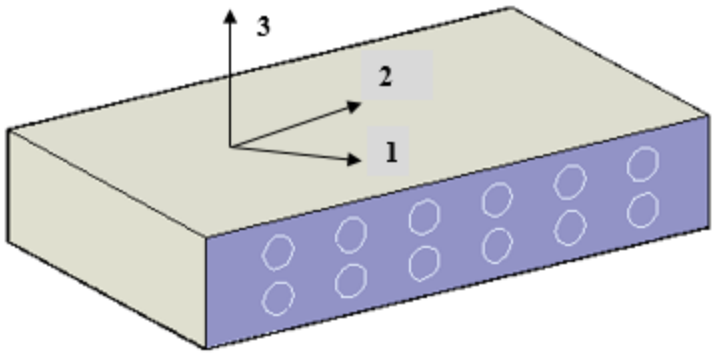

Figure 2.1. Principal material directions in an orthotropic material [34, 36].

As composite materials are considered as orthotropic material, the stiffness matrix is given by;

$$[C]=\begin{bmatrix} C_{11} & C_{12} & C_{13} & 0 & 0 & 0 \\ C_{21} & C_{22} & C_{23} & 0 & 0 & 0 \\ C_{31} & C_{32} & C_{33} & 0 & 0 & 0 \\ 0 & 0 & 0 & C_{44} & 0 & 0 \\ 0 & 0 & 0 & 0 & C_{55} & 0 \\ 0 & 0 & 0 & 0 & 0 & C_{66} \end{bmatrix} \quad (2.3)$$

Therefore, it can be shown that only 9 elastic constants need to be solved in order to determine the stress-strain relationship of composite materials. It is expressed as:

$$\begin{bmatrix}\sigma_1\\ \sigma_2\\ \sigma_3\\ \tau_{23}\\ \tau_{31}\\ \tau_{12}\end{bmatrix}=\begin{bmatrix}C_{11} & C_{12} & C_{13} & 0 & 0 & 0\\ C_{21} & C_{22} & C_{23} & 0 & 0 & 0\\ C_{31} & C_{32} & C_{33} & 0 & 0 & 0\\ 0 & 0 & 0 & C_{44} & 0 & 0\\ 0 & 0 & 0 & 0 & C_{55} & 0\\ 0 & 0 & 0 & 0 & 0 & C_{66}\end{bmatrix}\begin{bmatrix}\varepsilon_1\\ \varepsilon_2\\ \varepsilon_3\\ \gamma_{23}\\ \gamma_{31}\\ \gamma_{12}\end{bmatrix} \tag{2.4}$$

By substituting the stiffness matrix [C] with engineering constants, we get:

$$[C]=\begin{bmatrix}\frac{1-V_{23}V_{32}}{E_2E_3\Delta} & \frac{V_{21}+V_{23}V_{31}}{E_2E_3\Delta} & \frac{V_{31}+V_{21}V_{32}}{E_2E_3\Delta} & 0 & 0 & 0\\ \frac{V_{21}+V_{23}V_{31}}{E_2E_3\Delta} & \frac{1-V_{23}V_{32}}{E_1E_3\Delta} & \frac{V_{32}+V_{12}V_{31}}{E_1E_3\Delta} & 0 & 0 & 0\\ \frac{V_{31}+V_{21}V_{32}}{E_2E_3\Delta} & \frac{V_{32}+V_{12}V_{31}}{E_1E_3\Delta} & \frac{1-V_{12}V_{21}}{E_1E_2\Delta} & 0 & 0 & 0\\ 0 & 0 & 0 & G_{23} & 0 & 0\\ 0 & 0 & 0 & 0 & G_{31} & 0\\ 0 & 0 & 0 & 0 & 0 & G_{12}\end{bmatrix} \tag{2.5}$$

Where $\Delta=\frac{1-V_{12}V_{21}-V_{23}V_{32}-V_{13}V_{31}-2V_{21}V_{32}V_{13}}{E_1E_2E_3}$ (2.6)

$$\begin{bmatrix}\varepsilon_1\\ \varepsilon_2\\ \varepsilon_3\\ \gamma_{23}\\ \gamma_{31}\\ \gamma_{12}\end{bmatrix}=\begin{bmatrix}S_{11} & S_{12} & S_{13} & 0 & 0 & 0\\ S_{21} & S_{22} & S_{23} & 0 & 0 & 0\\ S_{31} & S_{32} & S_{33} & 0 & 0 & 0\\ 0 & 0 & 0 & S_{44} & 0 & 0\\ 0 & 0 & 0 & 0 & S_{55} & 0\\ 0 & 0 & 0 & 0 & 0 & S_{66}\end{bmatrix}\begin{bmatrix}\sigma_1\\ \sigma_2\\ \sigma_3\\ \tau_{23}\\ \tau_{31}\\ \tau_{12}\end{bmatrix} \tag{2.7}$$

Where [S] is the compliance matrix

Since the symmetrical properties exist in the stiffness matrix, the relation between Poisson's ratio and young's modulus is:

$$\frac{V_{ij}}{E_i}=\frac{V_{ji}}{E_j} \quad \text{for } i \neq j \text{ and } i, j = 1, 2, 3 \tag{2.8}$$

2.1.2.1. Constitutive Relations for a Lamina

In the analysis of fiber-reinforced composite materials, the assumption of plane stress is usually used for each layer (lamina). This is mainly because fiber reinforced materials are utilized in beams, plates, cylinders, and other structural shapes which have at least one characteristic geometric dimension in an order of magnitude less than the other two dimensions. In this case, the stress components σ_3 , τ_{23}, and τ_{13} are set to zero with the assumption that the 1-2 plane of the principal material coordinate system is in the plane of the layer (lamina). Therefore, the stresses σ_1,σ_2 and τ_{12} lie in a plane, while the stresses σ_3,τ_{23}, and τ_{13} are perpendicular to this plane and are zero (figure. 2.1).

By assuming two-dimensional orthotropic material properties for each unidirectional ply, the number of material properties reduced four. A unidirectional ply is shown in figure 2.1, the 1 and 2 axes are the longitudinal and transverse directions respectively.

In this case equation 2.7 reduced to:

$$\begin{bmatrix} \varepsilon_1 \\ \varepsilon_2 \\ \gamma_{12} \end{bmatrix} = \begin{bmatrix} S_{11} & S_{12} & 0 \\ S_{21} & S_{22} & 0 \\ 0 & 0 & S_{66} \end{bmatrix} \begin{bmatrix} \sigma_1 \\ \sigma_2 \\ \tau_{12} \end{bmatrix} \tag{2.9}$$

Where

$$S = \begin{bmatrix} \frac{1}{E_1} & -\frac{V_{21}}{E_2} & 0 \\ -\frac{V_{12}}{E_1} & \frac{1}{E_2} & 0 \\ 0 & 0 & \frac{1}{G_{12}} \end{bmatrix} \tag{2.9 a}$$

The 3 x 3 matrix in equation (2.9) is called the reduced compliance matrix. The inverse of the reduced compliance matrix is the reduced stiffness matrix given as follows:

$$\begin{bmatrix} \sigma_1 \\ \sigma_2 \\ \tau_{12} \end{bmatrix} = \begin{bmatrix} Q_{11} & Q_{12} & 0 \\ Q_{21} & Q_{22} & 0 \\ 0 & 0 & Q_{66} \end{bmatrix} \begin{bmatrix} \varepsilon_1 \\ \varepsilon_2 \\ \gamma_{12} \end{bmatrix} \tag{2.10}$$

Where the elements Q_{ij} are the reduced stiffness coefficients, which are related to the compliance matrix by:

$$Q_{11} = \frac{S_{22}}{S_{11}S_{22} - S^2_{12}} \quad (2.10\ a)$$

$$Q_{12} = -\frac{S_{12}}{S_{11}S_{22} - S^2_{12}} \quad (2.10\ b)$$

$$Q_{22} = \frac{S_{11}}{S_{11}S_{22} - S^2_{12}} \quad (2.10\ c)$$

$$Q_{66} = \frac{1}{S_{66}} \quad (2.10\ c)$$

2.1.2.2. Hooke's Law for a Two-Dimensional Angle Lamina

Generally, a laminate does not consists only of unidirectional laminae because of their low stiffness and strength properties in the transverse direction. Therefore, in most laminates, some laminae are placed at an angle. It is thus necessary to develop the stress-strain relationship for an angle lamina.

The coordinate system used for showing an angle lamina is given in below figure. The axes in the 1-2 coordinate system are called the local axes or the material axes. The direction 1 is parallel to the fibers and the direction 2 is perpendicular to the fibers. In some literature, direction 1 is also called the longitudinal direction L and the direction 2 is called the transverse direction T. The axes in the x-y coordinate system are called the global axes or the off-axes and the 1-2 coordinate systems are called the local axes. The angle between the two axes was denoted by angel θ.

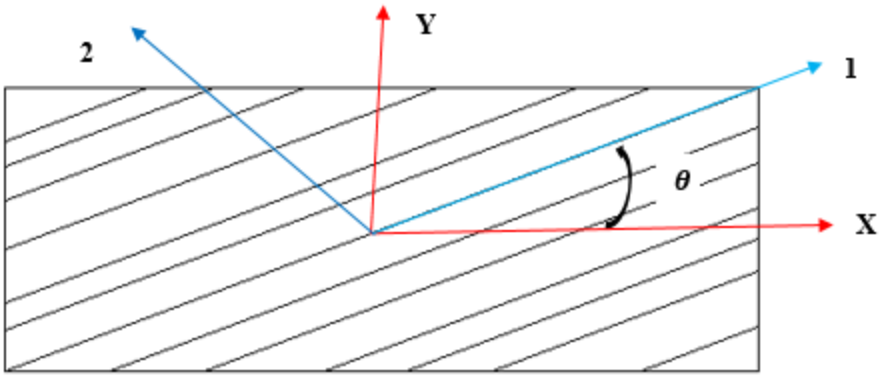

Figure 2.2. Local and global axes of an angle lamina [34].

The global and local stress in an angle lamina are related each other through the angle of the lamina, θ:

$$\begin{bmatrix}\sigma_x\\ \sigma_y\\ \sigma_{xy}\end{bmatrix}=[T]^{-1}\begin{bmatrix}\sigma_1\\ \sigma_2\\ \tau_{12}\end{bmatrix} \tag{2.11}$$

Where T is called the transformation matrix and it is defined as:

$$[T]^{-1}=\begin{bmatrix}c^2 & s^2 & -2sc\\ s^2 & c^2 & 2sc\\ sc & -sc & c^2-s^2\end{bmatrix} \tag{2.12}$$

Where c= cos (θ)

S= sin (θ)

Using the stress-strain equation (2.10) in the local axes, equation (2.11) can be written as

$$\begin{bmatrix}\sigma_x\\ \sigma_y\\ \sigma_{xy}\end{bmatrix}=[T]^{-1}[Q]\begin{bmatrix}\sigma_1\\ \sigma_2\\ \tau_{12}\end{bmatrix} \tag{2.13}$$

By using transformation matrix and some simplification procedure, equation (2.13) can be written as:

$$\begin{bmatrix}\sigma_x\\ \sigma_y\\ \sigma_{xy}\end{bmatrix}=\begin{bmatrix}\bar{Q}_{11} & \bar{Q}_{12} & \bar{Q}_{16}\\ \bar{Q}_{12} & \bar{Q}_{22} & \bar{Q}_{26}\\ \bar{Q}_{16} & \bar{Q}_{26} & \bar{Q}_{66}\end{bmatrix}\begin{bmatrix}\varepsilon_1\\ \varepsilon_2\\ \gamma_{12}\end{bmatrix} \tag{2.14}$$

Where $\bar{Q}_{ij}$ are called the elements of the transformed reduced stiffness matrix $[\bar{Q}]$ and are given by:

$$\bar{Q}_{11}= Q_{11}c^4 + Q_{22}s^4+2(Q_{12}+ 2Q_{66})s^2c^2 \tag{2.15a}$$

$$\bar{Q}_{12}= (Q_{11}+Q_{22} - 4Q_{66})\, s^2c^2 + Q_{12}(c^4 + s^2) \tag{2.15b}$$

$$\bar{Q}_{22}= Q_{11}s^4+Q_{22}c^4 + 2(Q_{12} + 2Q_{66})s^2c^2 \tag{2.15c}$$

$$\bar{Q}_{16}= (Q_{11}-Q_{12}-2Q_{66})\, c^3\text{s} - (Q_{22} - Q_{12} - 2Q_{66})s^3c \tag{2.15d}$$

$$\bar{Q}_{26}= (Q_{11}-Q_{12}-2Q_{66})\, s^3c - (Q_{22} - Q_{12} - 2Q_{66})c^3\text{s} \tag{2.15 e}$$

$$\bar{Q}_{66}= (Q_{11}+Q_{22}-2Q_{12}-2Q_{66})\ s^2c^2+ Q_{66}(s^4+c^4) \tag{2.15f}$$

Then inverting equation (2.14) gives:

$$\begin{bmatrix}\varepsilon_1\\ \varepsilon_2\\ \gamma_{12}\end{bmatrix}=\begin{bmatrix}\bar{S}_{11} & \bar{S}_{12} & \bar{S}_{16}\\ \bar{S}_{12} & \bar{S}_{22} & \bar{S}_{26}\\ \bar{S}_{16} & \bar{S}_{26} & \bar{S}_{66}\end{bmatrix}\begin{bmatrix}\varepsilon_1\\ \varepsilon_2\\ \gamma_{12}\end{bmatrix} \quad (2.16)$$

Where $\bar{s}_{ij}$ are the elements of the transformed reduced compliance matrix and are given by:

$$\bar{S}_{11}= S_{11}c^4 + S_{22}s^4+2(S_{12}+ 2S_{66})s^2c^2 \quad (2.17a)$$

$$\bar{S}_{12}= (S_{11}+S_{22} - 4S_{66})\, s^2c^2 + S_{12}(c^4 + s^2) \quad (2.17b)$$

$$\bar{S}_{22}= S_{11}s^4+Sc^4 + 2(S_{12} + 2S)s^2c^2 \quad (2.17c)$$

$$\bar{S}_{16}= (S_{11}\text{-}S_{12}\text{-}2S_{66})\, c^3\text{s} - (S_{22} - S_{12} - 2S_{66})s^3c \quad (2.17d)$$

$$\bar{S}_{26}= (S_{11}\text{-}S_{12}\text{-}2S_{66})\, s^3c - (S_{22} - S_{12} - 2S_{66})c^3\text{s} \quad (2.17e)$$

$$\bar{S}_{66}= (S_{11}+S_{22}\text{-}2S_{12}\text{-}2S_{66})\ s^2c^2+ S_{66}(s^4+c^4) \quad (2.17\ f)$$

2.2. Classical Lamination Theory

Classical lamination theory is useful in calculating stresses and strain in each lamina of a thin laminated structure. Beginning with the stiffness matrix of each lamina, the step-by step procedure in lamination theory includes:

1. Calculation of stiffness matrices for the laminate.
2. Calculation of midplane strains and curvatures for the laminate due to a given set of applied forces and moments.
3. Calculation of in-plane strains ε_{xx},ε_{yy} and γ_{xy} for each lamina.
4. Calculation of in-plane stressesσ_{xx},σ_{yy} and τ_{xy} in each lamina.

2.2.1. Assumptions

The following basic assumptions are made in the classical laminate theory to develop the relationships:

1. Each lamina is orthotropic
2. Laminate is thin and wide (width>> thickness).
3. A perfect interlaminar bond exists between various laminas.
4. Strain distribution in the thickness direction is linear.
5. All laminas are macroscopically homogeneous and behave in a linearly elastic manner.

6. A line straight and perpendicular to the middle surface remains straight and perpendicular to the middle surface during deformation ($\tau_{xz,yz}$=0).

2.2.2. Strain and Stress Variation in a Laminate

Following assumption 3, laminate strains are linearly related to the distance from the midplane as

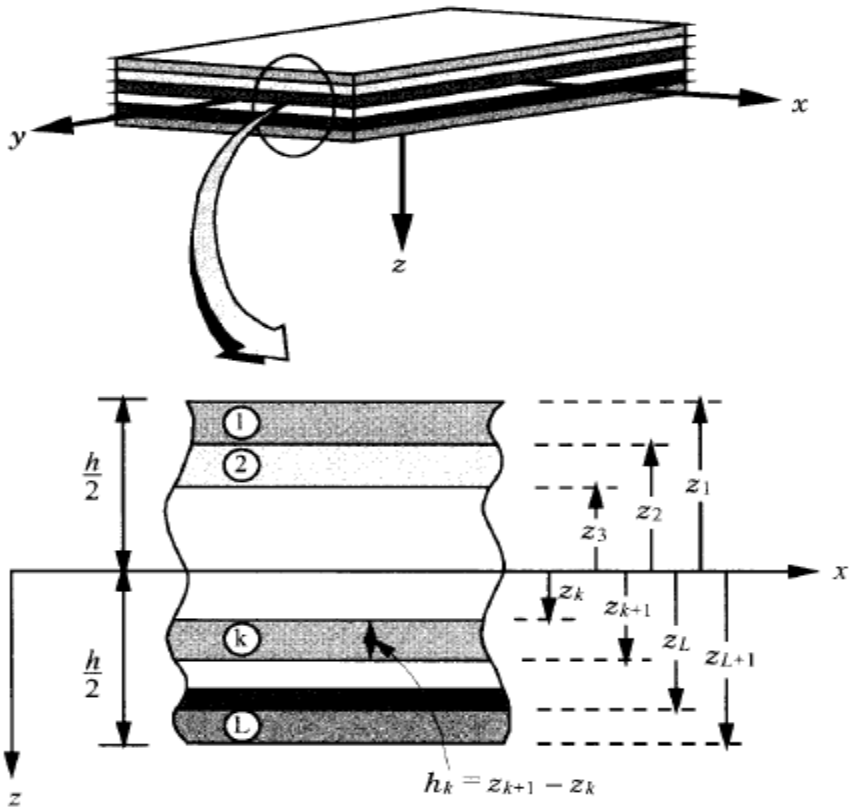

Figure 2.3. Laminate geometry [35].

$$\begin{Bmatrix} \varepsilon_x \\ \varepsilon_y \\ \gamma_{xy} \end{Bmatrix} = \begin{Bmatrix} {\varepsilon_x}^0 \\ {\varepsilon_y}^0 \\ {\gamma_{xy}}^0 \end{Bmatrix} + z \begin{Bmatrix} K_x \\ K_y \\ K_{xy} \end{Bmatrix} \tag{2.18}$$

Where:

${\varepsilon_x}^0$, ${\varepsilon_y}^0$ = midplane normal strain in the laminate

$\gamma_{xy}{}^{0}$ = midplane shear strain in the laminate.

K_x, K_y =bending curvatures of the laminates.

K_{xy} =twisting curvature of the laminate.

Z = distance from the midplane in the thickness direction.

By substitution of the strain variation through the thickness, Equation (2.18), in the stress-strain relation, Equation (2.14), the stresses in the K^{th} layer can be expressed in terms of the laminate middle surface strains and curvatures as:

$$\begin{Bmatrix}\sigma_x\\ \sigma_y\\ \tau_{xy}\end{Bmatrix}_K = \begin{bmatrix}\bar{Q}_{11} & \bar{Q}_{12} & \bar{Q}_{16}\\ \bar{Q}_{12} & \bar{Q}_{22} & \bar{Q}_{26}\\ \bar{Q}_{16} & \bar{Q}_{26} & \bar{Q}_{66}\end{bmatrix} \left\{ \begin{Bmatrix}\varepsilon_x{}^{0}\\ \varepsilon_y{}^{0}\\ \gamma_{xy}{}^{0}\end{Bmatrix} + z \begin{Bmatrix}K_x\\ K_y\\ K_{xy}\end{Bmatrix} \right\} \tag{2.19}$$

Since the $\overline{Q_{ij}}$ can be different for each layer of the laminate, the stress variation through the laminate thickness is not necessarily linear, even though the strain variation is linear.

2.2.3. Resultant Laminate Forces and Moments

Applied force and moment resultant (figure 2.4) on a laminate are related to the midplane strains and curvatures by the following equations:

$$\begin{Bmatrix}N_x\\ N_y\\ N_{xy}\end{Bmatrix} = \begin{bmatrix}A_{11} & A_{12} & A_{16}\\ A_{12} & A_{22} & A_{26}\\ A_{16} & A_{26} & A_{66}\end{bmatrix} \begin{Bmatrix}\varepsilon_x{}^{0}\\ \varepsilon_y{}^{0}\\ \gamma_{xy}{}^{0}\end{Bmatrix} + \begin{bmatrix}B_{11} & B_{12} & B_{16}\\ B_{12} & B_{22} & B_{26}\\ B_{16} & B_{26} & B_{66}\end{bmatrix} \begin{Bmatrix}K_x\\ K_y\\ K_{xy}\end{Bmatrix} \tag{2.20a}$$

$$\begin{Bmatrix}M_x\\ M_y\\ M_{xy}\end{Bmatrix} = \begin{bmatrix}B_{11} & B_{12} & B_{16}\\ B_{12} & B_{22} & B_{26}\\ B_{16} & B_{26} & B_{66}\end{bmatrix} \begin{Bmatrix}\varepsilon_x{}^{0}\\ \varepsilon_y{}^{0}\\ \gamma_{xy}{}^{0}\end{Bmatrix} + \begin{bmatrix}D_{11} & D_{12} & D_{16}\\ D_{12} & D_{22} & D_{26}\\ D_{16} & D_{26} & D_{66}\end{bmatrix} \begin{Bmatrix}K_x\\ K_y\\ K_{xy}\end{Bmatrix} \tag{2.20b}$$

The complete set of the equations can be expressed in matrix form as :

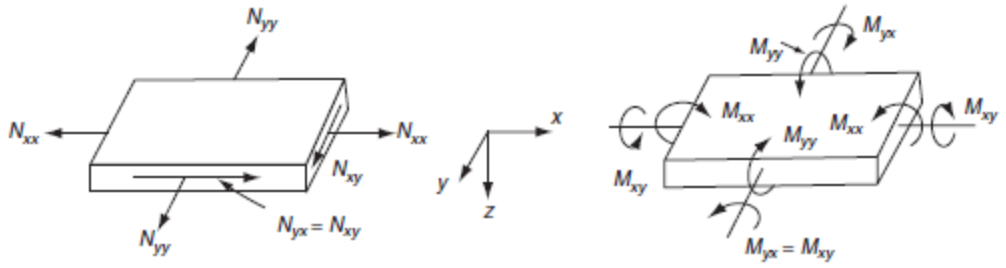

Figure 2.4. In-plane, bending, and twisting loads applied on a laminate[41].

$$\begin{Bmatrix} N_x \\ N_y \\ N_{xy} \\ M_x \\ M_y \\ M_{xy} \end{Bmatrix} = \begin{bmatrix} A_{11} & A_{12} & A_{16} & B_{11} & B_{12} & B_{16} \\ A_{12} & A_{22} & A_{26} & B_{12} & B_{22} & B_{26} \\ A_{16} & A_{26} & A_{66} & B_{16} & B_{26} & B_{66} \\ B_{11} & B_{12} & B_{16} & D_{11} & D_{12} & D_{16} \\ B_{12} & B_{22} & B_{26} & D_{12} & D_{22} & D_{26} \\ B_{16} & B_{26} & B_{66} & D_{16} & D_{26} & D_{66} \end{bmatrix} \begin{Bmatrix} {\varepsilon_x}^0 \\ {\varepsilon_y}^0 \\ {\gamma_{xy}}^0 \\ K_x \\ K_y \\ K_{xy} \end{Bmatrix} \tag{2.21}$$

Or in partitioned form as

$$\begin{Bmatrix} N \\ M \end{Bmatrix} = \begin{bmatrix} A & B \\ B & D \end{bmatrix} \begin{Bmatrix} \epsilon^0 \\ K \end{Bmatrix} \tag{2.22}$$

Where

N_x = normal force resultant in the x direction (per unit width)

N_y = normal shear resultant in the y direction (per unit width)

N_{xy} = shear force resultant (per unit width)

M_x = bending moment resultant in the yz plane (per unit width)

M_y =bending moment resultant in the xz plane (per unit width)

M_{xy} =twisting moment (torsion) resultant (per unit width)

$[A]$ = extensional stiffness matrix for the laminate (N/m)

$[B]$ = coupling stiffness matrix for the laminate (N)

$[D]$ = bending stiffness matrix for the laminate (Nm)

2.2.4. Elements in Stiffness Matrices

The elements in [A], [B], and [D] matrices are calculated from

$$A_{ij} = \sum_{k=1}^{N} \left(\bar{Q}_{ij}\right)_k (Z_k - Z_{k-1}) \text{ , i=1, 2,6 ; j=1,2,6,} \quad (2.23a)$$

$$B_{ij} = \frac{1}{2} \sum_{k=1}^{N} \left(\bar{Q}_{ij}\right)_k (Z^2{}_k - Z^2{}_{k-1}), \text{ i= 1,2,6 ; j=1,2,6 ,} \quad (2.23b)$$

$$D_{ij} = \frac{1}{3} \sum_{k=1}^{N} \left(\bar{Q}_{ij}\right)_k (Z^3{}_k - Z^3{}_{k-1}), \text{ i= 1,2,6 ; j= 1,2,6 .} \quad (2.23c)$$

The relations above are expressed in terms of three laminate stiffness matrices. [A], [B] and [D], which are functions of the geometry, material properties and stacking sequence of the individual plies, as described in Equation (2.23). They are average elastic parameters of the multidirectional laminate with the following significance:

$\mathbf{A_{ij}}$ are extensional stiffness's, or in-plane laminate moduli, relating in-plane loads to in-plane strains. $\mathbf{B_{ij}}$ are called coupling stiffness, or in-plane flexure coupling laminate moduli, relating in-plane loads to curvatures and moments to in-plane strains. Thus, if $\mathbf{B_{ij}} \neq 0$, in-plane forces produce flexural and twisting deformations; moments produce extension of the middle surface in addition to flexure and twisting. $\mathbf{D_{ij}}$ are bending or flexural laminate stiffness's relating moments to curvatures.

2.2.5. Symmetric Laminates

A laminate is called symmetric when for each layer on one side of a reference plane (middle surface) there is a corresponding layer at an equal distance from the reference plane on the other side with identical thickness, orientation, and properties. The laminate is symmetric in both geometry and material properties.

For symmetric laminate coupling stiffness is equal to zero ($[B]$ =0). This means that bending-stretching coupling will not be present in such laminates. Consequently, in plane loads will not generate bending and twisting curvatures that cause out-of-plane warping, and bending or twisting moments will not produce on extension of the middle surface.

The load-deformation relations in this case reduce to:

$$\begin{Bmatrix} N_x \\ N_y \\ N_{xy} \end{Bmatrix} = \begin{bmatrix} A_{11} & A_{12} & A_{16} \\ A_{12} & A_{22} & A_{26} \\ A_{16} & A_{26} & A_{66} \end{bmatrix} \begin{Bmatrix} {\varepsilon_x}^0 \\ {\varepsilon_y}^0 \\ {\gamma_{xy}}^0 \end{Bmatrix} \tag{2.24a}$$

$$\begin{Bmatrix} M_x \\ M_y \\ M_{xy} \end{Bmatrix} = \begin{bmatrix} B_{11} & B_{12} & B_{16} \\ B_{12} & B_{22} & B_{26} \\ B_{16} & B_{26} & B_{66} \end{bmatrix} \begin{Bmatrix} {\varepsilon_x}^0 \\ {\varepsilon_y}^0 \\ {\gamma_{xy}}^0 \end{Bmatrix} \tag{2.24b}$$

2.3. Damage and failure for fiber-reinforced composites

Damage in fiber-reinforced composite material is characterized by the degradation of material stiffness. Many such materials exhibit elastic-brittle behavior; that is, damage in these materials is initiated without significant plastic deformation. Consequently, plasticity can be neglected when modeling behavior of such materials.

Failure analysis of laminated composites is usually based on the stresses in each lamina [11]. To date various theories based on the normal and shear strengths of lamina have been developed. The stresses acting on the lamina are resolved into the normal and shear stresses in the local axes. Among all the failure criteria for composite materials, Tsai-Wu, Chang-Chang and Hashin are the most widely used criteria's.

2.3.1. Damage initiation for fiber-reinforced composites

Damage initiation refers to onset of degradation at a material point. In Abaqus the damage initiation criteria for fiber-reinforced composites are based on Hashin's theory (failure criteria). When the Hashine's failure criterion was satisfied at a material point, it is assumed that damage rather than failure initiates at that point of a composite laminate. These criteria consider four different damage initiation mechanisms such as; fiber tension, fiber compression, matrix tension and matrix compression.

The initiation criteria have the following general forms:

Fiber tension ($\hat{\sigma}_{11} \geq 0$):

$$F^t_f = \left(\frac{\hat{\sigma}_{11}}{X^T}\right)^2 + \alpha \left(\frac{\hat{\tau}_{12}}{S^L}\right)^2 \tag{2.25a}$$

Fiber compression ($\hat{\sigma}_{11} < 0$):

$$F^{c}_{f} = \left(\frac{\hat{\sigma}_{11}}{X^{C}}\right)^{2} \quad (2.25\ b)$$

Matrix tension ($\hat{\sigma}_{22} \geq 0$):

$$F^{t}_{m} = \left(\frac{\hat{\sigma}_{22}}{Y^{T}}\right)^{2} + \left(\frac{\hat{\tau}_{12}}{S^{L}}\right)^{2} \quad (2.25\ c)$$

Matrix compression ($\hat{\sigma}_{22} < 0$):

$$F^{c}_{m} = \left(\frac{\hat{\sigma}_{22}}{2S^{T}}\right)^{2} + \left[\left(\frac{Y^{C}}{2S^{T}}\right)^{2} - 1\right]\frac{\hat{\sigma}_{22}}{Y^{C}} + \left(\frac{\hat{\tau}_{12}}{S^{L}}\right)^{2} \quad (2.25\ d)$$

Where:

X^{T}: Longitudinal tensile strength;

X^{C}: Longitudinal compressive strength;

Y^{T}: Transverse tensile strength;

Y^{C} : Transverse compressive strength;

S^{L} : Longitudinal shear strength;

S^{T} : Transverse shear strength;

α : Is a coefficient that determines the contribution of the shear stress to the fiber tensile initiation criterion; and $\hat{\sigma}_{11}$, $\hat{\sigma}_{22}$, $\hat{\tau}_{12}$, are components of the effective stress tensor, $\hat{\sigma}$, that is used to evaluate the initiation criteria and which is computed from:

$$\hat{\sigma} = M\sigma, \quad (2.26)$$

Where σ the true stress and M is is the damage operator:

$$M = \begin{bmatrix} \frac{1}{(1-d_f)} & 0 & 0 \\ 0 & \frac{1}{(1-d_m)} & 0 \\ 0 & 0 & \frac{1}{(1-d_s)} \end{bmatrix} \quad (2.27)$$

d_f, d_m and d_s are internal (damage) variables that characterize fiber, matrix, and shear damage, which are derived from damage variables, d^{t}_{f} , d^{c}_{f} , d^{t}_{m} , and d^{c}_{m}, corresponding to the four modes previously discussed as follows:

$$d_f = \begin{cases} d^{t}_{f}, if\ \hat{\sigma}_{11} \geq 0 \\ d^{c}_{f},\ if\ \hat{\sigma}_{11} < 0 \end{cases} \quad (2.28\ a)$$

$$d_f = \begin{cases} d^{t}_{m}, if\ \hat{\sigma}_{22} \geq 0 \\ d^{c}_{m},\ if\ \hat{\sigma}_{22} < 0 \end{cases} \quad (2.28\ b)$$

$$d_s = 1 - (1 - d^{t}_{f})(1 - d^{c}_{f})(1 - d^{t}_{m})(1 - d^{c}_{m}) \quad (2.28\ c)$$

Prior to any damage initiation and evolution the damage operator, M, is equal to the identity matrix, So $\hat{\sigma}$ = . Once damage initiation and evolution has occurred for at least one mode, the damage operator becomes significant in the criteria for damage initiation of other modes.

The initiation criteria presented above can be specialized to obtain the model proposed in Hashin and Rotem (1973) by setting α=0.0 and $S^T = \frac{Y^C}{2}$ or the model proposed in Hashin (1980) by setting α=1.

CHAPTER THREE

EXPERIMENTAL DETERMINATION OF COMPOSITE MATERIAL PROPERTIES

3.1. Introduction

In this chapter, the manufacturing process of the sisal fiber reinforced epoxy resin composite material has been presented starting from the extraction of the sisal fiber, and also their material property was fully characterized experimentally in order to prepare complete set of input data for FEM analysis. The static experimental procedure for measuring the stiffness and strength of the unidirectional laminate under compression, tension, and in-plane shear loading conditions and its results with discussion are then presented.

3.2. Material and Method

3.2.1. Materials

For this study the materials such as sisal fiber and epoxy resin with hardener are utilized in order to manufacture the composite material specimen. Also sodium hydroxide (NaOH) and distilled water was used in order to treat the sisal fiber to improve the interfacial adhesive property. The sisal fiber was extracted from sisal plants that coming from Derban Town and the epoxy resin with its hardener was obtained from Dejen Aviation (DAVI), Debreziet, Ethiopia, and also the NaOH and distilled water was obtained from local market in Addis Ababa.

3.2.1.1. Sisal fiber

Extraction process of sisal fiber

Sisal fibers can be extracted from the sisal plants through different techniques such as by mechanical means (a process known as decortication) and hand/manual extraction process. In a decortication process, the leaves are crushed and beaten by a rotating wheel set with blunt knives, so that only fiber remains. However, in this study the sisal fiber was extracted using hand extraction technique/manual extraction techniques due to the unavailability of the decortication machine.

In general the extraction process of the sisal fiber from sisal plants was concisely summarized as below:

All lower leaves, standing at an angle of more than 45 degrees to the vertical, are cut away from the bole of the plants with a sharp flexible knife.

Then the leaves are trimmed in a longitudinal direction in to different strips for ease of fiber extraction.

The peeling part is clamped between the wood table and knife. Then it hand-pilled gently through in longitudinal direction in order to remove the resinous materials as shown in below figure 3.1. Then the extracted fiber washed gently with pure water in order to loosen, and separate the fiber until individual fibers are obtained. Then the extracted fibers are then dried over the sun for three days.

3.2.1.2. Sodium hydroxide treatment

Alkali treatment or mercerization using sodium hydroxide (NaOH) is the most commonly used treatment for bleaching and cleaning the surface of the natural fibers to maximize the efficiency of the fiber as reinforcement.

Sodium hydroxide (NaOH) is a highly caustic metallic base and alkali salt. Pure sodium hydroxide is a whitish solid, which is available in pellets, flakes, granules, and as a 50% saturated solution [17]. Sodium hydroxide is soluble in water, ethanol and methanol. This alkali is deliquescent and readily absorbs moisture and carbon dioxide in air.

After drying of the extracted sisal fiber, the chemical treatment process was proceeded using NaOH. For this study 500 gm of NaOH in pellets form was used that purchased from local suppliers with the Brand name of RANKEM and code of S0290 to perform a chemical treatment of sisal fiber.

3.2.1.3. Epoxy resin with hardener

A. Epoxy resin

Low cost composites are successfully fabricated by reinforcing the natural fiber with the many thermoset hydrophobic matrixes like polyester, phenolic, epoxies and others. The role of matrix in the composite is to transfer the stress in to the fiber, prevent the fiber-fiber interaction, keeps the position of the fiber intact in the composite to form a stable structure, prevent the fiber from the abrasions.

Figure 3.1. Manual extraction process of sisal fiber.

a. *Sisal plants*
b. *Longitudinally trimmed sisal plant*
c. *peeling of sisal plant for sisal fiber extraction*
d. *Extracted sisal fiber before washing with water and drying*
e. *Extracted sisal fiber in drying process after washing.*

Figure 3.2 Extracted and dried sisal fiber

Epoxy is the most commonly used resin in polymer matrix composites. It is one of the advanced thermosetting resin types which do not give off reaction products when they cure and so have low shrinkage. It also has good adhesion to other materials, good chemical and environmental resistance, good chemical properties and insulating properties [17].

Epoxy resins has a superior advantages over the other resin types; such as:

- Curing convenience (0-180 °*c* temperature range curing)
- Low shrinkage during cure.
- Diverse form.
- Strong adhesive properties (the ability to bond to the reinforcement or core).
- Good mechanical properties (particularly strength and stiffness).
- Superior dimensional and chemical stability.
- Improved resistance to fatigue and micro cracking.
- Reduced degradation from water ingress (diminution of properties due to water penetration).
- Increased resistance to osmosis (surface degradation due to water permeability).

Due to this advantageous properties, the epoxy resin with a brand name of EPOXY MAS RESIN was used in this study, which is manufactured by fiber Glass development Corporation Company

B. Hardener (catalyst)

Epoxy resin is cured by adding a catalyst, which causes a chemical reaction without changing its own composition. This catalyst initiate the chemical reaction of the epoxy resin and monomer ingredient from liquid to a solid state.

The curing agent uses in this study for the liquid Epoxy resin is the hardener that manufactured by fiber Glast development Corporation Company with a brand name of HARDNER MAS with the ratio of 2:1 for epoxy and hardener respectively as recommended.

3.2.2. Preparation of the composite testing specimens

In this study before the reinforcement of the sisal fiber with the mixture of the epoxy resin and harder, the sisal fibers was chemically treated in order to improve its adhesion properties. After that using the rule of mixture the fiber and matrix mass fraction was determined. Then finally the unidirectional sisal/epoxy composite was fabricated using hand layup vacuum assisted techniques.

3.2.2.1. Alkali Treatment of sisal fiber

Natural fibers are hydrophilic in nature so as sisal fibers, as they are derived from lignocelluloses, which contains strongly polarized hydroxyl groups. The surface of the sisal fiber is coated with waxy substances and having lower surface tension. The major limitations of using these fibers as reinforcements in polymer matrices include poor interfacial adhesion between polar-hydrophilic fiber and non-polar hydrophobic matrix that lead to the poor wetting of fiber with the matrix and lower bond strength. This in turn led to the composites with weak interface. The bond strength can be improved by following operations [32]:

a) Dissolving the fatty substances and the layer of cuticle from the fiber.
b) Making the fiber hydrophobic by reacting with some reagents.
c) Increasing the compatibility of the fiber with the resin by grafting it with some suitable polymers.
d) Removal of trap air from the resin-fibre mixture by degassing it before cure.

So in order to enhance the compatibility and bond strength of the fiber with its matrix, surface modification of the fiber is essential [32]. Surface modifications include:

- Chemical modifications.
- Physical treatments, like the use of microwave or any other high energy radiation.

Among various chemical treatment, alkali treatment or mercerization using sodium hydroxide (NaOH) is an old and commercially bleaching and cleaning the surface of the sisal fibers to produce high-quality fibers. The alkali treatment can cause an increase of the fiber surface free energy. Moreover the alkali treatment can make the fiber surface become 'clean' due to the removal of waxes, hemicellulose, pectin and parts of lignin. The removal of this substance enhances the surface adhesion properties and roughness of the sisal fiber.

In general, removal of these fatty like components from sisal fiber leads the fibers to:

- Improve an adhesive properties for fibre–matrix interface;
- Improve fiber's shear strength;
- Improve fiber's rigidity and stiffness;
- Improve moisture absorption problems;
- Reduce fiber's weight; etc.

However when the percentage of NaOH is increased it affect the fibers properties by reduce the bonding capacity during preparation of the composites. Based on several literatures, the medium percentage of NaOH (i.e. 8%) was used for this work. In general, for this study 500gm of NaOH pellet was mixed with 6.25 liter of distilled water at ambient temperature. The sisal fiber then dipped in the solution for four hour. Then it washed several time with distilled water in order to neutralize it. Lastly, the fibers were allowed to dry in sun light for at least 3 day as shown in figure 3.3.

In this process the solution of the sisal fiber and NaOH must kept under the vacuum, since NaOH can react with air, as a result that can absorb moisture. This cause to increase the water content in the solution. Due to this as shown in below figure 3.3 (b), the bucket was covered with plastic sheet in order to create the vacuum inside the bath.

Figure 3.3. Alkaline treatment of sisal fiber.

a. *Equipment needed for alkali treatment processes(including safety equipment)*
b. *Sisal fiber soaked by NaOH*
c. *Sisal fiber after soaked by NaOH*
d. *Sisal fiber washed by distilled water several time after soaking.*

3.2.2.2. Fiber and matrix mass fraction content of the composites

i. Fibre and matrix mass fraction (M_F, M_M)

Total mass of composite = mass of fiber + mass of matrix

$$M_c = M_f + M_m \quad (3.1)$$

$$\text{Fiber mass fraction} = \frac{\text{mass of fiber}}{\text{total mass}}$$

$$M_F = \frac{M_f}{M_f + M_m} \quad (3.2)$$

$$\text{Matrix mass fraction} = \frac{\text{mass of matrix}}{\text{total mass}}$$

$$M_M = \frac{M_m}{M_f + M_m} \quad (3.3)$$

And;

$$M_F + M_M = 1 \quad (3.4)$$

ii. Fiber and matrix volume fraction (V_F , V_M)

$$\text{Volume of fiber} = \frac{\text{mass of fiber}}{\text{density of fiber}}$$

$$V_f = \frac{M_f}{\rho_f} \quad (3.5)$$

$$\text{Volume of matrix} = \frac{\text{mass of matrix}}{\text{density of matrix}}$$

$$V_m = \frac{M_m}{\rho_m} \quad (3.6)$$

$$V_c = V_m + V_c \quad (3.7)$$

$$\text{Fiber volume fraction} = \frac{\text{volume of fiber}}{\text{total volume}}$$

$$V_F = \frac{V_f}{V_f + V_m} \quad (3.8)$$

$$\text{Matrix volume fraction} = \frac{\text{volume of matrix}}{\text{total volume}}$$

$$V_M = \frac{V_m}{V_f + V_m} \quad (3.9)$$

Let ρ_f and ρ_m are density of fiber and matrix respectively. Then we have:

$$V_F = \frac{M_f + \rho_m}{M_f x \rho_m + M_m \, x \rho_f} \tag{3.10}$$

Similarly:

$$V_M = \frac{M_m + \rho_f}{M_f x \rho_m + M_m \, x \rho_f} \tag{3.11}$$

i. density of ply (ρ):

$$\rho = \frac{Total\ mass}{total\ volume} = \frac{mass\ of\ fiber}{total\ volume} + \frac{mass\ of\ matrix}{total\ volume}$$

$$\rho = \frac{volume\ of\ fiber}{total\ volume}\ \rho_f + \frac{volume\ of\ matrix}{total\ volume}\rho_m$$

$$\rho = \rho_f \text{ x } V_F + \rho_m \text{ x } V_M \tag{3.12}$$

ii. Ply thickness , h

The thickness of plies is simply the number of grams of mass of fibers (W_f) per unit area.

Total volume = h x1(m^2)

$$h = \frac{\text{total volume}}{1(m^2)}$$

$$h = \frac{M_f}{V_F \text{ x } \rho_f} \tag{3.13}$$

In terms of mass of fraction of fibers, thickness expressed as :

$$h = M_f \left[\frac{1}{\rho_f} + \frac{1}{\rho_m}\left(\frac{1 - M_F}{W_F}\right)\right] \tag{3.14}$$

Where:

h : Lamina(ply) thickness (mm)

V_m : Volume of matrix (cm^3)

ρ_f : Density of fiber (gm/cm^3)

M_M :Matrix mass fraction

ρ_m : Density of matrix (gm/cm^3)

M_F : Fiber mass fraction

V_F : Fiber volume fraction

M_f : Mass of fiber(gm)

V_M : Matrix volume fraction M_m : Mass of matrix(gm)

V_f : Volume of fiber (cm^3) M_c : Mass of composite (gm)

A. Calculation to find the unidirectional longitudinal tensile specimen properties

Several literatures [28, 32, 37,54,55,56, & etc], are used 30-50% volume fraction of natural fibers in their researches. In this study the average 40% volume fraction sisal fibers and 60% of the matrix are used.

Volume of the moulds = 280 x 150 x3 = 126,000mm^3=126cm^3.

From the literature the density of the sisal fibre and epoxy resin is 1.33 g/cm^3 and 1.2 g/cm^3 respectively.

Density of the composites:

$\rho_c = \rho_f V_f + \rho_m V_m$

ρ_c = (1.33 g/cm^3. x 0.4) + (1.2 g/cm^3. x 0.6) = 0.532 g/cm^3. + 0.72 g/cm^3. = 1.252g/cm^3

Mass of the composites:

$m_c = \rho_c$ x V_c = 1.252g/cm^3.x 126cm^3 = 157.752gms

Mass of the matrix:

m_m= 0.6 x 157.752gms = 94.6512 gms.

Mass of the fiber:

m_f= 0.4 x 157.752gms = 63.1008 gms

Volume of the fiber:

$$V_f = \frac{M_f}{\rho_f} = \frac{63.1008}{1.33} = 47.444 cm^3$$

Volume of the matrix:

$$V_m = \frac{M_m}{\rho_m} = \frac{94.6512 \text{ gms}}{1.2} = 78.876 \text{ cm}^3 ,$$

And the other testing specimen calculation was calculated in similar manner and the final calculated results was presented in below table 3.1. Also the thickness of the lamina(h) was calculated using equation 3.13:

$$h=\frac{M_f}{V_F x \rho_f}=\frac{289.28\ gms}{0.4\ x\ 1.33\ gm/cm3}\approx 0.54mm$$

	90 degree tensile	***0 degree compression***	***90 degree compression***	***In plane shear***
Volume of the composite	205 x 230 x 3 =141.45 cm^3	185 x 115 x 3 = 63.825 cm^3	185 x 230 x 3 =127.650 cm^3	280 x 150 x3 = 126cm^3.
Mass of the composite	177.1 gms	77.91 gms	159.8178 gms	157.752gms
Mass of the fiber	70.84 gms	31.964 gms	60.72712 gms	63.1008 gms
Mass of the matrix	106.26 gms	47.946 gms	95.89 gms	94.6512 gms
Volume of the matrix	88.55 cm^3	39.955 cm^3	79.91 cm^3	78.876 cm^3
Volume of the fiber	53.26 cm^3	24,033 cm^3	48.066 cm^3	47.444cm^3

Table 3.1. Testing specimen different fraction calculated results.

3.2.2.3.Composite fabrication process

In the mechanical property characterization process, it was crucial to keep the fibers alignments at desired direction and well in place. However due to the natural properties of the sisal fiber, its alignment at desired direction is difficult. Due to this, dimensioned metallic frame was used in study in order to keep the fiber alignments properly as shown in figure 3.4. Then the composite laminate was fabricated by using hand layup insisted vacuum bagging produces by removing the frame from the unidirectional sisal fibers.

Figure 3.4. Unidirectional sisal fiber with frame

Vacuum bagging Assisted Hand Lay-up technique (VBAHT)

Hand lay-up is one of the oldest and the least capitally intensive composite manufacturing techniques. A one-sided mold in the final shape of the part is constructed with the desired surface finish. The mold surface is treated with mold release compounds consisting of wax and/or other chemical compositions. Epoxy resin and hardener mixture are impregnated by hand into the fibres. This is usually accomplished by rollers or brushes, with an increasing use of nip-roller type impregnators for forcing resin into the fabrics by means of rotating rollers and a bath of resin. Then the laminates are left to cure under standard atmospheric conditions. Advantages of hand lay-up are the relatively lower mold costs and strength requirements, the tools required for production are readily available, the molds are easy to maintain and the part's lay-up can usually be changed without altering the mold. However, the disadvantages are many. Hand lay-up is a manual process, and therefore results are very subject to the user that is doing the work. Since the fibers have the superior mechanical properties, it is often desirable to control and typically maximize the fiber volume percent, which is relatively difficult with hand lay-up [41]. However by using the vacuum bagging, this hand lay-up techniques was greatly improved.

Vacuum bagging Assisted Hand Lay-up technique (VBAHT) is basically an extension of the hand lay-up process described above where pressure is applied to the laminate once laid-up during its curing cycle in order to improve its consolidation .This is achieved by sealing a plastic film over the wet laid-up laminate and onto the tool. The air under the vacuum bag is extracted by a vacuum pump and thus up to one atmosphere of pressure can be applied to the laminate to consolidate it.
The main goal of VBAHT is to produce a homogeneous laminated composite by:

- Removes the trapped air between laminate layers.
- Compacts the fibre layers for more efficient force-transmission amongst fibre bundles
- Prevents shifting of fibre orientation throughout the curing process.
- Reduces humidity.

So, if the VBAHT procedure is properly used as shown in figure 3.5 and the universally, there is no any doubt about the homogeneity of fabricated laminate.

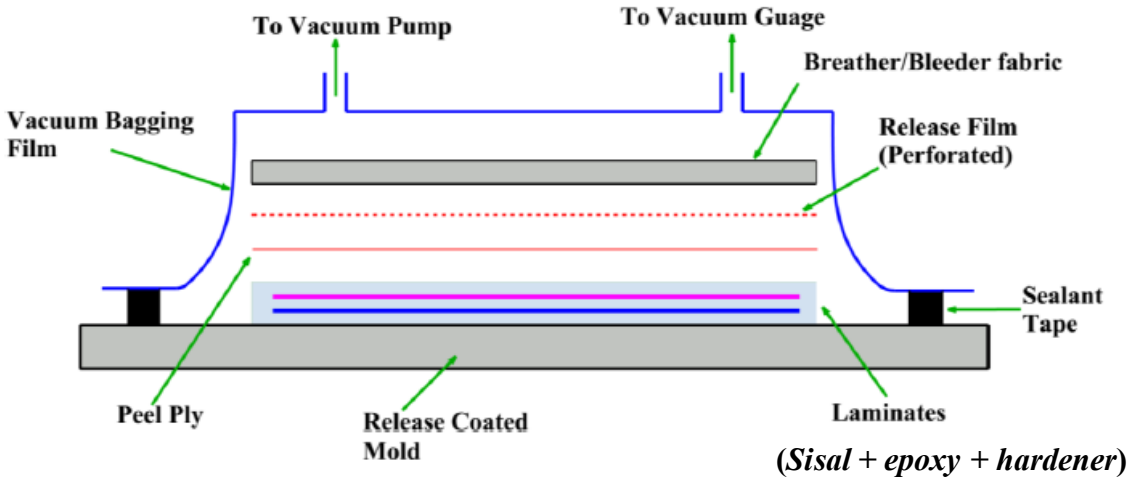

Figure 3.5. Hand Lay-up Assisted by Vacuum bagging technique.

The epoxy resin and hardener mixture was impregnated with the unidirectional sisal fiber in order to give consolidated composites that has light, stiff & strong properties, as the flow chart of this process is depicted in figure 3.6.

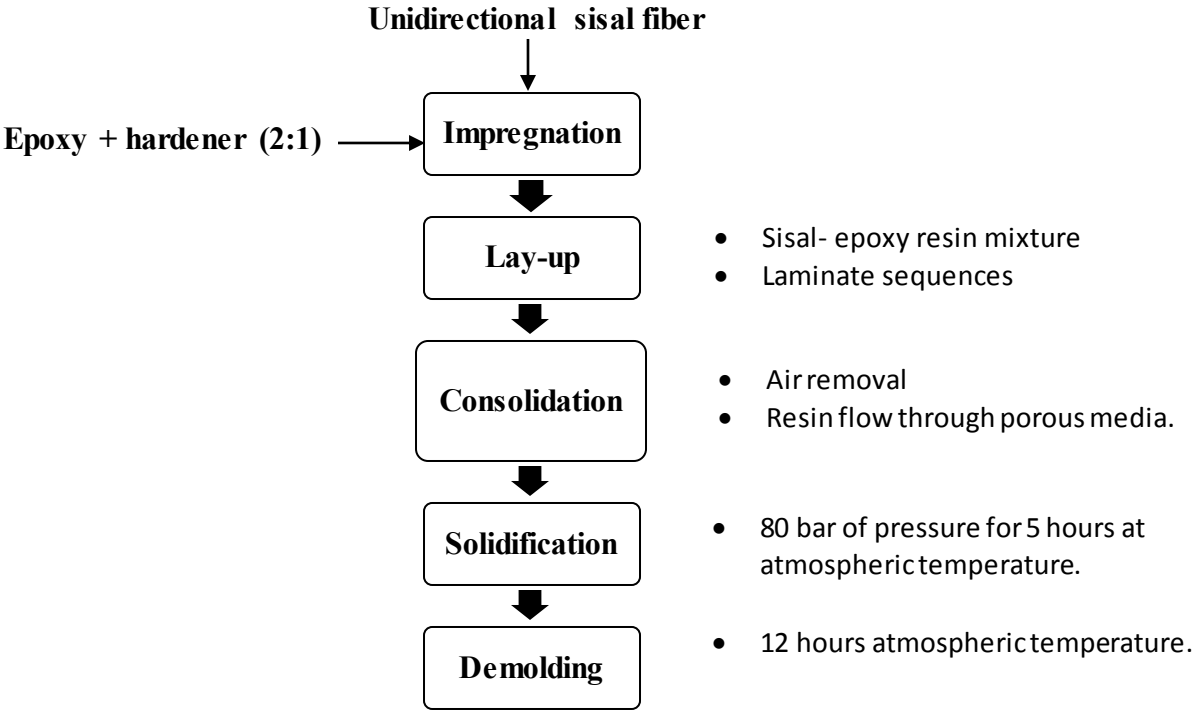

Figure 3.6. Fabrication process flowchart of laminated composite using VBAHT.

The full Composite fabrication by vacuum bagging system was shown in below figure 3.8. As shown in figure 3.8 (a) the hand lay-up process was first used manually in the impregnation process. Also as shown in part (b) the different vacuum bagging equipment was used for composite manufacturing process.

In general the VBAHT process that shown in figure 3.8 was concisely summarized as below:

First the mould was cleaned gently three times by using mould release agent such as wax in order to preventing the epoxy- hardener mixture from sticking to the mold when laminating a parts and then sealed it by using vacuum tape before the vacuum process is under taken.

Then the unidirectional sisal fibers is placed in the mould and impregnated it with epoxy resin and hardener mixture by using hand layup process. After the end of full hand lay-up processes, the dimensioned release peel ply, release film, breather fabric and vacuum bagging film are orderly placed over the composite layups as shown in figure 3.5 and figure 3.8. Then the vacuum pumps and reservoir is connected with the vacuum hose and T-shaped vacuum ports. After that the vacuum bagging film is attached with the mold by using vacuum tape in order to create the vacuum inside the mould area. Then finally by opening the vacuum bagging switch, the process is started and check there is no partial air draw from the vacuum bagging film. If the air is draw from the vacuum bagging film, the process is stop and fix the problem immediately and then start switch again.

3.2.2.3.1. Main Vacuum Bagging Equipment

1. Vacuum pump

Vacuum pump is the hearts of a VBAHT system. Vacuum pumps are designated by their vacuum pressure potential or "Hg maximum", their displacement in cubic feet per minute (CFM) and the horsepower required to drive the pump.

The pump used for this work is taken from Dejen Aviation, Unmanned Air Vehicle department which has the following specification:

Type: rotary

Model No: 2TW-4C

Capacity: 8cfm

Vacuum: 6.7×10^{2}Pa

Power: 220-240v/50Hz

Figure 3.7. Vacuum pump.

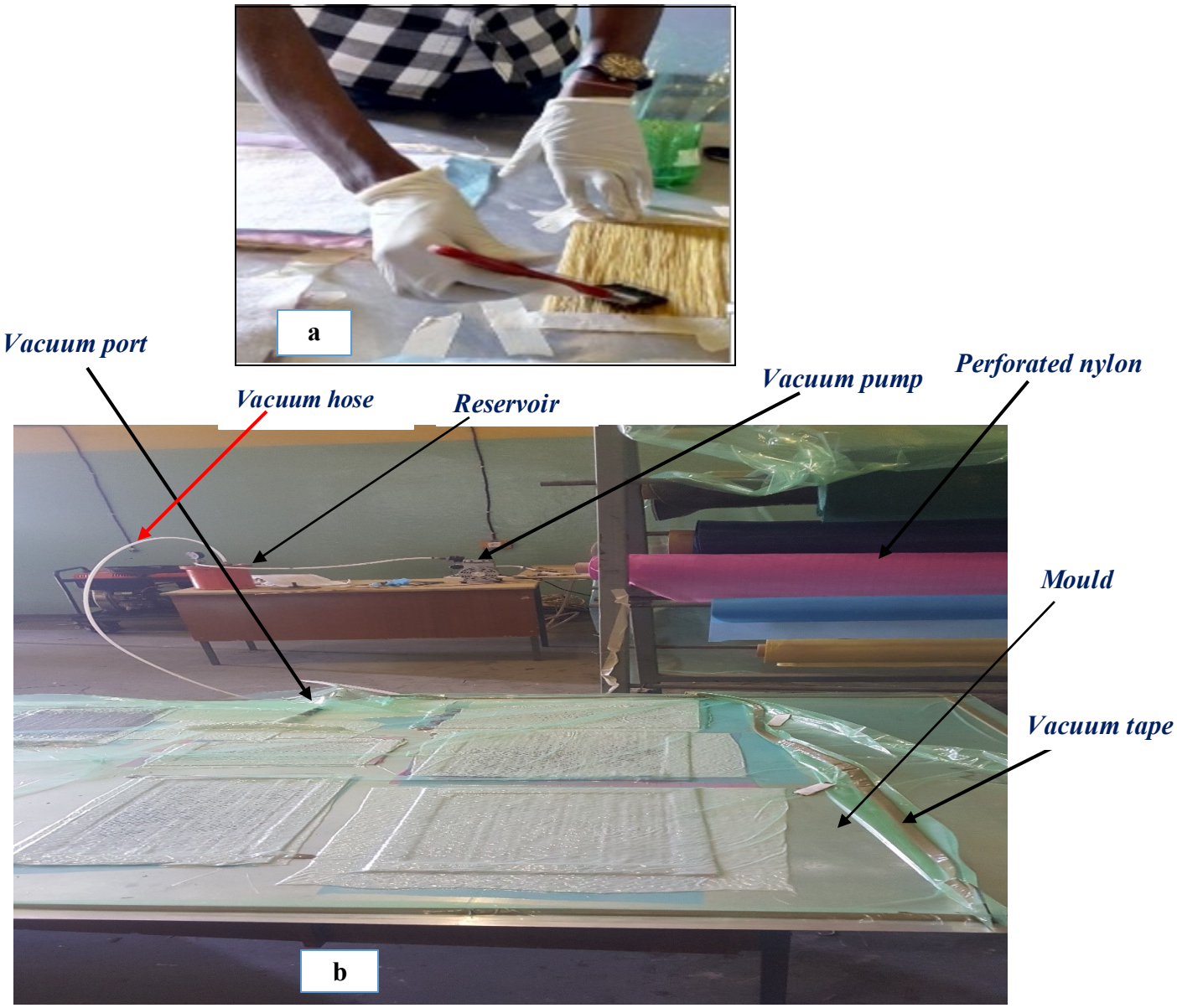

Figure 3.8. Composite fabrication process using VBAHT.

A. Impregnation & hand lay-up process.

B. Vacuum bagging process.

2. Release Fabric

Commonly known as peel plies, they are placed against the laminate to provide a moulded surface suitable for secondary bonding or painting. After peeling off from the laminate the fabric leaves an impression of its weave pattern. They can be applied dry or impregnated with the same resin as

the laminate. Dry peel ply bleeds out a controlled amount of resin from the laminate without bonding to it. Impregnated peel ply does not bleed any resin from the laminate stack, which is particularly useful when processing thin laminates using zero bleed resin systems.

3. Breather

Non-woven polyester bleeder or breather fabrics are used to allow the free passage of air across the bag face of a laminate while under vacuum or autoclave pressure. This allows air and volatiles to be pulled from the laminate and an even pressure applied to it. The secondary use of these fabrics is the absorption of any excess resin which is bled from the laminate during cure.

4. Vacuum nylon

These materials are used to form the vacuum bag. The film is sealed to the edge of the mould with vacuum bag sealant tape. Vacuum bags must be completely airtight to ensure no leaks occur at full vacuum during the final cure. The most commonly used material is nylon film due to its excellent physical properties. As well as being extremely tough, it has good flexibility and high elongation. Special additives allow it to be used at high temperatures and make it the most cost effective material available.

5. Sealant Tape (mastic sealant)

Also known as "tacky tape", it is used to provide an airtight seal between the tool / master model and bagging film. The tape must have sufficient tack to adhere well to the mould surface but not so much tack that the bag cannot be stripped away from the tape for re-positioning during lay-up. The tape must also strip cleanly from the mould surface after the cure cycle has been completed.

6. Mold Release

It is commonly used in vacuum bagging process in order to prevent the epoxy and hardener mixture from stacking to the mould when laminating the composite parts. Generally there are three types of mould release used in the industry depending on the mold material and desired characteristic of the finished part. The most common type is carnauba based paste wax. This is usually put on it up to 5 composite layers for new moulds and at least one layer before each new part is moulded.

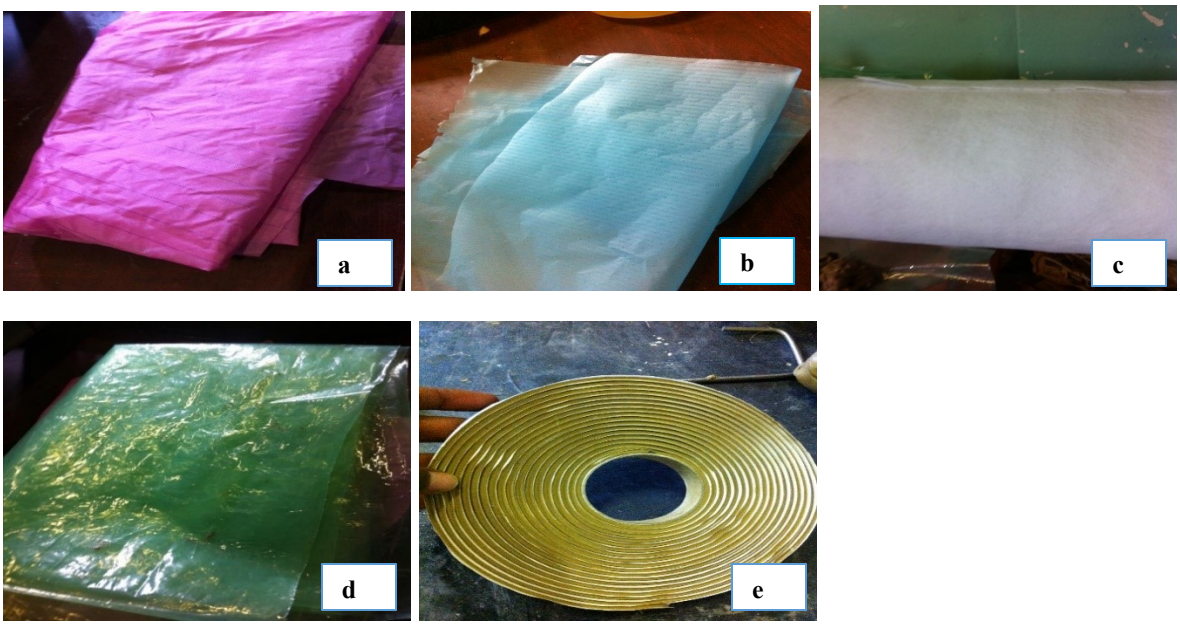

*Figure 3.9 vacuum bagging system materials - **(a)**. Release fabric/peel ply **(b)**. Perforated nylon **(c)**. Breather **(d)**. Vacuum nylon **(e)**. Mastic sealant.*

3.2.3. Dimension of Test specimens

As shown in figure 3.10; all the testing specimen for compression (longitudinal and transverse), tensile (longitudinal and transverse) and in plane shear testing composite specimen is prepared based on ASTM D3410 , ASTM D 3039, and ASTM D 3518, standards respectively [43,44,45].

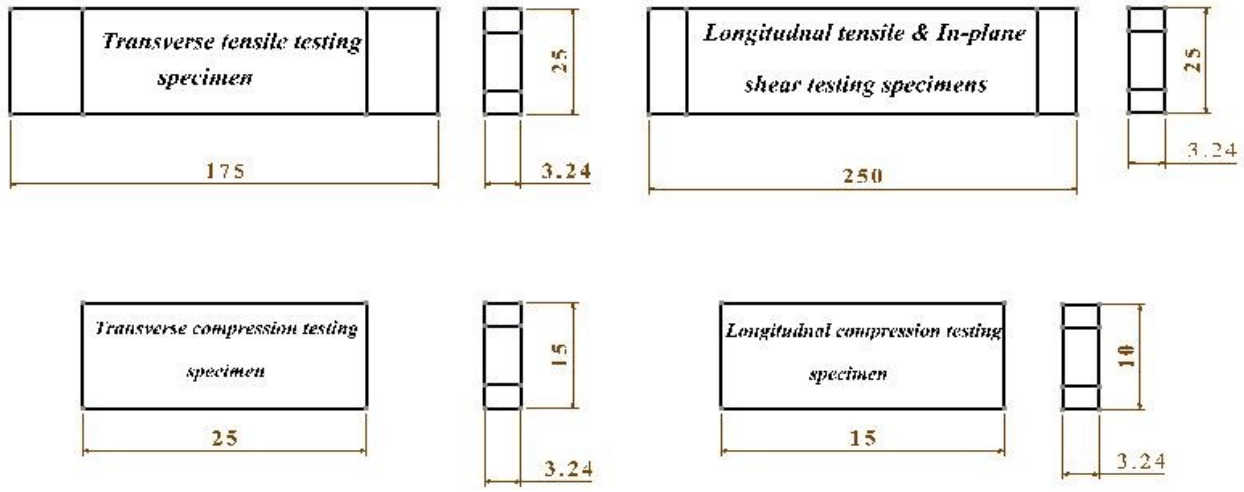

Figure 3.10. Testing specimens dimension in millimeter.

3.2.4. Testing Procedure

After manufacturing of the laminated composite materials, the specimen was cut in to smaller piece of testing specimen using Band saw machine that found in AAiT mechanical work shop based on their respective ASTM standards. The Band saw machine has a cutting speed of 500-1000 mm/min, with blade length 2560 mm. For this study generally 30 different testing specimens was used for all different tests.

Universal testing machine (UTM)

Universal testing machine is basically used to test the tensile, compression and shear stress, and strength of the different materials. For this study all the material properties testes was done in AAiT Mechanical engineering workshop by using Computer Controlled Electro-Hydraulic Servo Universal Testing Machine model: WAW-600; which has a capacity of up to 600 kN, with 0.01 - 500 mm /min test speed. Also a computer is connected to the testing machine for data acquisition, and displacement (mm) and loads (N) are monitored for this static experiments.

Figure 3.11. Universal testing machine (AAiT workshop).

Generally the required sisal fibre reinforced epoxy resin composite material properties are characterized under three primary loading modes such as the tension, compression and in-plane shear modes.

3.2.4.1.Determination of the Tensile Properties of Unidirectional composite

The sisal/epoxy laminate tensile properties such as the longitudinal young's modulus (E_1), the transverse young's modulus (E_2), the longitudinal ultimate tensile strength (X_t)and the transverse ultimate tensile strength (Y_t)are measured by static tension testing of longitudinal $[0^0]_6$and transverse $[90^0]_6$ unidirectional testing specimens according to ASTMD 3039/D 3039M testing procedures.

The tensile testing specimen is placed under the universal testing machine and pulled at a cross-head speed of 0.5 mm/min. The specimens are loaded step by step up to failure under this uni-axial tensile loading. A continuous record of load and deflection is obtained by a digital data acquisition system. Also the typical the stress-strain curve for under both tensile loading was obtained from the testing machine.

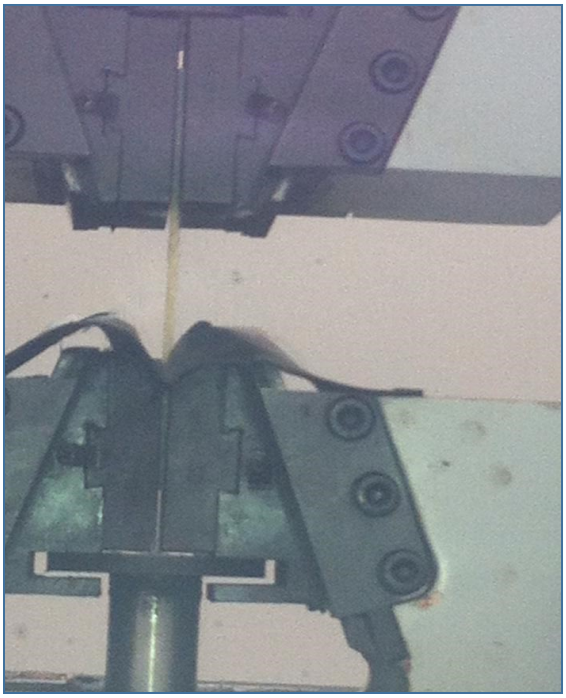

Figure 3.12. Typical tensile specimen under tensile test.

The value of stress (σ), E_1 , E_2 , F^{1tu} and F^{2tu} are determined from the tensile testing data using the following formula:

$$X_t = \frac{P^{1max}}{A_1} \qquad \sigma_i = \frac{P_i}{A}$$

$$Y_t = \frac{P^{2max}}{A_2} \qquad \varepsilon_i = \frac{\Delta L}{L_0} \tag{3.15}$$

Where:

X_t, Y_t= ultimate longitudinal and transvers tensile strength, Mpa

P^{1max}= maximum load before failure for longitudinal tensile testing specimen, N

P^{2max}= maximum load before failure for transverse tensile testing specimen, N

A_1, A_2= w x h = the perpendicular cross sectional area of the longitudinal and transverse testing specimen respectively, mm^2

σ_i= tensile stress at i^{th} data point, Mpa

ε_i= tensile strain at i^{th} data point.

P_i= load at i^{th} data point, N

ΔL= change in gage length (L-L_0), mm

L_0 = original gage length of the specimen, mm

The Major Young's modulus ($E_{1)}$ and minor young's modulus (E_2) was determined from the stress-strain graph using the ASTM D3039 standard,

$$E = \frac{\Delta\sigma}{\Delta\varepsilon} \tag{3.16}$$

This formula was applied to two separate data points. These two separate data points were based on the ASTM standard, which stated that the first data point be taken near a strain value of 25% and that the second data point be taken near a value of 50% of the total strain . The main reason for choosing these values is because the specimen should deform in a linear fashion between thes e pairs of data points, and linearity between these points is essential in order to determine an accurate Young's modulus. From these two data points the stress values were taken and the change in stress

over the change in strain was determined and Major Young's Modulus could therefore be calculated.

The major Poisson's ratio (V_{12}) was calculated using below formula based on the micromechanics analysis because of the lack of relevant universal testing machine with the strain gauge.

$$V_{12} = V_f v_f + V_m v_m \tag{3.17}$$

However the determination of the Poisson's ratio of the natural fiber (V_f) was difficult, and different literatures uses different Poisson's ratio of sisal fiber ranging from 0- 0.35 [24]. For this study the average poisonous ratio of 0.175 used and also Poisson's ratio of epoxy resin of 0.4 was used.

$$V_{12} = v_f V_F + v_m V_M = 0.175 * 0.4 + 0.4 * 0.6 = 0.07 + 0.24 = 0.31$$

3.2.4.2. Determination of the Compressive Properties of Unidirectional composite

Compression testing of composites is one of the most difficult types of testing owing to sidewise buckling of the specimen. Many test methods have been developed and used to overcome the buckling problem, incorporating variety of specimen designs and loading fixtures. Due to this, the specimens with a very short but unsupported gage-length is used for this study based on ASTM 3410.

Compressive load is applied to $[0]_6$ and $[90]_6$ sisal/epoxy composite specimens and maximum failure load are recorded to find longitudinal and transverse compression strengths of the laminate respectively.

The stress-strain graph for both longitudinal and transverse testing specimens are plotted and characterized as the same way with tensile testing.

3.2.4.3. Determination of the in plane- Shear Properties of Unidirectional composite

Generally there are different kind of in-plane shear property testing method for unidirectional composites such as rail shear, crossbeam sandwich, thin-walled tube torsion, the Iosipescu shear test and etc. In this study the in-plane shear property test was conducted by using off-axis tensile tests of a ±45° based on ASTM D3518. The main reason for choosing this testing method was due

to its simplicity to perform when compared to the others and also due to the unavailability of the other testing fixture. Such a uniaxial tension test of a $\pm 45^0$ laminate is performed in accordance with Test Method of D3039, although with specific restriction on stacking sequence and thickness. As shown in the ASTM D3518-standards, the specimens for this test was prepared from the $\pm 45^0$ laminate composites such as a balanced lay-up composed only of $+45^0$ plies and -45^0 plies.

Figure 3.13. Typical specimens under transverse and longitudinal compression test.

The maximum in plane shear stress and young's modulus are calculated using the following formulas:

$$\tau_{12}{}^{m} = \frac{P^m}{2A} \tag{3.18}$$

Where:

$\tau_{12}{}^{m}$ = maximum in-plane shear stress, Mpa

P^m = maximum load at or below 5% of shear strain, N

A= cross-sectional area in accordance with Test method D 3039/3039M, mm^2

Also the shear modulus:

$$G_{12} = \frac{\Delta\tau_{12}}{\Delta\gamma_{12}} \tag{3.19}$$

Where:

G_{12}= shear modulus of elasticity, GPa.

$\Delta\tau_{12}$= difference in applied shear stress between two shear strain points.

$\Delta\gamma_{12}$ = difference between the two shear strain points.

3.3. Experimental testing Result and Discussion

3.3.1. Tensile test

By using the data's records from the universal testing machine, the force-displacement, stress-strain curve and the required tensile testing properties were displayed in below figures both for longitudinal and transverse testing specimens.

As shown from figure 3.14- 3.19, the force-displacement and stress-strain behavior for longitudinal and transverse tensile testing specimens was linear and final failure occurs catastrophically. Also from the standard deviation value, it's noticed that the tensile testing graph of the specimens are little different from each other; the main reason includes the mechanical and material factors, specimen preparation and measurement errors [43].

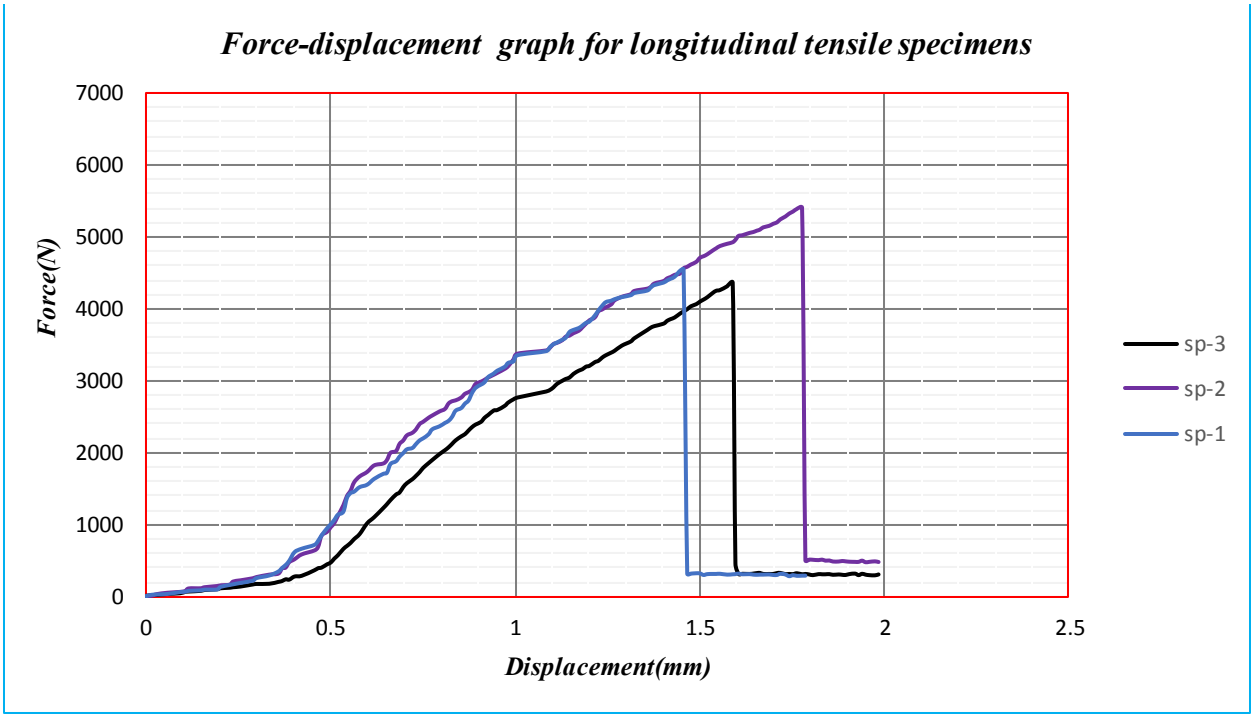

Figure 3.14. Force –displacement graph for longitudinal tensile specimens.

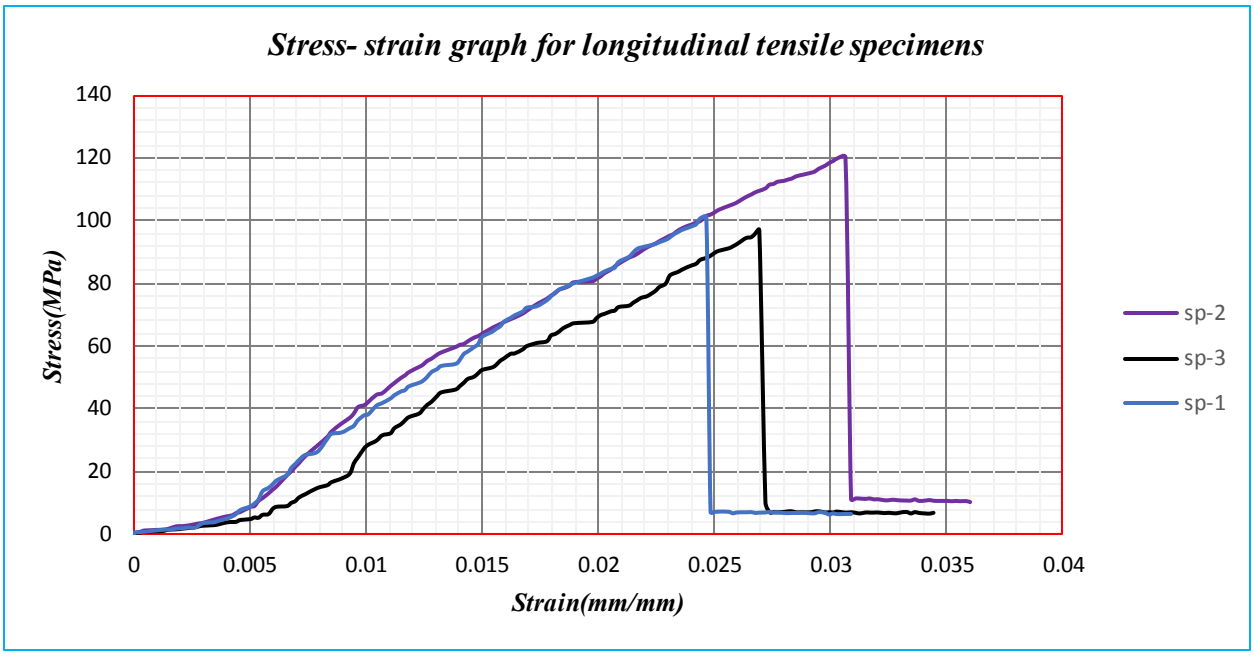

Figure 3.15. Engineering stress-strain graph for longitudinal tensile specimens.

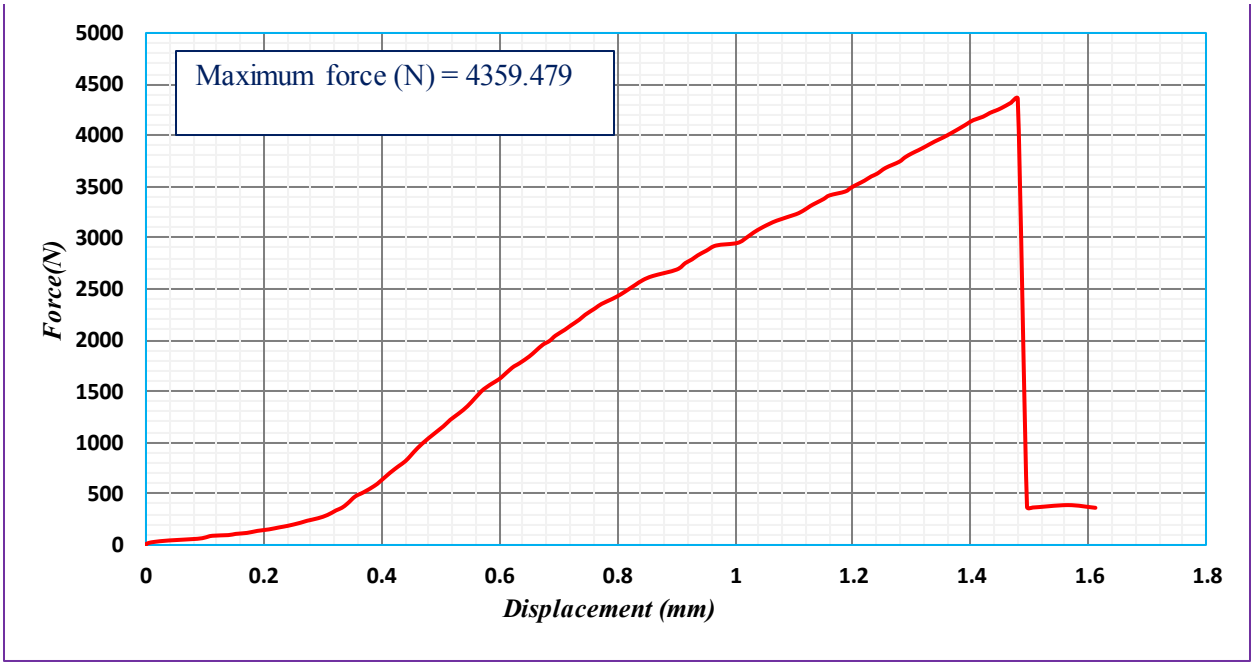

Figure 3.16. Average force-displacement graph of the longitudinal tensile testing specimens.

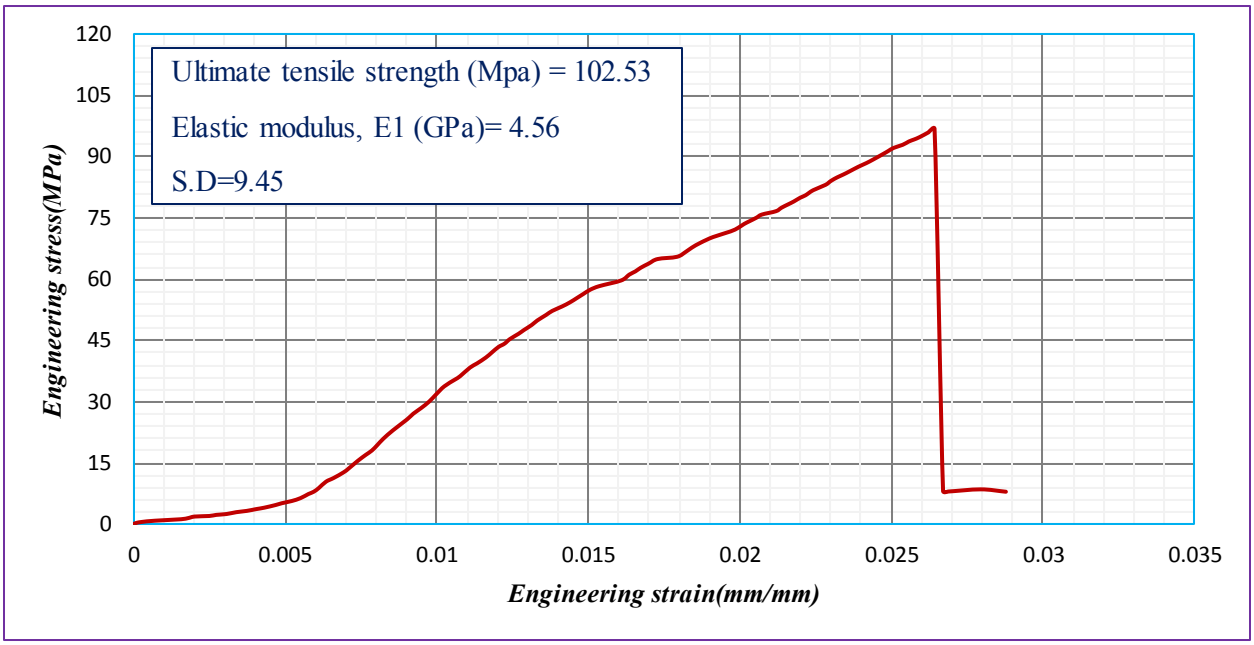

Figure 3.17. Average engineering stress-strain graph for longitudinal tensile testing specimens.

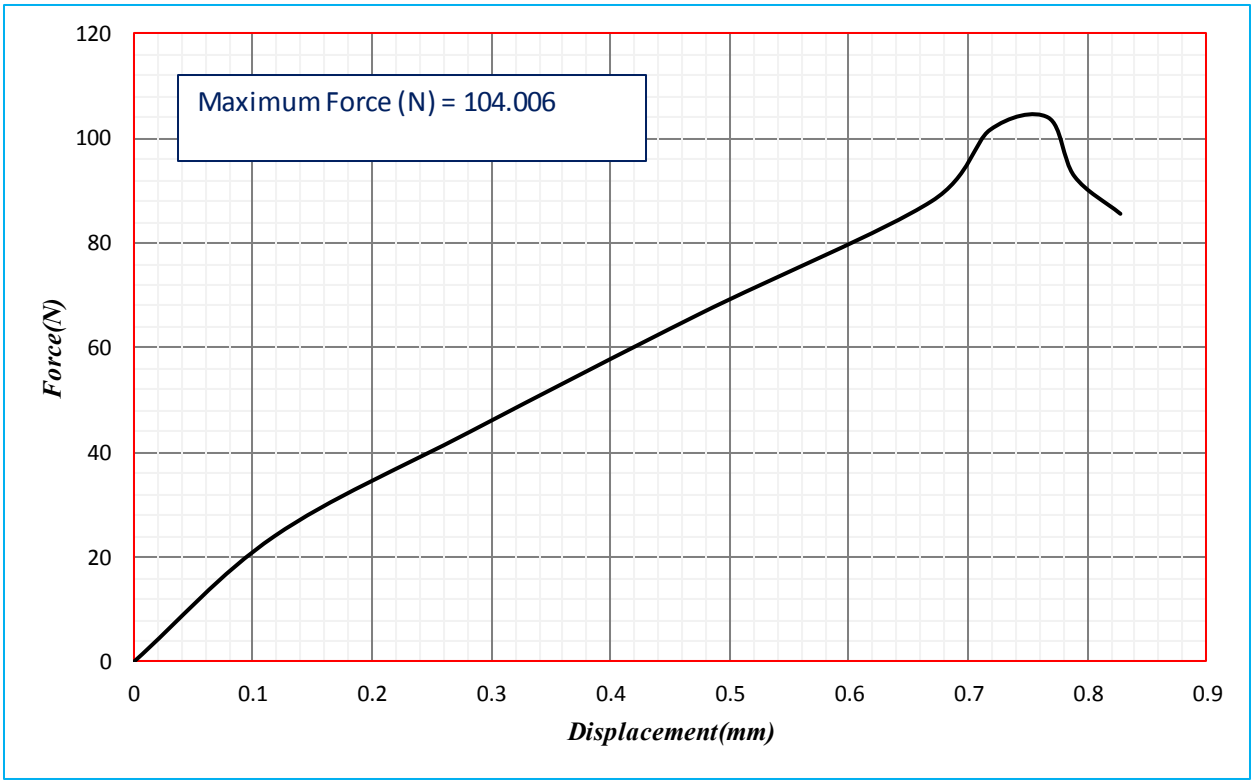

Figure 3.18. Average force-displacement graph of the transverse tensile testing specimens.

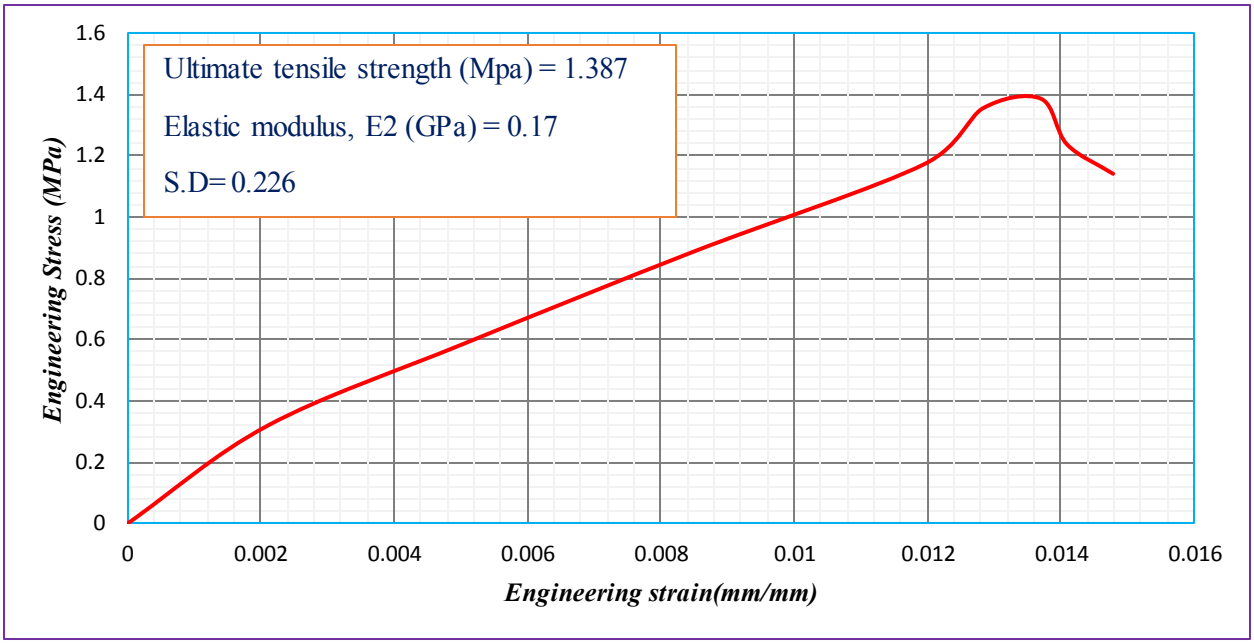

Figure 3.19.Average engineering stress-strain graph of the transverse tensile testing specimens.

3.3.2. Compression test

As shown from figure 3.20- 3.23 of the force-displacement and stress-strain curve of the compression test; the compressive strength is increased with increase the load until it reaches their ultimate compressive strength and then they fail catastrophically.

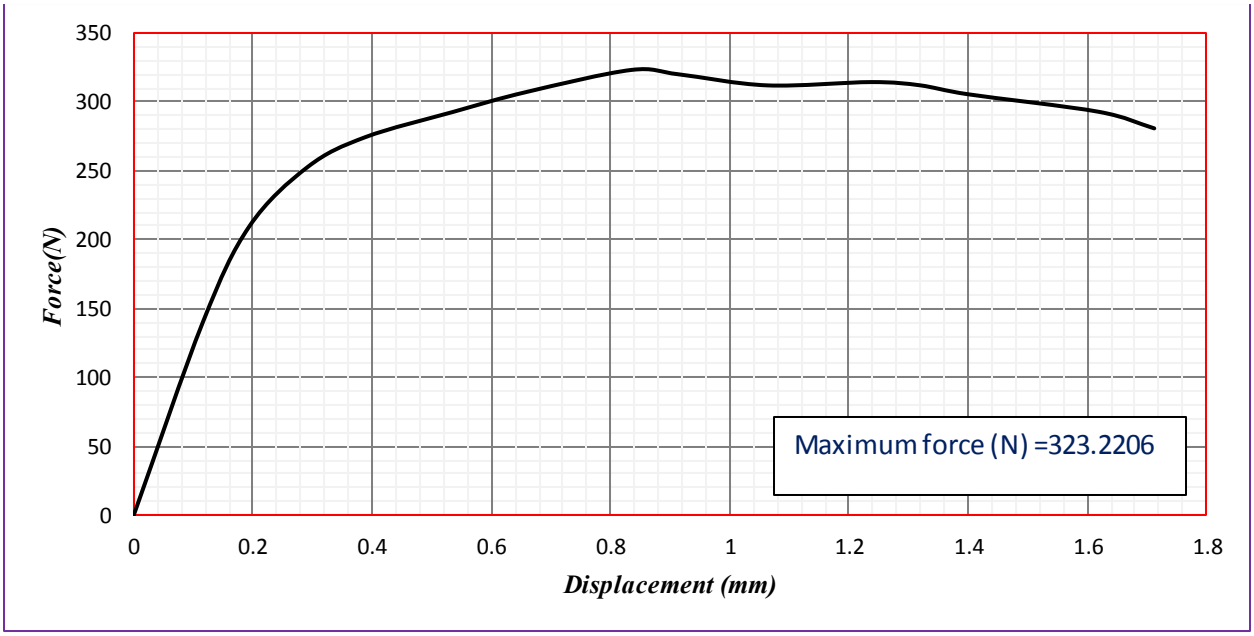

Figure 3.20.Average force- displacement curve for longitudinal compression specimens.

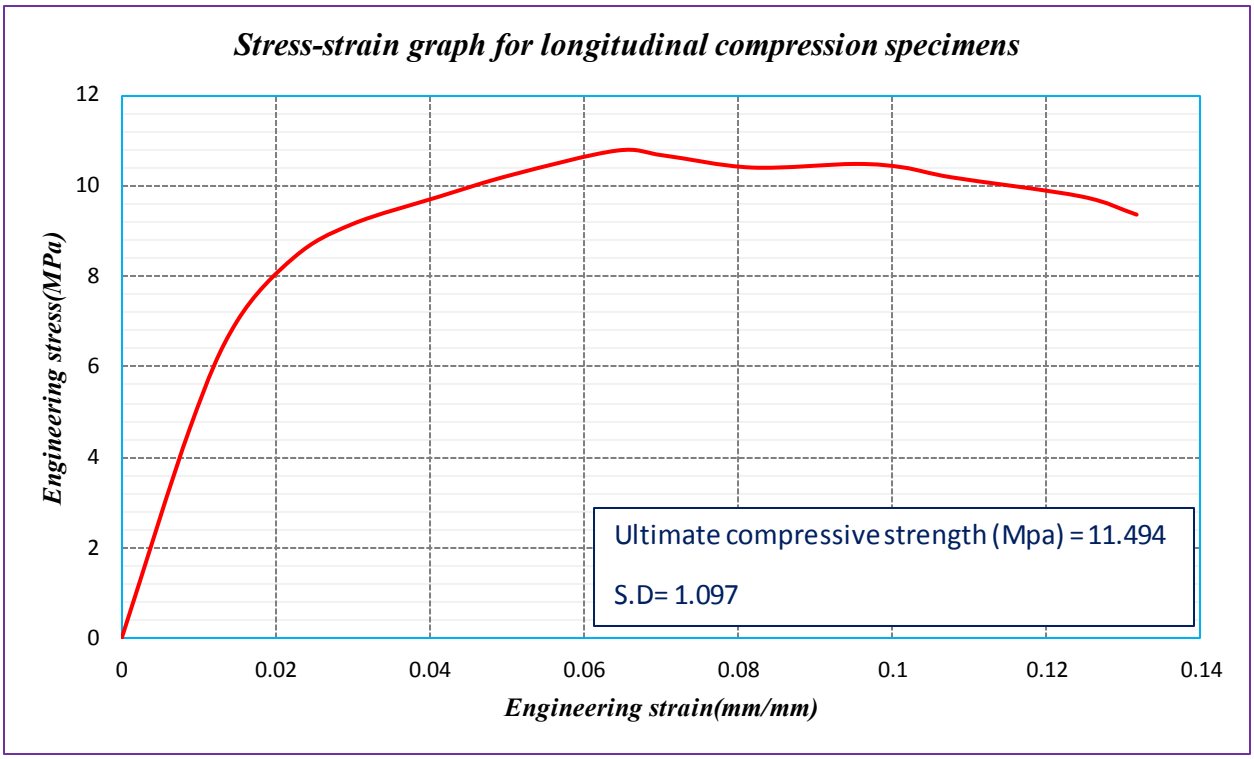

Figure 3.21. Average engineering Stress-strain curve of the longitudinal compression specimens.

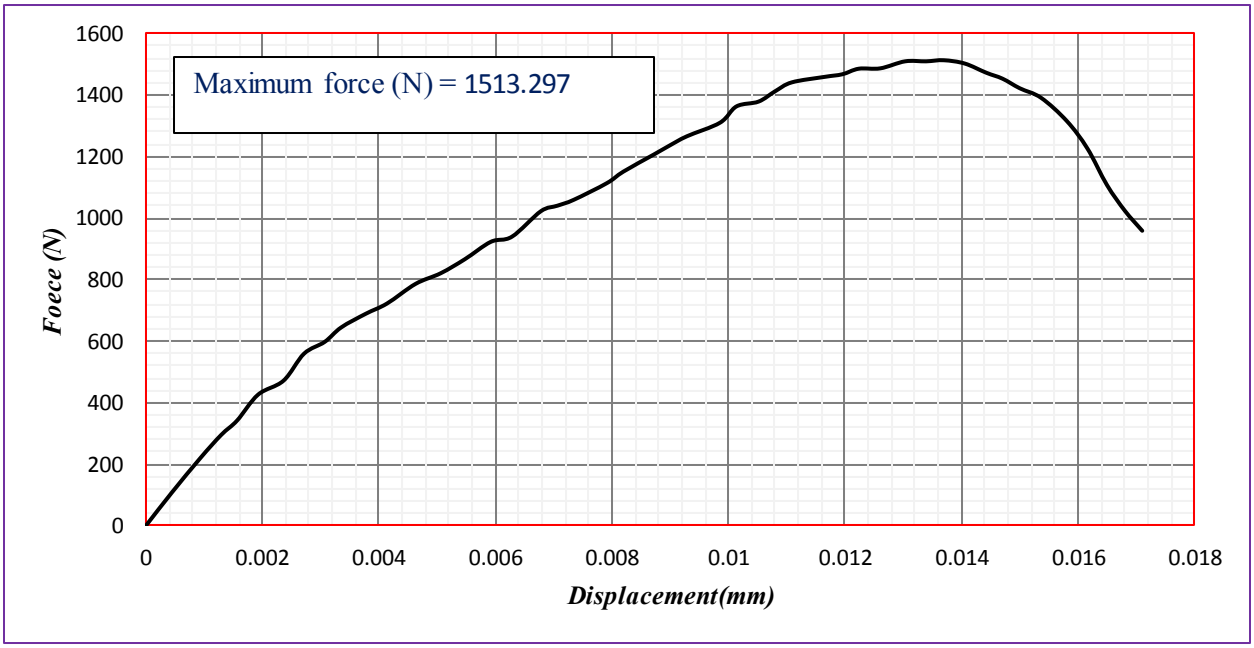

Figure 3.22. Average force-displacement curve of the transverse compression specimens.

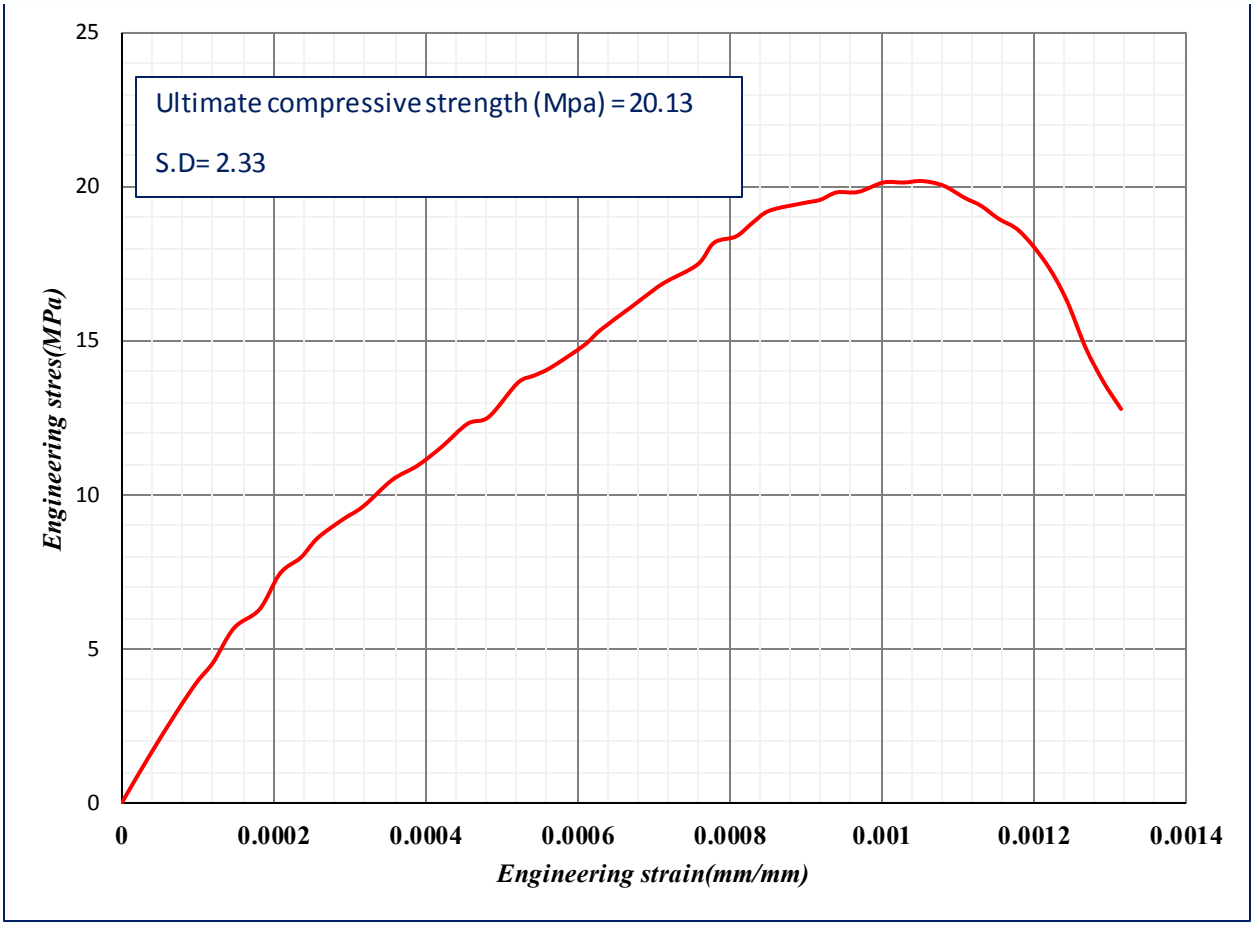

Figure 3.23. Average engineering stress-strain curve for transverse compression specimens.

3.3.3. In-plane shear test

The individual and average force-displacement and stress-strain curve of the different in-plane shear specimens are presented in below figures.

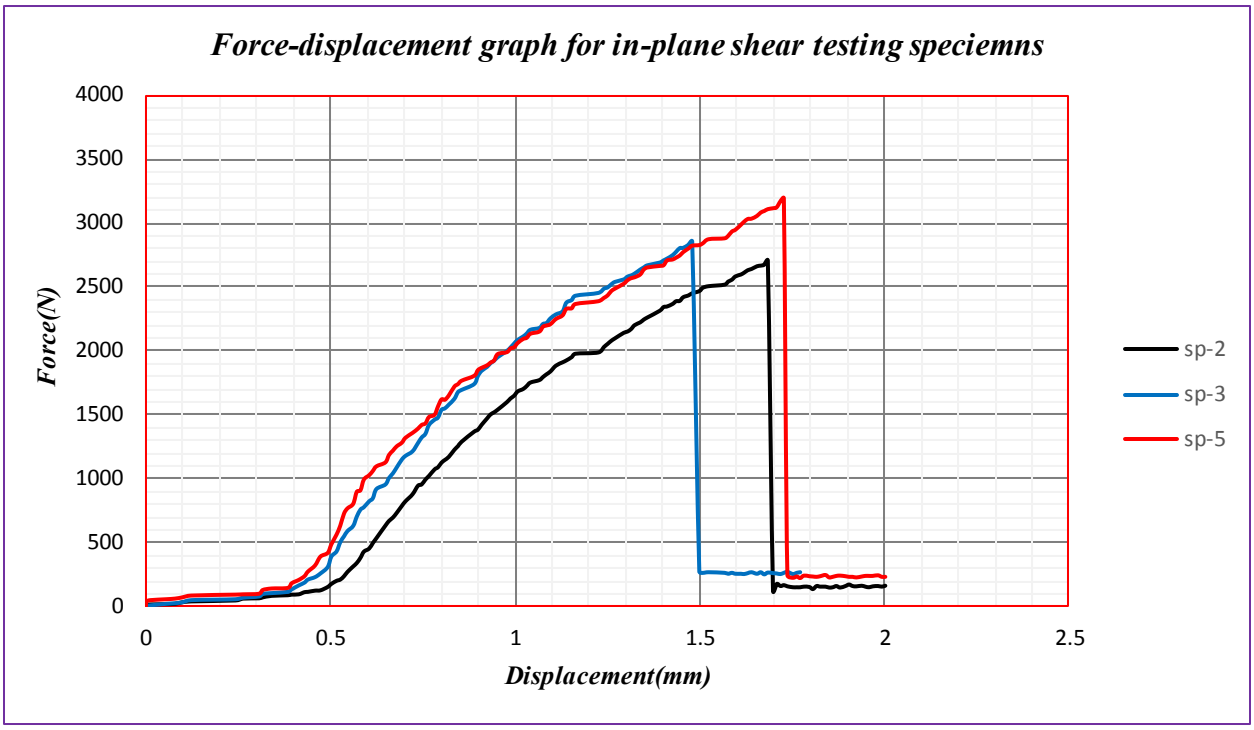

Figure 3.24. Force-displacement graph for in-plane shear testing specimens.

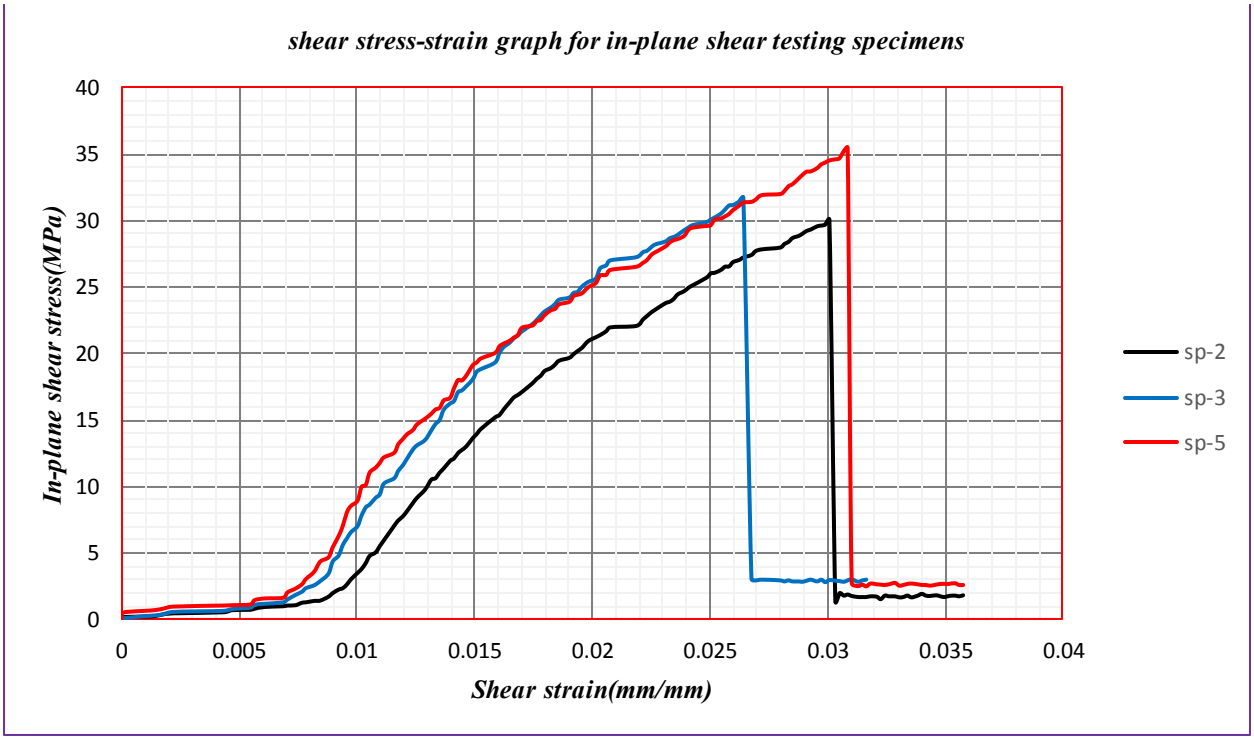

Figure 3.25. In-plane shear stress-strain graph for testing specimens.

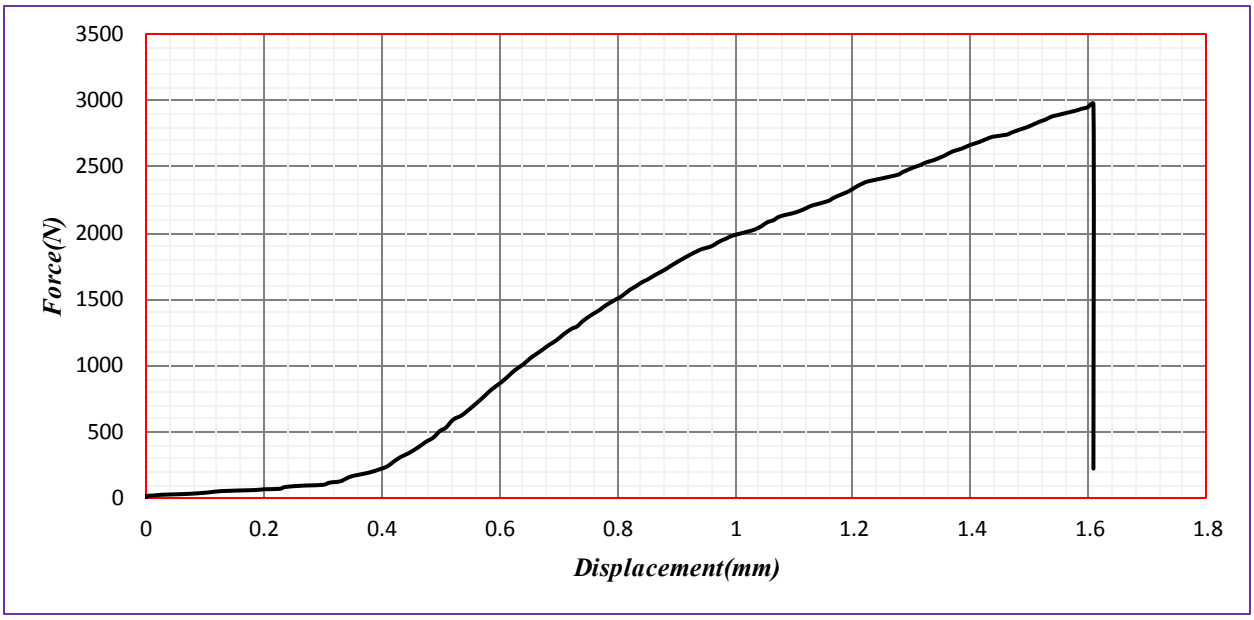

Figure 3.26.Average force-displacement curve of the in plane-shear testing specimens.

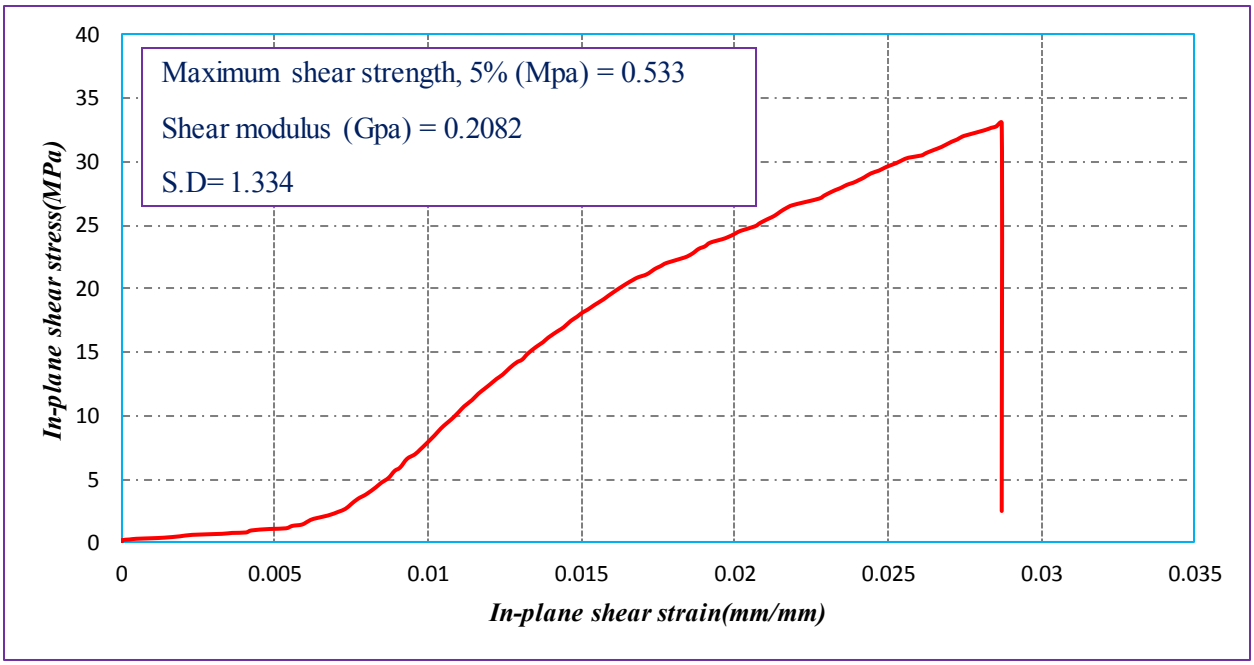

Figure 3.27.Average In-plane shear stress-strain curve of the in plane-shear testing specimens.

Generally from the final material property result, it's observed that the unidirectional sisal fibre reinforced epoxy resin composite material has a good mechanical properties especially in the

longitudinal direction. However, they have low in-plane shear strength. Full mechanical properties comparison are depicted in below two figures.

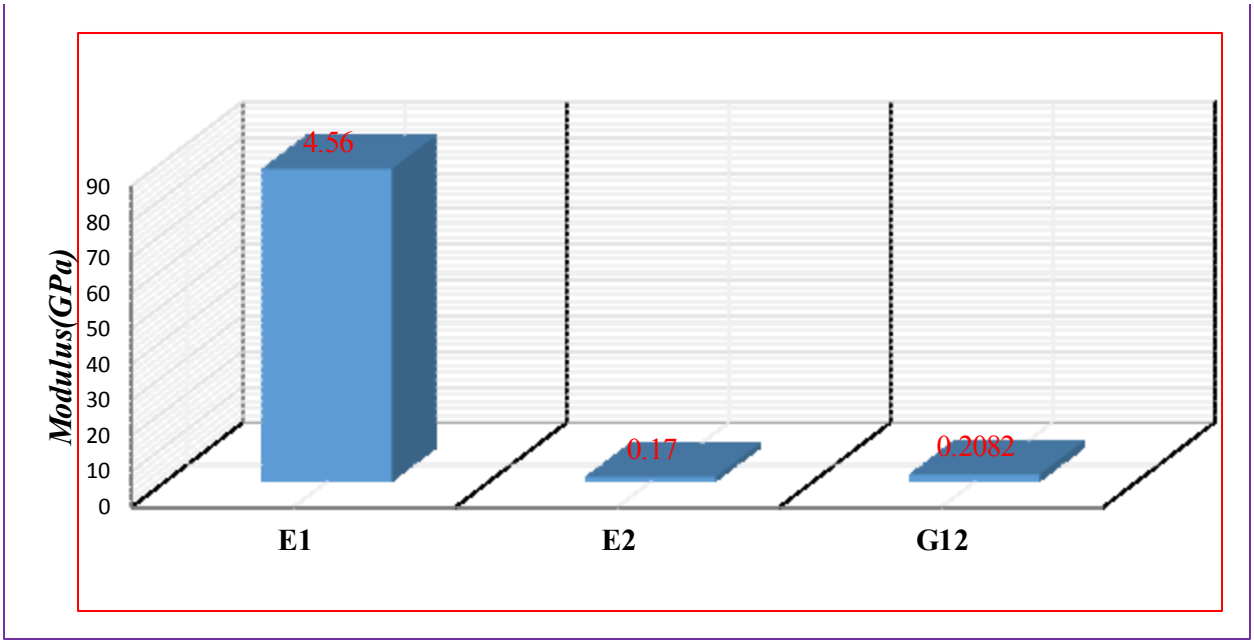

Figure 3.28. Comparisons of the modulus of elasticity for different tests.

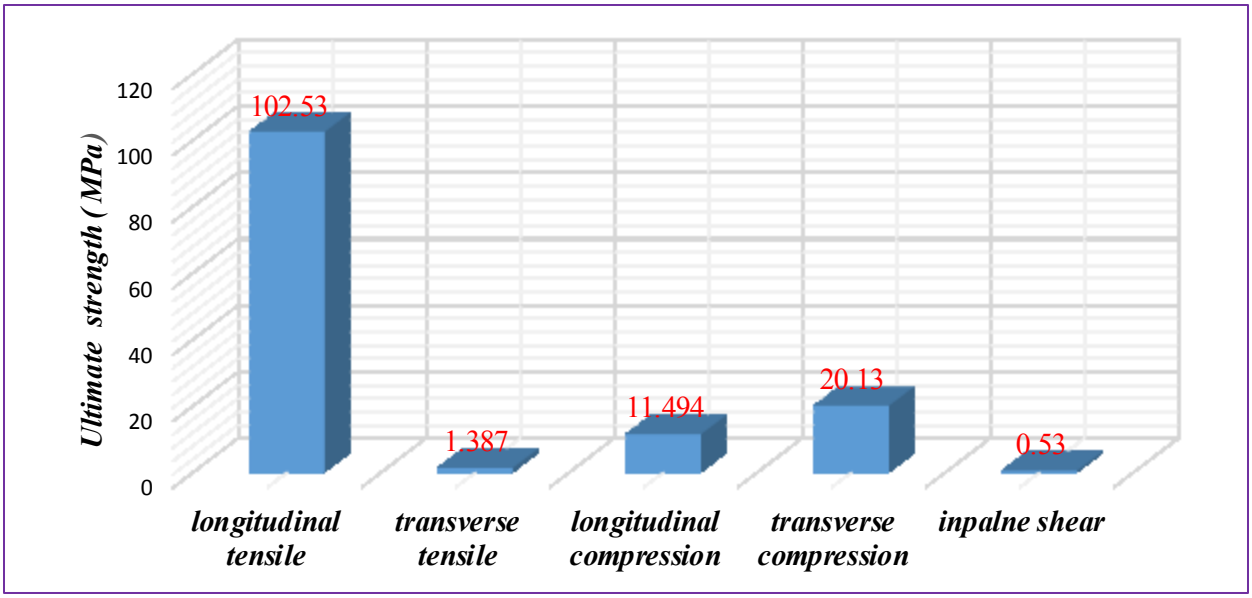

Figure 3.29. Comparisons of the ultimate strength results for different tests.

3.3.4. Failures Modes

The tensile, in-plane shear and compression testing specimens before and after testing are depicted in below figure 3.30 and figure 3.31 respectively.

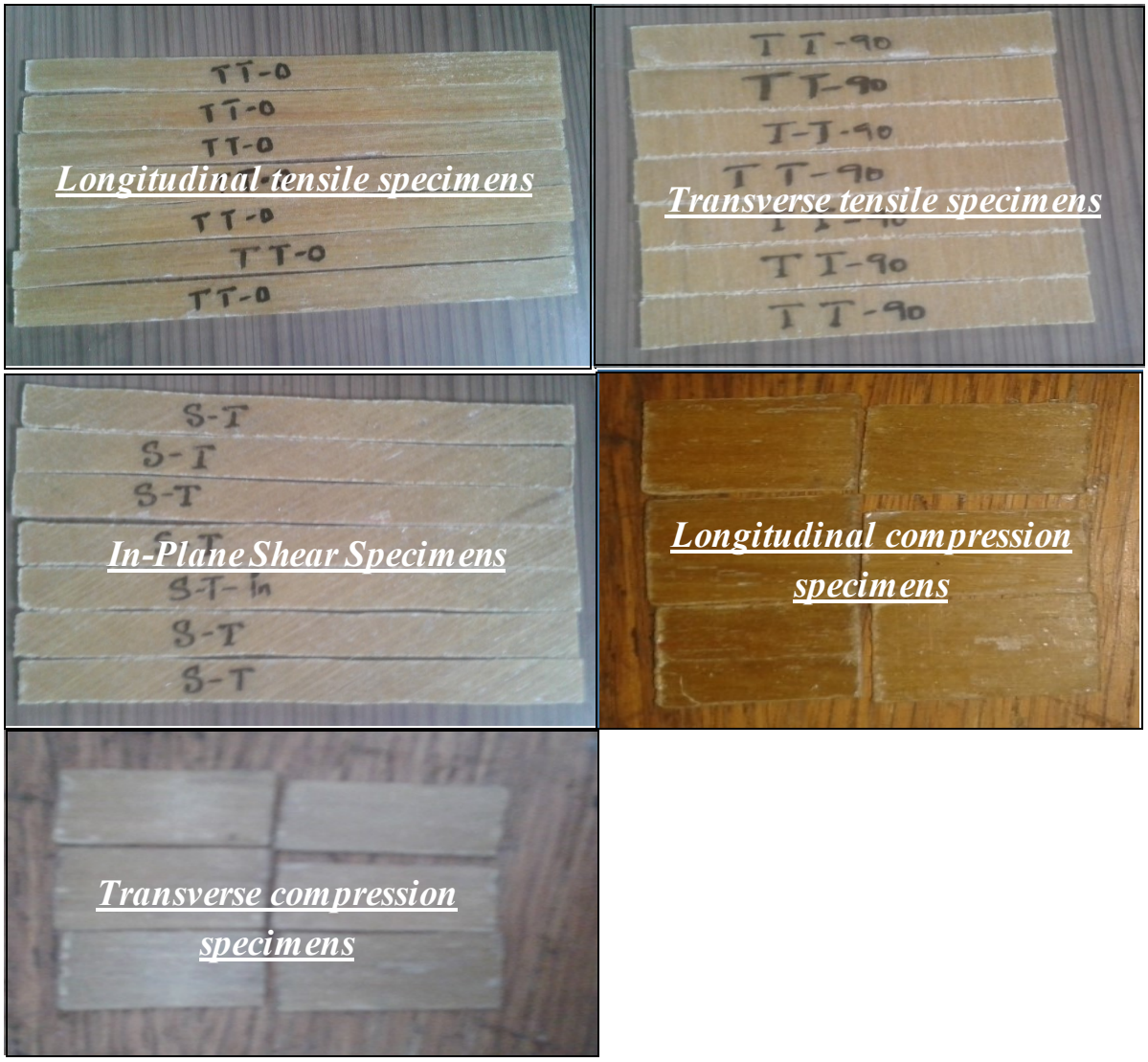

Figure 3.30. Specimens before test.

From below figure 3.31, it's noticed that most of the specimen's failure are occurred at the gauge length sections. Also it observed that some specimens are failed at out of the gauge length such as at grips or at multimode types. However, such testing specimens that failed out of the gauge section was omitted from the data.

Figure 3.31. Specimens after test.

For all testing specimens , it observed that the matrix damage mode is first occurred and then followed by fibres failure through then fracture propagate spontaneously starting from the first layer to the other layers. Also from both the compression final failure test it noticed that the buckling problem is reduced due using the shortened specimen dimension.

Loading conditions	**ASTM standards**	**Mode of failure**
Tensile(Longitudinal, Transverse)	D3039	AGM, AGM(2),LGM
Compression(Longitudinal, Transverse)	D3410	SVG,BGM
In-plane shear	D3518	AGM,LGM

Table 3.2. Mode of failures under different loading conditions.

NB: The term of failure mode code definition is elaborated/presented in appendix –E

3.3.5. Determination of composite material orientation defect (orientation error)

In the mechanical property characterization of the unidirectional composite, the orientation of the composite at required absolute direction is very crucial. However due to the different reasons including the manufacturing process and the property of fiber and matrix, the absolute orientation was deviated at some angle especially for the natural fiber which has very low thickness .Therefore measuring the amount of orientation defect is very important in ordered to assess the reliability of the final mechanical properties of the unidirectional composite materials. However measuring this full orientation defect is a very difficult task especially for the defects which is microscopic in nature without using different advanced technology.

In this work due to the properties of the sisal fiber such as its very low thickness and its high flexibility, and due to the inexperienced manufacturing process such as hand-lay-up process, using vacuum pump and etc., the sisal epoxy lamina (basically the fibers) are disordered at some amount from its absolute direction. Therefore, in order to measure the manufactured composite orientation defect (Macroscopic orientation defect), first the sample specimen was selected randomly from all the fabricated specimen type. Then the deviated angle from the original was marked gently using sharp panicle and ruler which clearly visible to the naked eye. Then using AUTOCAD 2007 software, the marked parts are dimensioned properly as shown in below figure 3.32. Finally by measuring the amount of the angle deviation and the deviated area, the correction factor is calculated as shown in table 3.3 for all testing specimens except the compression test. For both longitudinal and transverse compression specimen due to their small dimension when compared to the other testing specimens, it's assumed that their deviation is negligible when compared to the other.

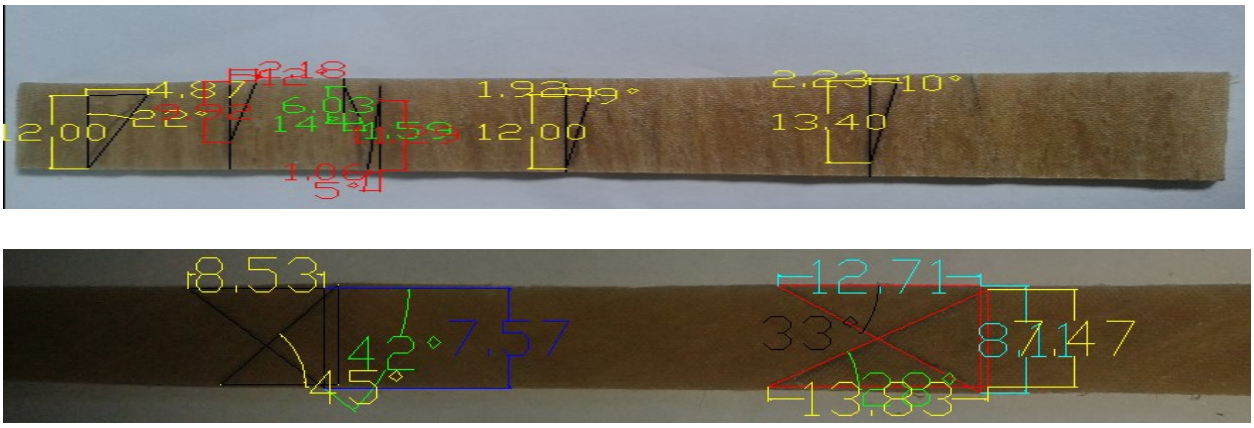

Figure 3.32. A typical sample of dimensioned longitudinal tensile and in-plane shear testing specimens (in mm).

Testing specimens samples	**Disordered total area (%)**	**Deviated angle (degree)**	**Correction factor (%)**
Longitudinal tensile	0.33	13.25	+ 7.36
Transverse tensile	0.172	12.316	+ 6.84
In-plane shear	0.41	5.335	-2.96

Table 3.3. Calculated results of the composite orientation defect.

From the final calculated error(relative error) due to the misalignment of the sisal fiber, the experimental measured results has the + 7.36 %, + 6.84 %, -2.96 % percentage of correction for longitudinal tensile, transverse tensile and in-plane shear specimens results respectively .Therefore the measured results from the experimental tests for all cases should be corrected with this factors as shown in below table.

	Experimental		***Actual(corrected)***	
Testing mode	***Strength(Mpa)***	***Modulus(Gpa)***	***Strength(Mpa)***	***Modulus(Mpa)***
Longitudinal tensile	102.53	4.56	110.076	4.896
Transverse tensile	1.387	0.17	1.482	0.182
In-plane shear	0.53	0.2082	0.514	0.202

Table 3.4. Corrected ultimate strength and modulus results for different testing modes.

3.4. Conclusion

The sisal fiber was extracted manually from the sisal plant that comes from Derban town, and then the alkaline treatment was carried out using 8 % of NaOH in order to improve its interfacial adhesion properties. After that the sisal fiber reinforced epoxy resin composite material was successfully manufactured using Vacuum bagging Assisted Hand Lay-up technique (VBAHT) and mechanical property characterization such as the tensile, compression and in-plane shear test was done on it using universal testing machine.

From the mechanical characterization results, it observed that the treated unidirectional sisal fibre reinforced composite material have a good mechanical performance (modulus of elasticity and strength) basically in the longitudinal direction. However, it has moderate mechanical properties in the transverse direction.

CHAPTER FOUR

FINITE ELEMENT IMPACT SIMULATION USING ABAQUS SOFTWARE

4.1. General description of the Finite element software

4.1.1. Introduction

Abaqus is a suite of powerful engineering simulation programs, based on the finite element method (FEM), which can solve problems ranging from relatively simple linear analysis to the most challenging nonlinear simulations. Abaqus software contains an extensive library of elements that can model virtually any geometry. It has a various list of material models that can simulate the behavior of most typical engineering materials including composites, metals, polymers and reinforced concrete [46].

Abaqus offers a wide range of capabilities for simulation of linear and nonlinear applications. Problems with multiple components are modeled by associating the geometry defining each component with the appropriate material models and specifying component interactions. In a nonlinear analysis, Abaqus automatically chooses appropriate load increments and convergence tolerances and continually adjusts them during the analysis to ensure that an accurate solution is obtained efficiently. A complete Abaqus finite element analysis (FEA) usually consists of three distinct stages: preprocessing, simulation, and post-processing [46, 47].

Generally the majority of authors surveyed previously have used this software at some points in their works especially for low velocity impact problems, and it is a preferred choice for this study due to the comprehensive and intuitive modelling environment featured in the software, and the ability to readily perform dynamic explicit analysis.

4.1.2. Choosing between Abaqus/Explicit and Abaqus/Standard analysis

There are two main analysis procedure for solving structural problems in Abaqus, such as Abaqus/Standard (static implicit and dynamic implicit) and Abaqus/Explicit (includes dynamic Explicit). Also other procedures exist for frequency, thermal, electrical, fluid and etc. analysis.

For many analyses it is clear whether Abaqus/Standard or Abaqus/Explicit should be used. For example, Abaqus/Standard is more efficient for solving smooth nonlinear problems; on the other hand, Abaqus/Explicit is the clear choice for a dynamic (wave propagation) analysis. There are, however, certain static or quasi-static problems that can be simulated well with either program.

Typically, these are problems that are usually solved with Abaqus/Standard, but they may converge with difficulty, because of the contact or material complexities; this results in a large number of iterations. Such analysis are expensive in Abaqus/Standard because the iteration requires a large set of linear equations to be solved.

Whereas Abaqus/Standard must iterate to determine the solution to a nonlinear problem, Abaqus/ Explicit determines the solution without iterating by explicitly advancing the kinematic state from the previous increment. In fact, 'Explicit' stands for explicit time integration. Even though a given analysis may require a large number of time increments using the explicit method, the analysis can be more efficient in Abaqus/Explicit if the same analysis in Abaqus/Standard requires much iteration. Another advantage is that it requires much less disk space and memory than Abaqus/Standard for the same simulation. For problems in which the computational cost of the two programs are comparable, the disk space and memory savings of Abaqus/Explicit make it attractive [46, 47].

In this work the Abaqus/Explicit analysis method is used because this analysis step can handle large deformations, non-linear material model and complex contacts and also the time spent for running the analysis has been considerably reduced.

4.1.3. Finite element selection

The correct choice of element for a particular simulation is vital if accurate results are to be needed at a reasonable cost. Generally a wide range of elements are available in Abaqus and the most commonly used finite elements are presented in figure 4.1.

Shell elements are used to model structure in which one dimension (the thickness) is significantly smaller than the other dimension (typically whose thickness is less than 1/10 of a typical global structural dimension generally can be modeled with shell elements) and in which the stress in the thickness direction are negligible. There are two types of shell elements are available in Abaqus, such as conventional shell elements and continuum shell elements. Conventional shell elements discretize a reference surface by defining the element's planar dimensions, its surface normal, and its initial curvature. The nodes of a conventional shell element, however, do not define the shell thickness, the thickness is defined through section properties. Continuum shell elements, on the other hand, resemble three-dimensional body yet are formulated so that kinematic and constitutive behavior is similar to conventional shell elements. Continuum shell elements are more accurate in

contact modeling than conventional shell elements, since they employ two-sided contact taking into account changes in thickness. Therefore, in this work continuum general purposes shell element such as SC8R (8-node, quadrilateral, first-order interpoaltion ,stress/displacement continuum shell element with reduced integration) is used for the composite material in the impact simulation[46].

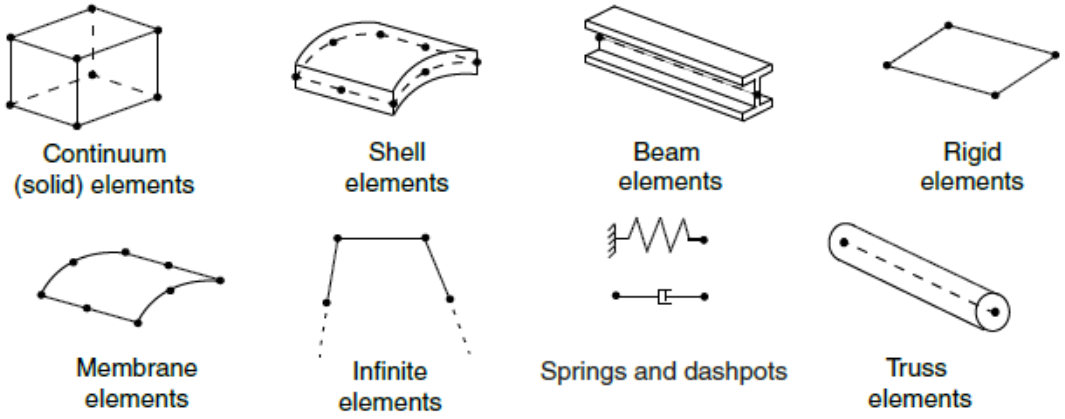

Figure 4.1. Commonly used element families in Abaqus [46].

4.2. Description of the problem

The numerical impact simulation is done based on ASTM D7136/7136M-07 standards which is basically designed for measuring the damage resistance of a fiber-reinforced polymer matrix composite to a drop weight impact events.

Based to this standards, the drop weight impact simulation was performed by using a balanced, symmetric $[0]_4$ unidirectional laminated sisal/epoxy composite with a dimension of 125 x 75 mm^2 as shown in below figure 4.2. Damage in the composite plate is imparted through out-of –plane, concentrated impact (perpendicular to the plane of the laminated composite plate) using a drop weight rigid impactor with a hemispherical striker tip. In this work the 0.5kg, 1kg ,2kg and 3kg of the impactor mass with smooth hemispherical striker tip of 16 mm diameter is used with three different velocities such as 1m/s, 2m/s and 3m/s to deal the influence of the velocity and mass of impactor on the composite materials. In this simulation a clamp boundary conditions was also implemented in the Abaqus software, and by using the advantage of symmetry, only the quarter

pars (1/4) of the composite plate is modeled and simulated in order to reduce the computational time cost. .

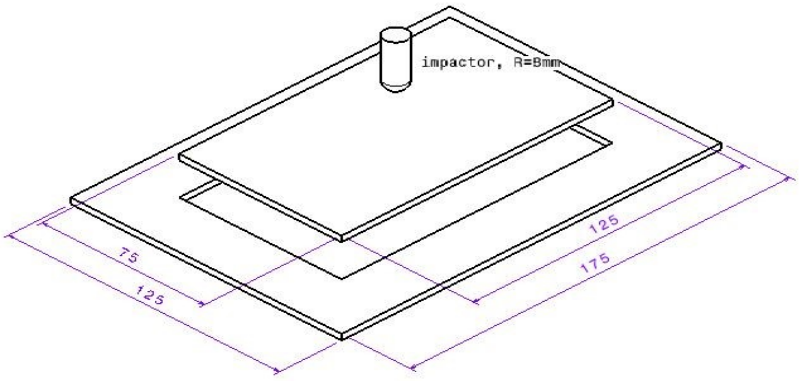

Figure 4.2. Description of the problem.

The nominal absorbed energy by the composite laminate was calculated using the below formula:

$$E_i = \frac{1}{2} m_i v_i^2 \quad (4.1)$$

Where:

E_i Impact energy (J)

m_i Mass of impactor (kg)

v_i Velocity of the impactor (m/s^2).

4.3. Procedures

The following procedures is followed based on the Abaqus module in order to visualize the low velocity impact simulation results.

4.3.1. Creating composite parts

Parts are the building blocks of an Abaqus/CAE model. The uses of the part module in Abaqus software is to create each parts. Using this module, the main parts of the simulation such as composite layer Plate and the impactor are created as shown in below figure. The composite Plate is created as a three dimensional deformable solid and the impactor as a three dimensional rigid.

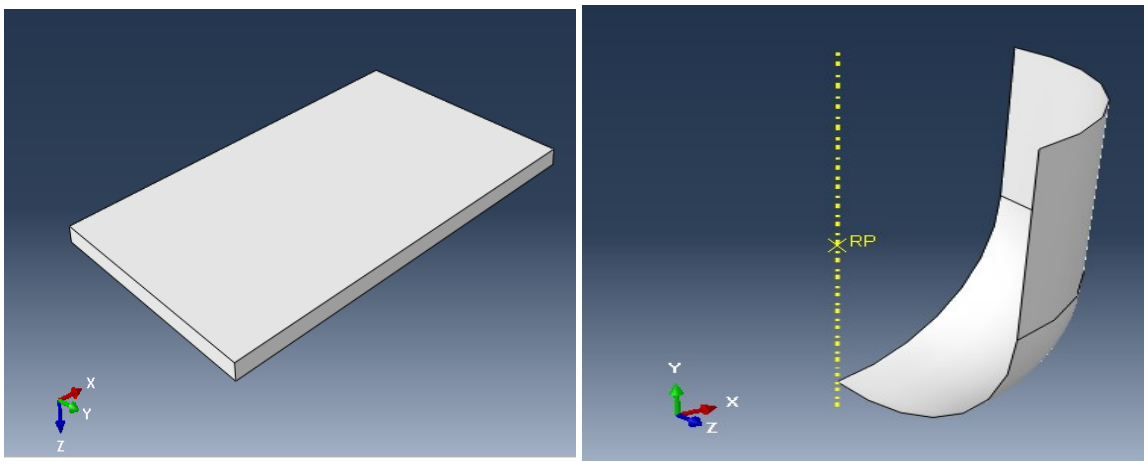

Figure 4.3. 3D model of the composite Laminate and impactor.

4.3.2. Material properties

The material library in Abaqus is intended to provide comprehensive coverage of linear and nonlinear, isotropic and anisotropic material behaviors. In this module the full material properties of the composite and the impactor are created.

- Units in Abaqus

Generally Abaqus has no units built into it except for angle and rotation measurements. Therefore, the considered unit must be self-consistent, which means that derived units of the chosen system can be expressed in terms of the fundamental units without conversion factors. A consistent system of units is chosen within the design, as following:

Entity	***unit***
Time	S
Mass	Kg
Length	m
Energy	J
Stress	Pa
Force	N

Table 4.1. Unit System Convention [46].

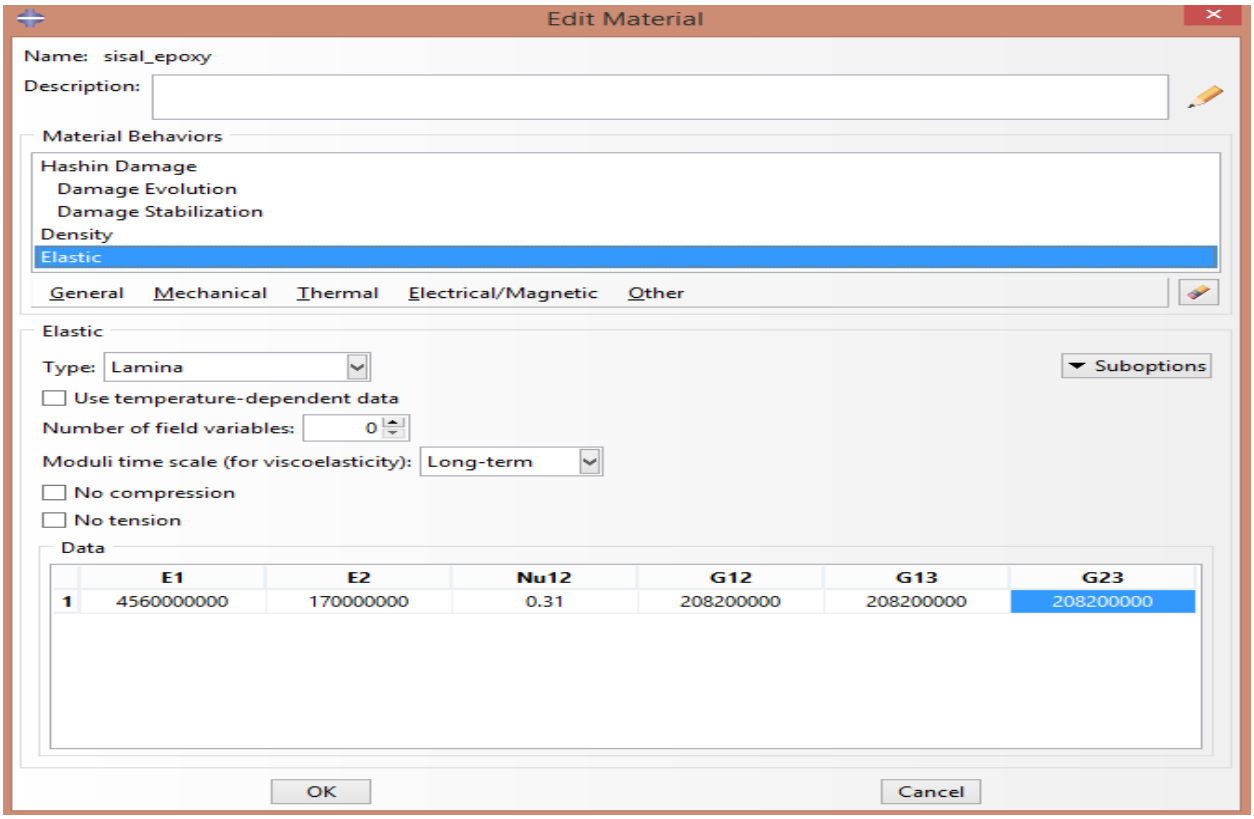

Figure 4.4. Material properties for the composite laminates.

As shown in above figure 4.4, due to the lack of experimental values, the out of plane shear moduli G_{13} and G_{23} were assumed to be equal to G_{12} in the simulation. Also the two dimensional Hashin failure criteria is used in order to predict the progressive failure damage of the sisal fibre reinforced epoxy resin composite laminates with including the sub-option of the damage evolution and damage stabilization option. The value of the damage evolution is calculated from the area under the stress-strain curve of each testing type. In order to stabilize the simulation process and overcome convergence difficulties, the stabilization coefficient was also used.

Also as it mentioned in previous section the impactor is strike the composite laminates at the center of the materials. So in order to simplify the machine meshing strategy and in order to overcome the excessive element distortion error, the partition (impact zone) around the impactor and composite laminate contact area is created. Then the composite layup was created using continuum shell elements.

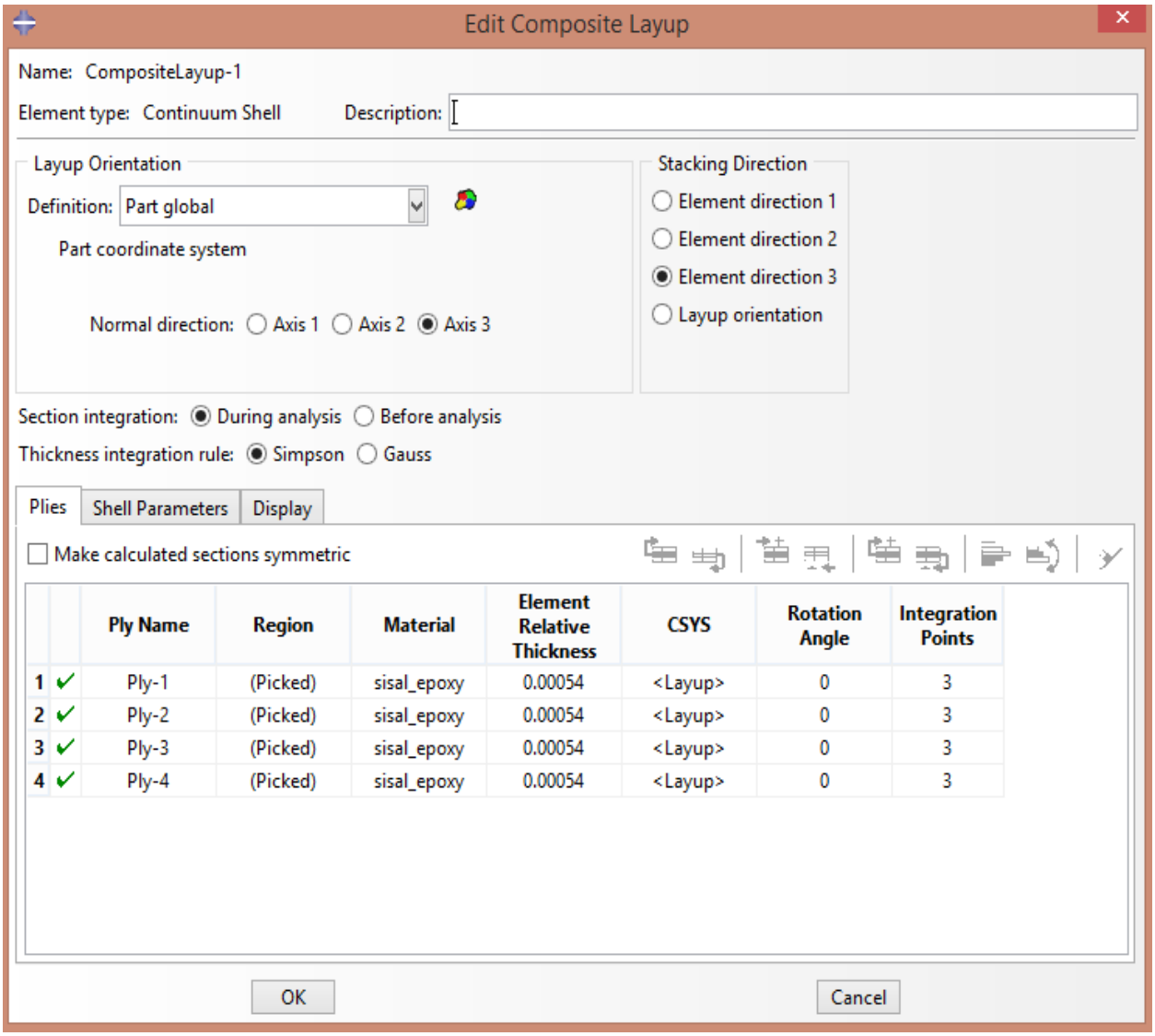

Figure 4.5. Composite lamina layup.

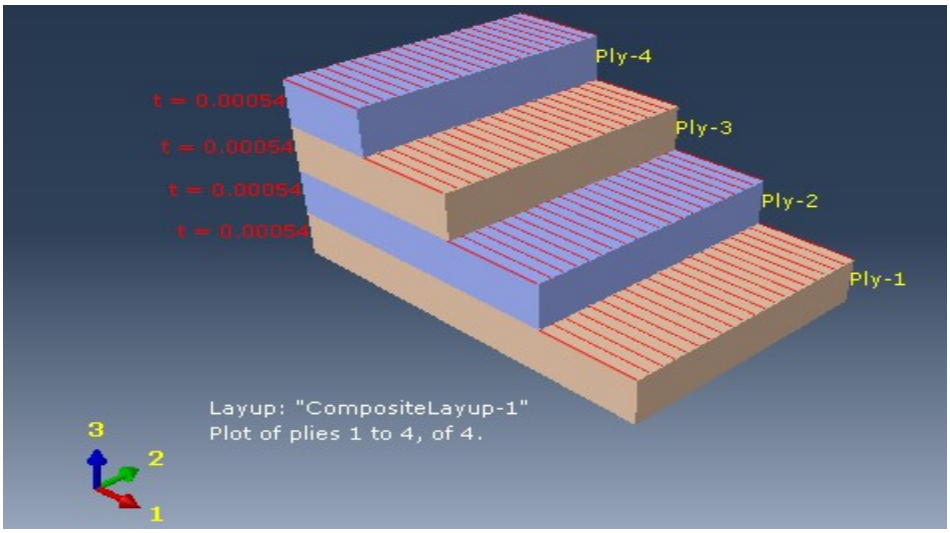

Figure 4.6. Sisal /epoxy composite ply stacking sequence.

4.3.3. Assembly of the parts

The main rule of the assembly module was to create and modify the assembly. In this module the parts that created in the previous section was assembled with the impactor.

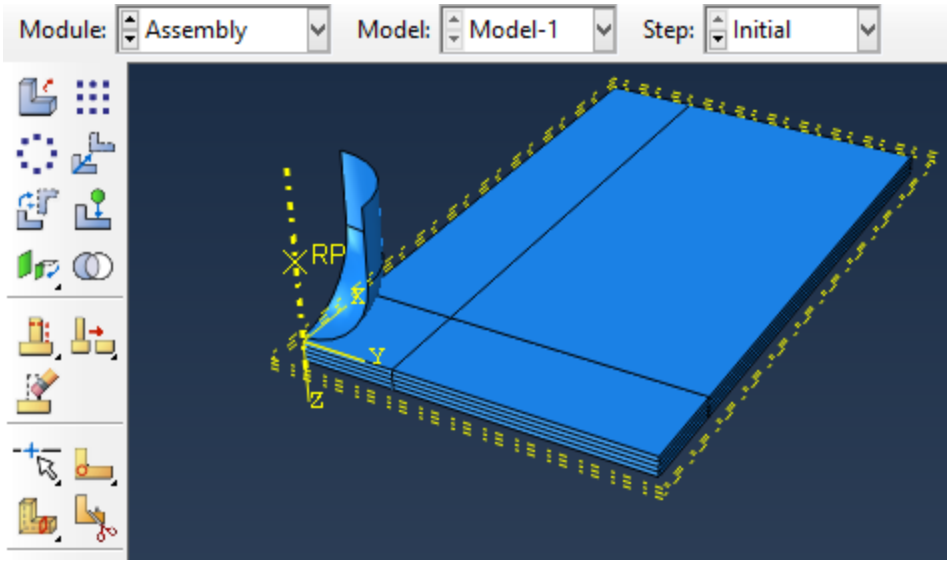

Figure 4.7. Assembly of the composite laminate and impactor.

4.3.4. Step module

After the initial step, the analysis step is created using General Dynamic Explicit procedure. In this study 20 millisecond of step time period was used, and the other parameter such as the incrimination, mass scaling & others are used its default values.

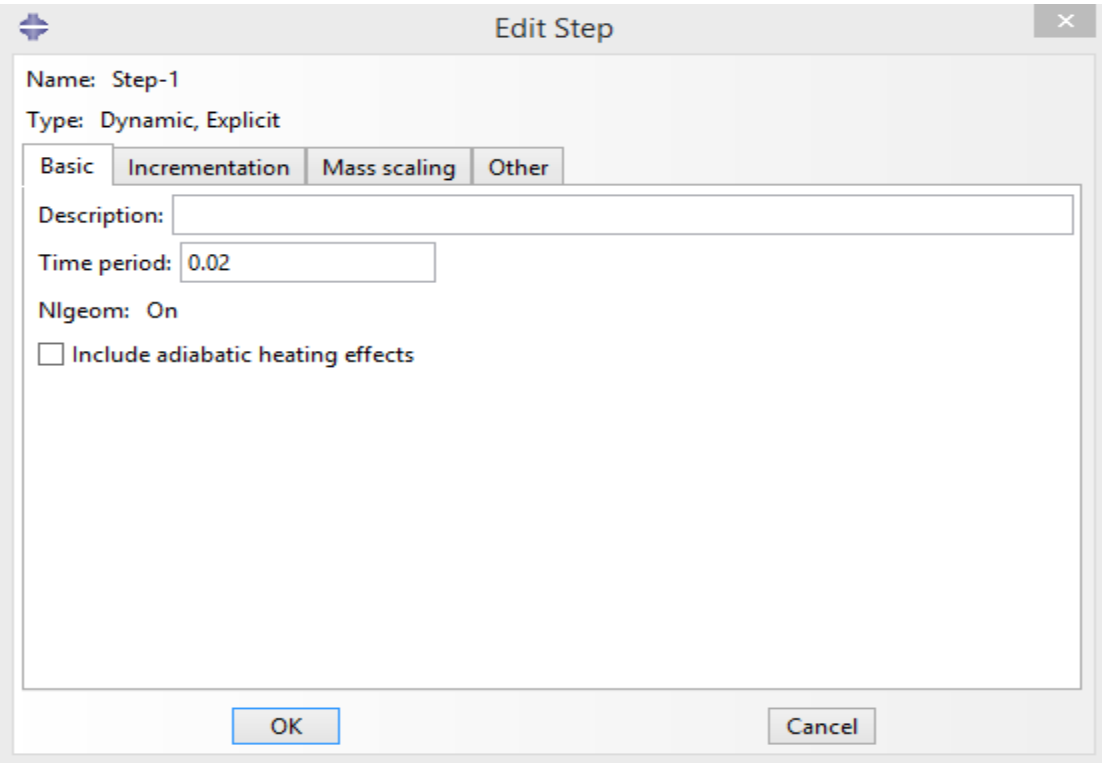

Figure 4.8. Typical step module of the simulation.

4.3.5. Interaction properties

The interaction module is one of the most important parts of the finite element analysis when two or more objects are in contact. Interactions are a step- dependent objects, which means that when you define them, you must indicate in which steps of the analysis they are active.

In this study the interaction properties was created using the general contact algorithm. A contact interaction property between the impactor and the composite laminate is defined using frictional tangential behavior with friction coefficient of 0.3 and hard contact normal behavior [53].

4.3.6. Boundary condition and initial velocity

The prescribed initial boundary conditions and the predefined velocity in the transverse direction (in Z-direction) is applied at this module. The clamped boundary condition are created using the pinned (U1=U2=U3=0) and symmetry boundary condition(X-SYM and Y-SYM). Also the impactor movement is only allowed in the Z direction (U1=U2=UR1=UR2=0) using displacement/ rotation boundary condition.

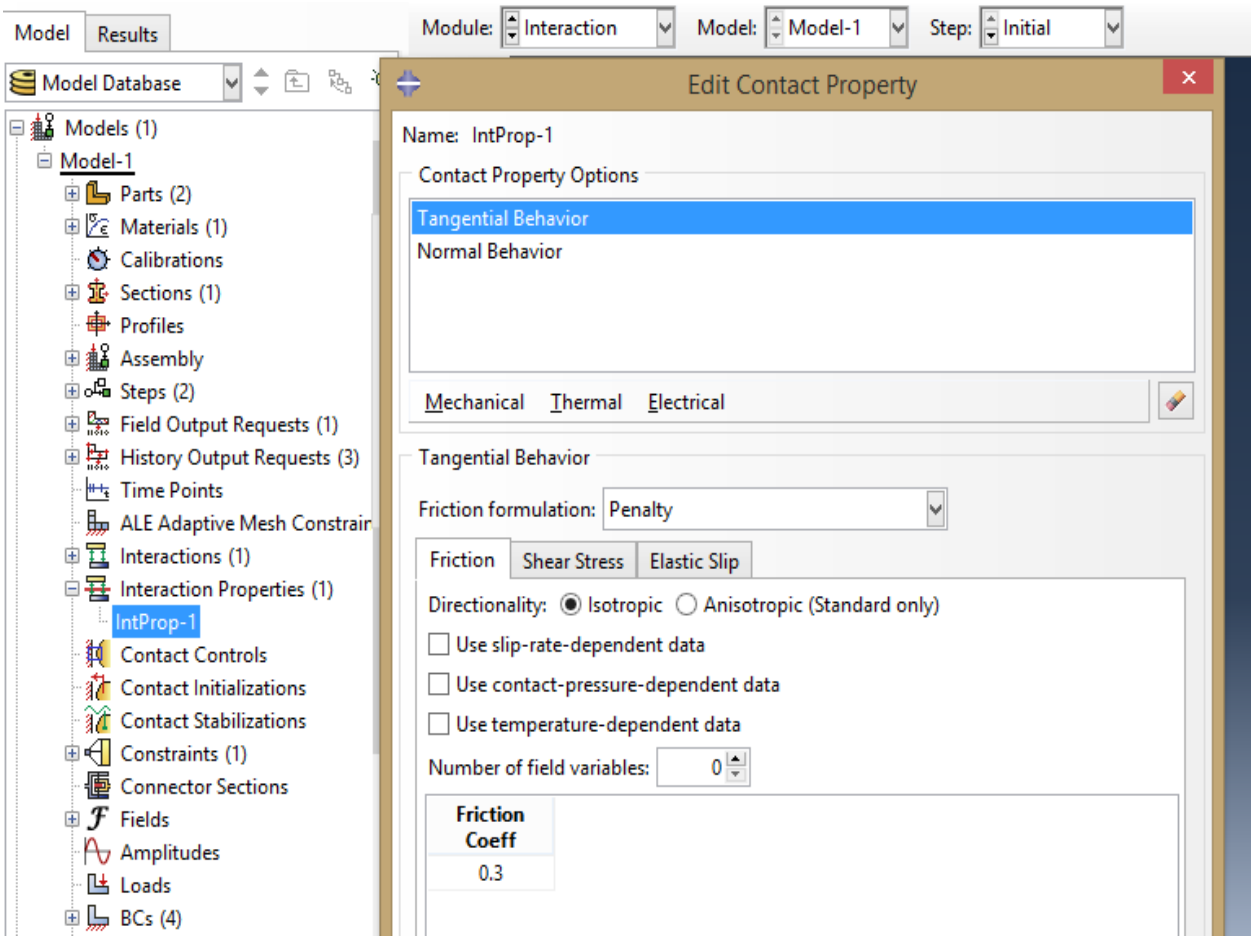

Figure 4.9. Interaction property.

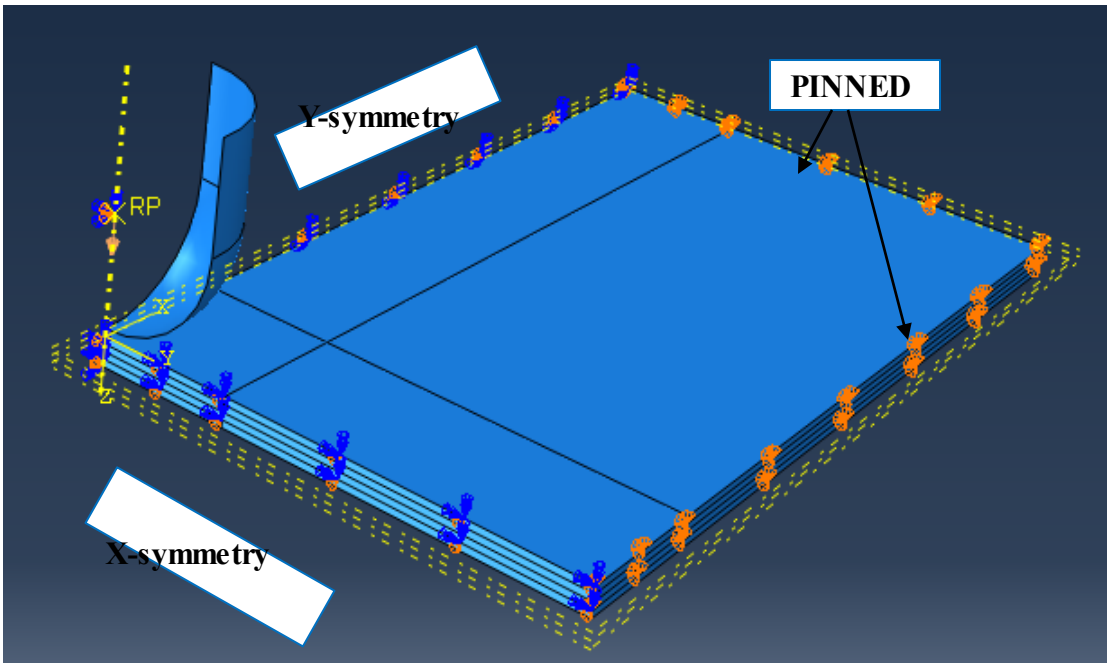

Figure 4.10. Boundary conditions.

4.3.7. Mesh module

The Mesh module provides a variety of tools that allow you to specify different mesh characteristics, such as mesh density, element shape, and element type. The composite plate is meshed with SC8R element type which describes an 8-node quadrilateral in-plane general-purpose continuum shell, reduced integration with hourglass control, finite membrane strain. The impact region is meshed with ($1x1mm^2$) also the other region is meshed with ($2 \times 2mm^2$). Also the metal impactor is meshed with R3D4 ($1 \times 1mm^2$) element type such as a 4-node 3-D bilinear rigid quadrilateral. Generally the finite element meshes hold over 3456 elements in total.

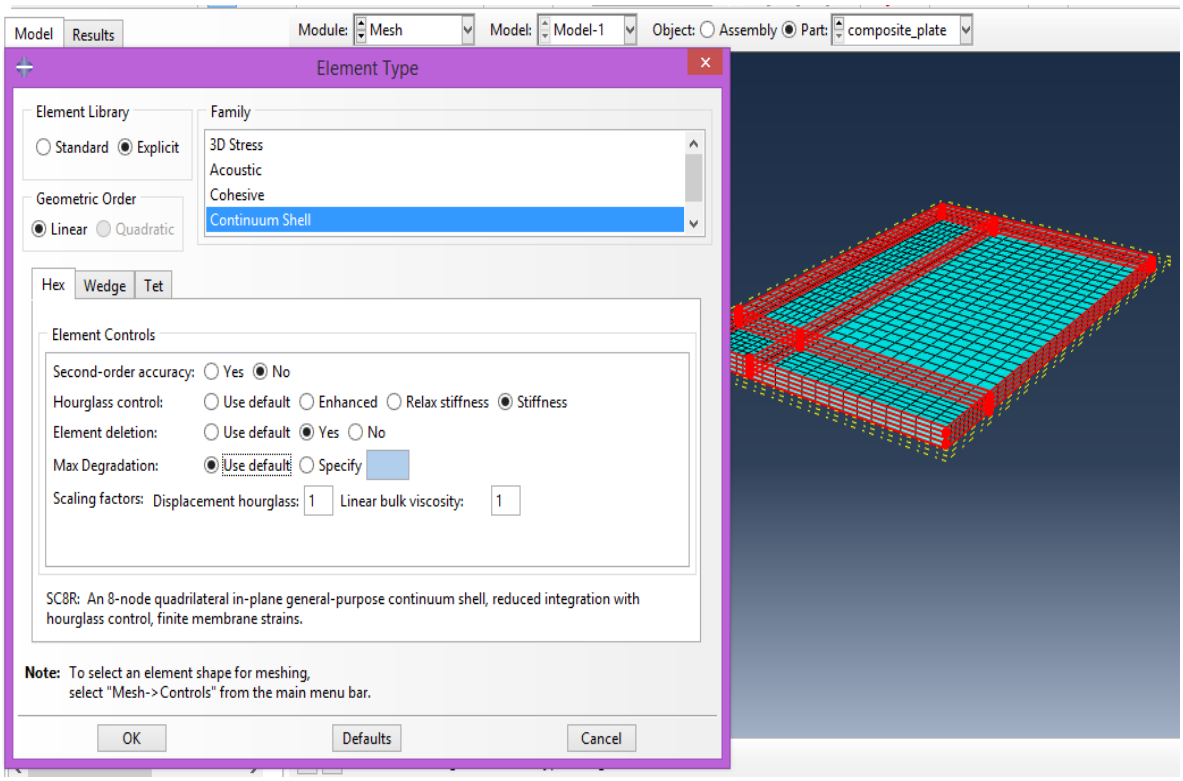

Figure 4.11. Element type dialog box for composite laminate.

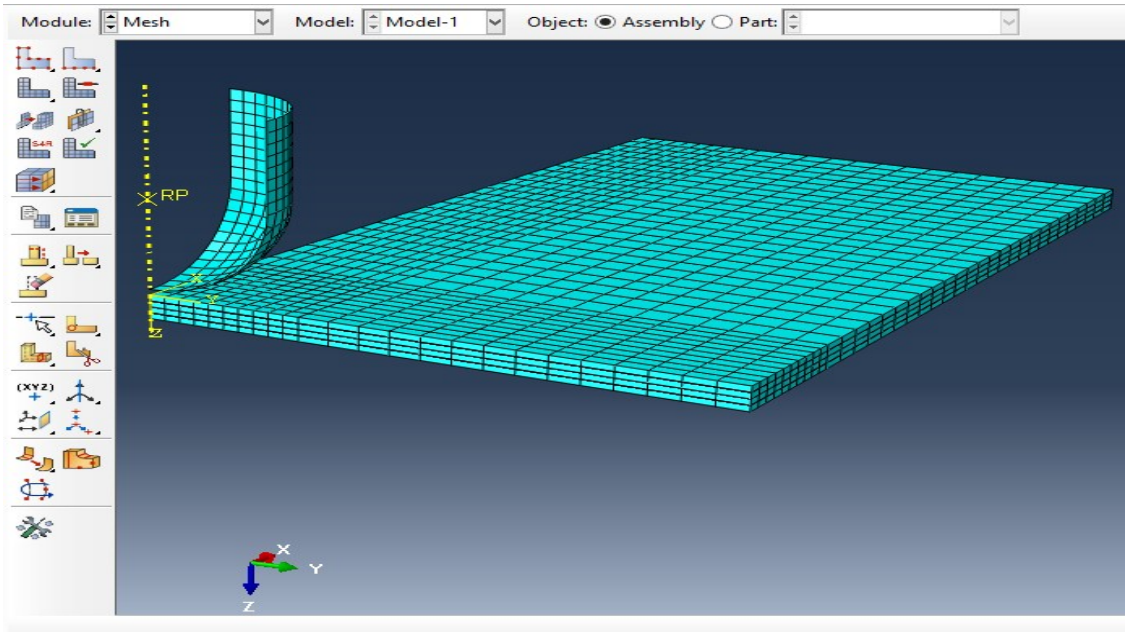

Figure 4.12. Final meshed impactor and composite laminate.

4.3.8. Job Module

Job model is the final step of the pre-processing. After you have defined your model, you are ready to analyze it. Analyzing a model involves some steps. Once you have finished all of the tasks involved in defining a model (such as defining the geometry of the model, assigning section properties, and defining contact), you can use the Job module to analyze your model. The Job module allows you to create a job, to submit it to ABAQUS/Explicit for analysis, and to monitor its progress;

4.3.9. Visualization module

In the post-processing, the Visualization module provides graphical display of finite element models and its results.

CHAPTER FIVE

RESULT AND DISCUSSION

In the previous chapter the numerical impact simulation procedure of sisal fiber reinforced epoxy resin composite laminate using Abaqus/CAE was discussed. In this chapter its result were presented and discussed briefly. Also the full simulations result was presented in appendix A-D.

5.1. Force - Time history

The force - time history shows the evolution of the contact force on the composite laminate with respect to time. The force - time history for 0.5 kg, 1 kg, 2 kg, and 3 kg mass of the impactor with respective 1 m/s, 2 m/s and 3 m/s graph is depicted in below figures.

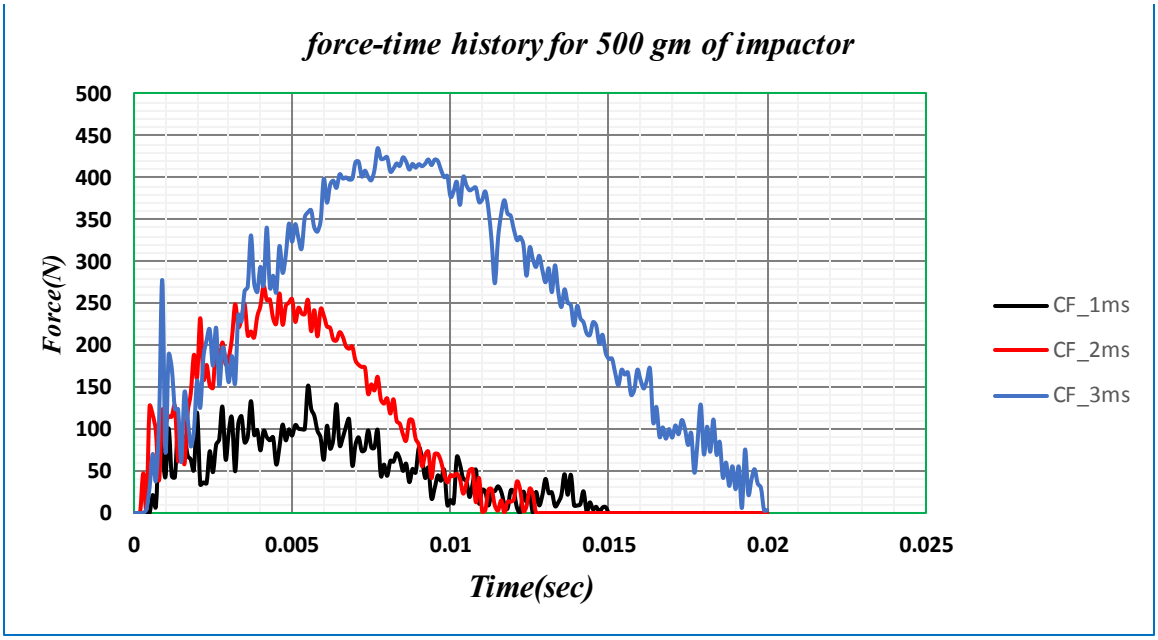

Figure 5.1. Force –time history for 500gm of impactor at different velocities.

As shown in above figure, the contact force of the composite plate was remain zero for very short period of time during the impact process up to the projectile comes in contact with the composite first layer. After such contact points (around 1millisecond), the contact force is gradually increased to its maximum value and then start decreases, and comes to zero.

When the impactor comes in contact with the composite plates, first the initial layer (upper most composite lamina) gets damage. Then for fraction of second contact is lost between the impactor and the specimens. This can be due to the damage of initial layer as so as the next layer comes in

contact with the impactor again the damage propagates. This goes on till all the energy is used by the specimen.

From force-time history graphs, it's noticed that the contact force was increased with increasing the mass and velocities of the impactor up to 1kg of the impactor. However, for 2kg and 3kg of the impactor, the contact force was decreased and the composite plate was highly damaged.

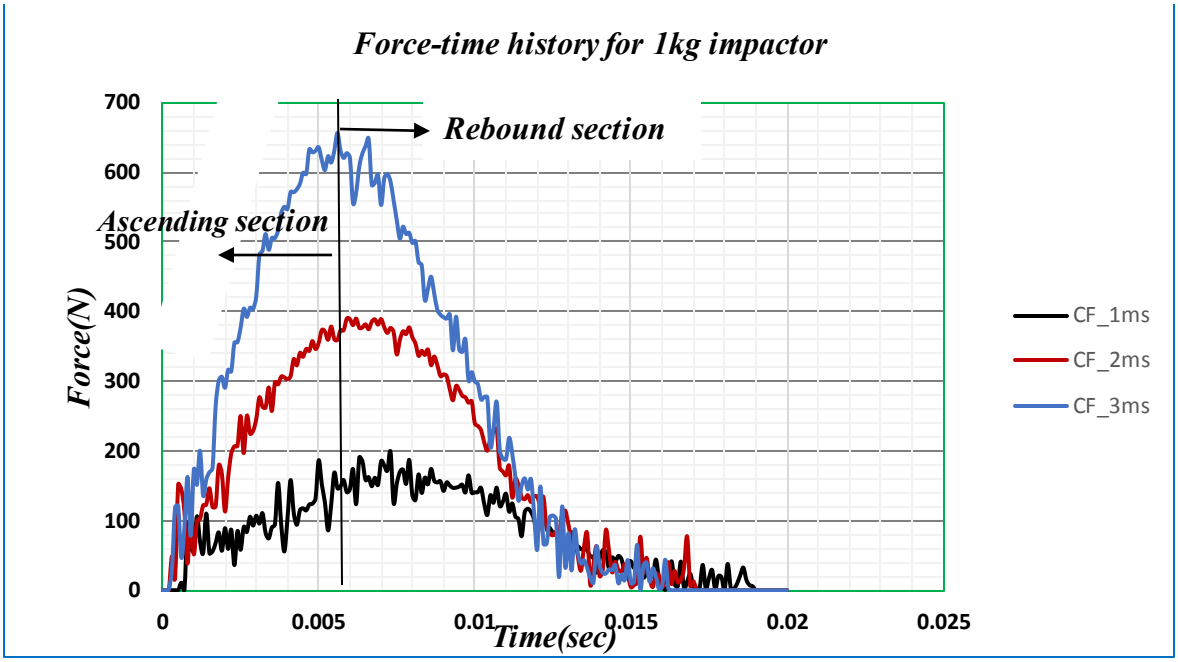

Figure 5.2. Force-time history for 1Kg of impactor.

For the 0.5kg and 1kg of the impactor, the force - time curves has two main parts such as the ascending and descending (rebound) parts. As shown in the figures, for ascending parts, the contact force is starting from zero and increased, and reached the peak value, almost when all the forces are absorbed by the composite plate, then the curves are starts fall down (rebound) and come to the initial points. These rebound section was the composite material response.

However for 2 kg and 3 kg of impactor at all of velocities such as 1, 2 and 3 m/s the curve does not have the rebound section, the curves reaches the peak load it can observe the sudden fall due to the damage of the composite layers. In these cases complete perforation of the plate has

occurred. Also the contact period between the impactor and composite plate was very small for this two impactor masses when compared to the others.

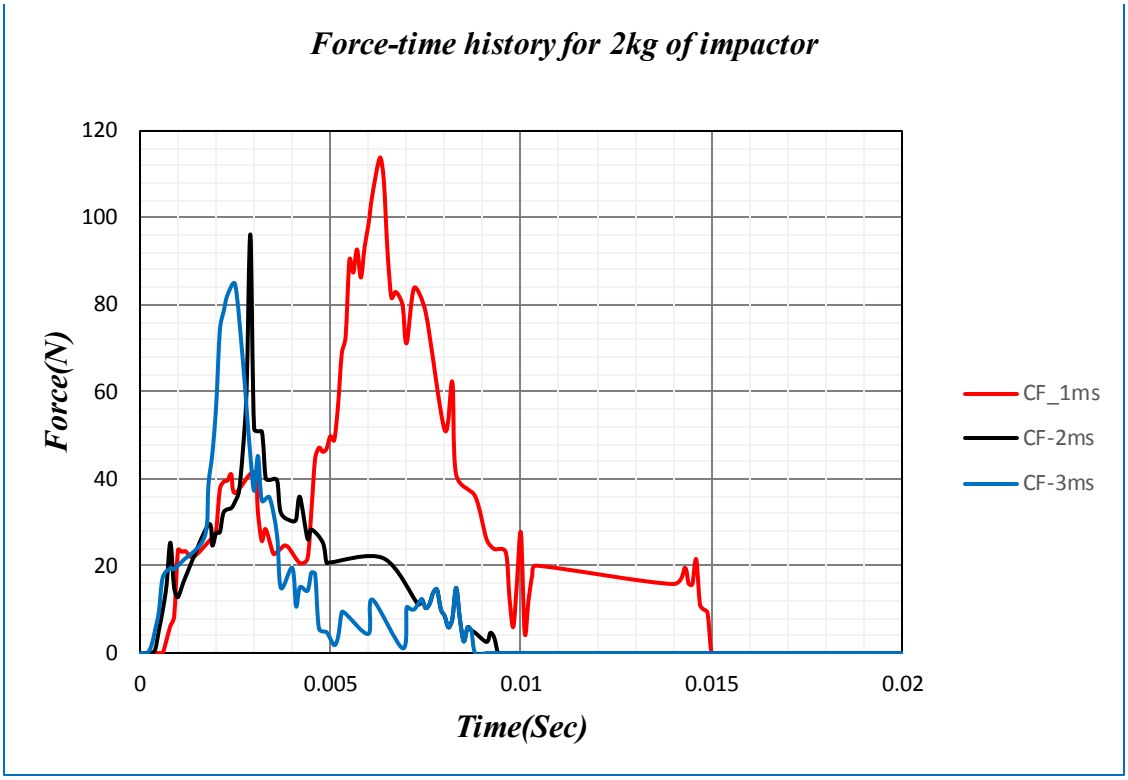

Figure 5.3. Force-time history for 2Kg of impactor.

The force-time history for this two impactor mass cases are highly wavy which caused by the rapid development of the impact damage and due to the vibration of the composite plate when compared to the other masses.

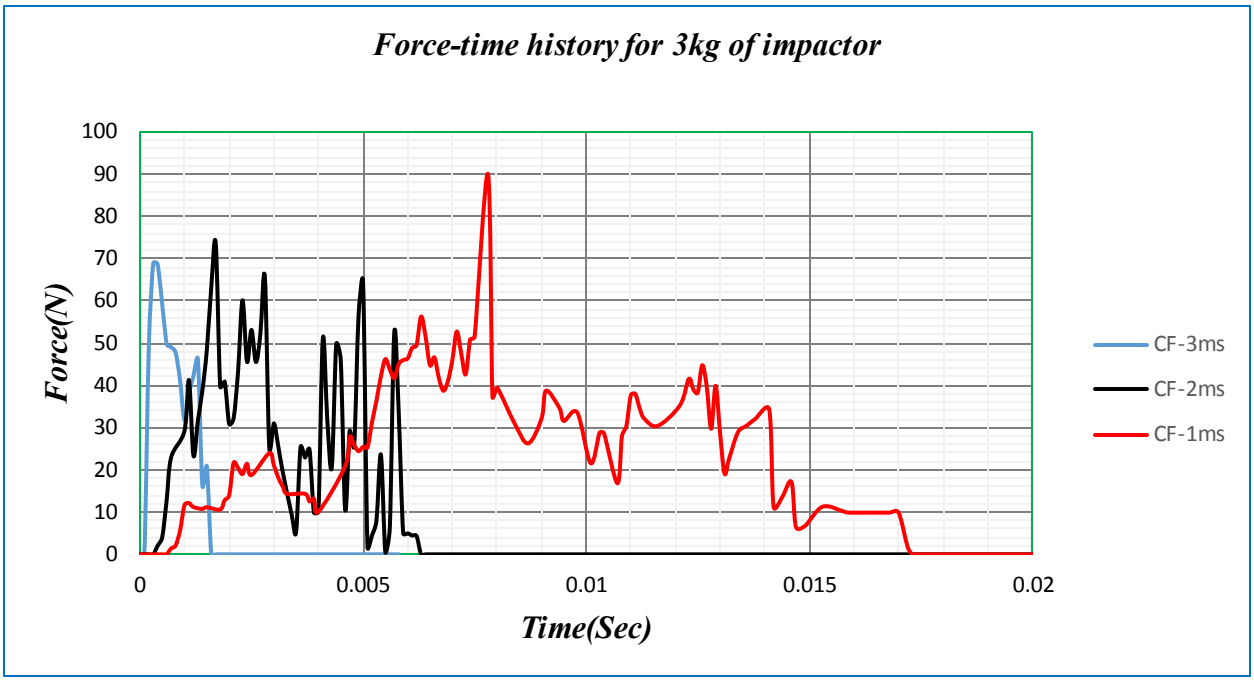

Figure 5.4. Force - time history for 3 kg of impactor.

From all force-time history graph, it observed that the highest reaction force is occurred at 1kg of impactor for 3m/s with peak load of 656.69N

5.2. Force-Deflection history

The force-deflection history shows the evolution of the contact force with respect to the specimen out of plane displacements. As shown in the figure 5.5, the slope of the ascending section of each force-deflection curve was termed as the impact bending stiffness section due to its representation of the stiffness of composite laminates under impact induced bending in the beginning of the impact process. According to the below figures, the maximum forces and deflection was increased as the mass and velocities of the projectile increased up to 1kg of impactor. For such cases, the force-deflection curve rises, reached a maximum level and returned back to the origin. It formed a close curve representing the projectile's impacting onto the composite plate and rebounding from the composite laminate. The area covered by this closed curve is the absorbed energy of the composite laminate under such specific impact. Apparently, as the impact energy continued to increases, the enveloped area was increased up to 1kg of the impactor mass. Apart from such impactor mass, as the impact energy continued to increase, perforation then take place due to

excessive fibre breakage. Once the perforation of the composite plate occurred, the force-deflection curve would no longer be a closed curve as shown in figure 5.6 and figure 5.7

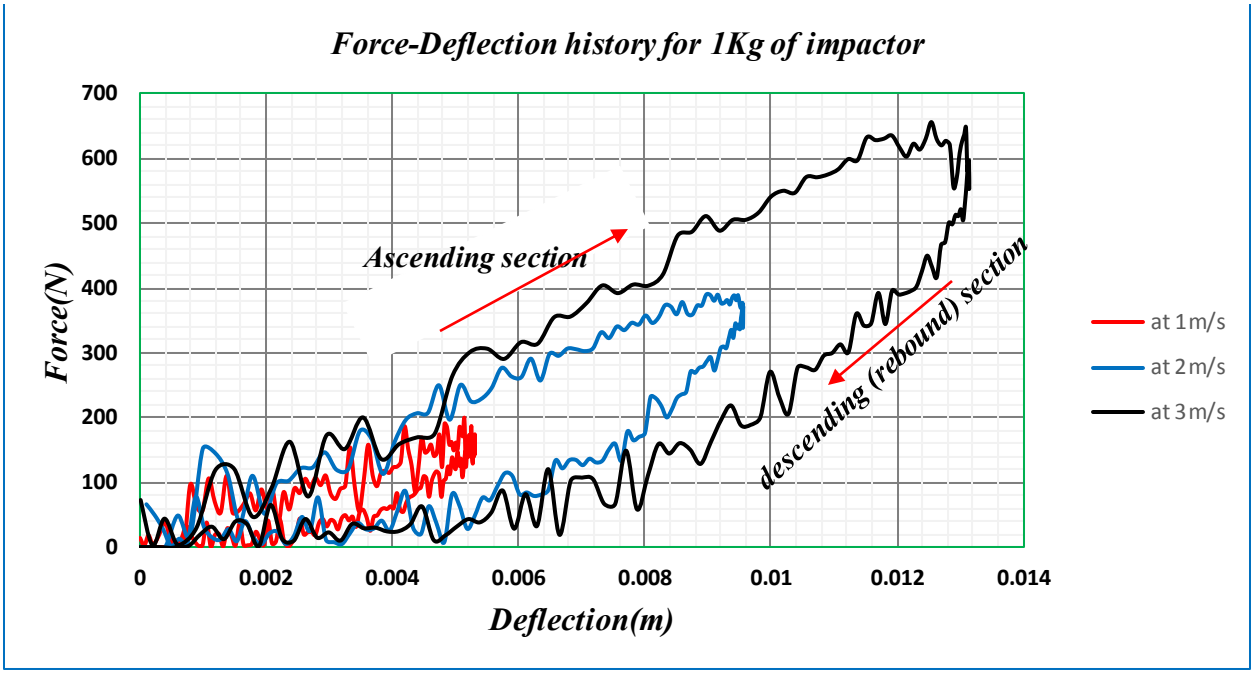

Figure 5.5. Force-deflection curve for 0.5Kg of impactor.

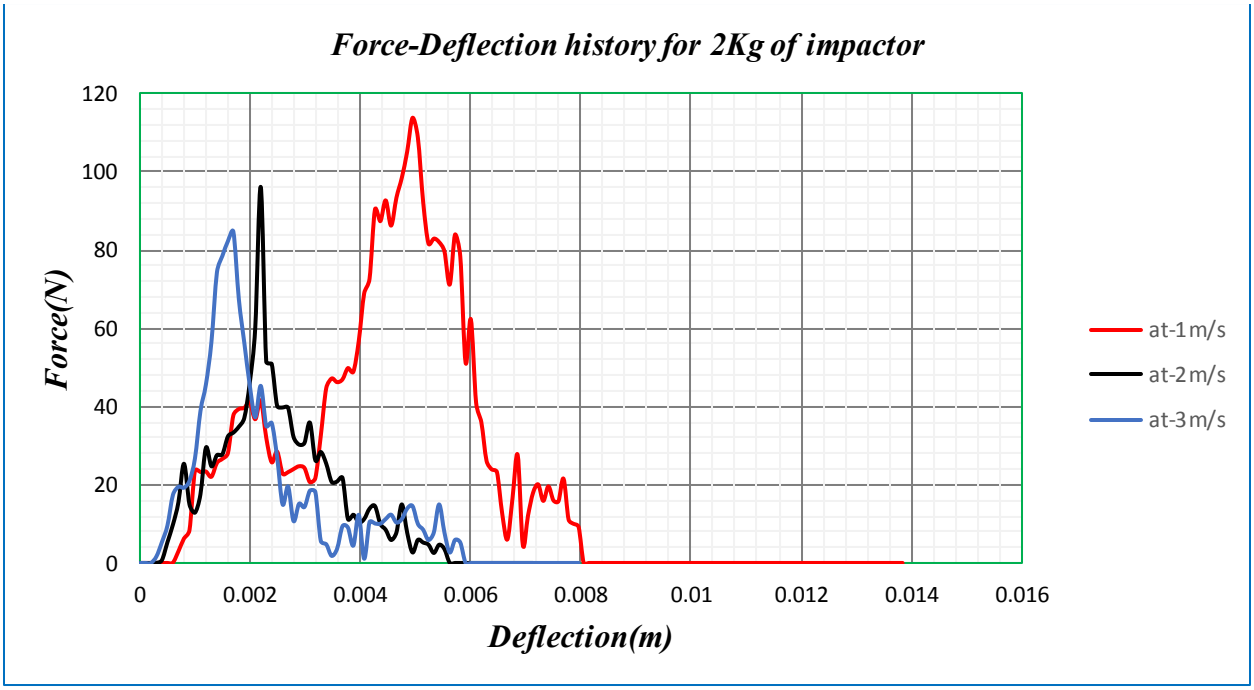

Figure 5.6. Force-deflection curve for 2Kg of impactor.

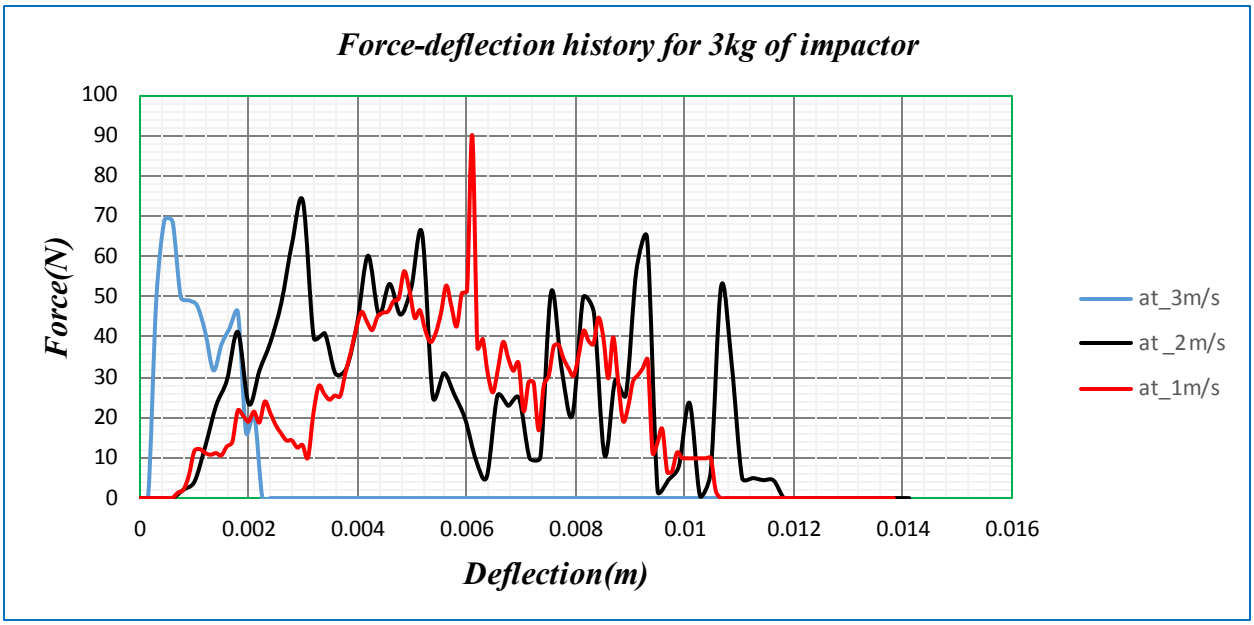

Figure 5.7. Force-deflection history for 3 kg of impactor.

5.3. Damage and failure mode of the composite laminate

During the transverse impact process of sisal fibre reinforced epoxy resin composite laminate, several damage is occurred starting from shear damage to perforation based on the mass and velocity of the impactor. In this section the shear damage, matrix damage, fibre damage and perforation mode of the composite plate was presented.

5.3.1. Shear damage

As shown in below the figures due to the out of plane impact, the shear effect on the composite plate is high basically due to their low shear strength of the laminates. The shear damage is starts from the points where the impactor and composite plate come in contact, and then spread into the whole composite plate. For example as depicted in below figure 5.8, for 0.5 kg of impactor with 1m/s, the shear damage starts at 1ms where the contacts begin and get the highest shear damage at time of 7ms that means when the contact force value reaches the highest value (at peak load).Also it is observed that the shear damage was occurred at constant level even at the rebound section of the impactor.

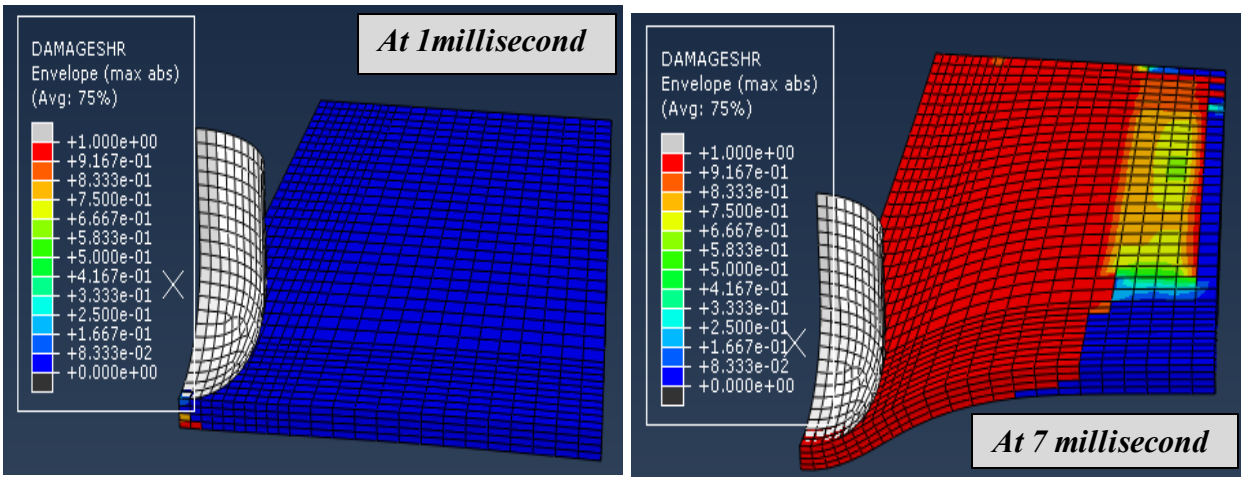

Figure 5.8. Typical shear damage for 0.5 kg of impactor at 1m/s.

Also from the simulation result, it's observed that the evolution of the shear damage is starts from the first layer and goes down to the other internal layer during the impactor life time. This shear effects can cause a significant reduction in the strength and stiffness of the material.

From the simulation result, it's noticed that the shear damage was increase with the increase of the impactor mass and velocity up to 1kg of impactor with 3m/s as a global damage. Apart from that, for 2kg and 3kg of impactor, the shear damage is starts to decrease at some extent when compared to the others.

As shown in the above figure, Abaqus was used different color mode in order to show the damage extent of the composite, and a red color shows the area that satisfied the damage criteria (≥ 1).

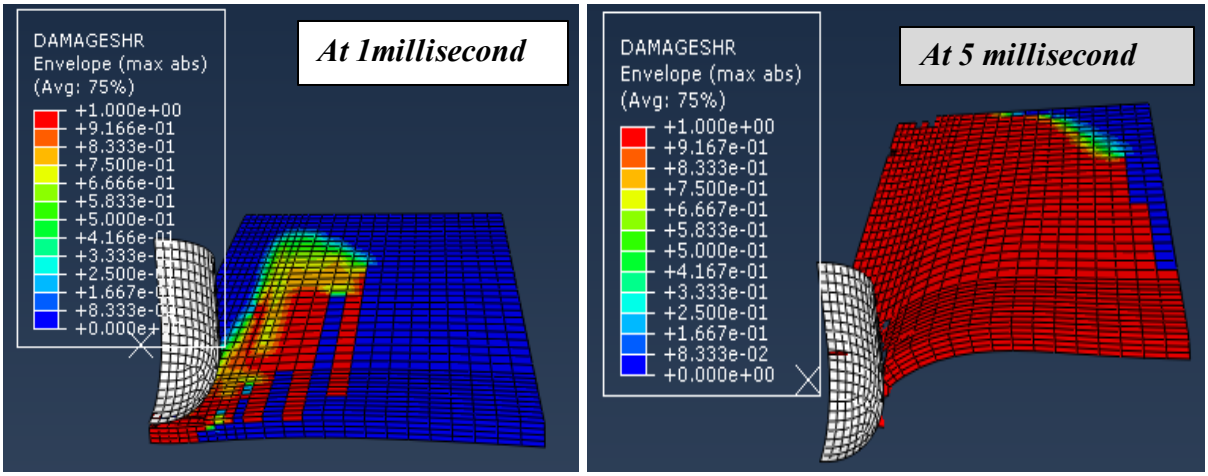

Figure 5.9. Typical shear damage mode for 2kg of impactor at 3m/s

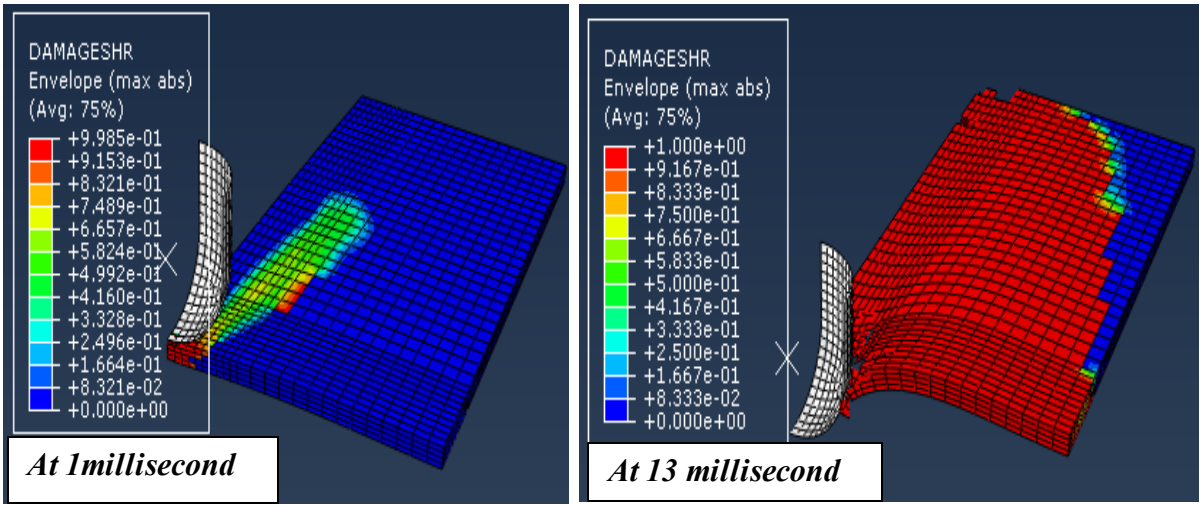

Figure 5.10. Typical shear damage mode for 3kg of impactor at 3m/s.

5.3.2. Matrix and fibre damage

Damage produced in the low velocity impact is generally initiated by matrix crack which induced delamination at the interfaces between plies with different orientation.

According to the two dimensional hashin damage criteria's of matrix damage such as HSNMTCRT(matrix tension) and HSNMCCRT (matrix compression), the composite matrix are highly damaged by the transverse impact even at low velocity and impactor masses. The evolution of the matrix damage (tension and compression) is starting from the point of contact between the projectile and composite plate and spread into the whole plate during the impact time which cause the global damage of the composite plate.

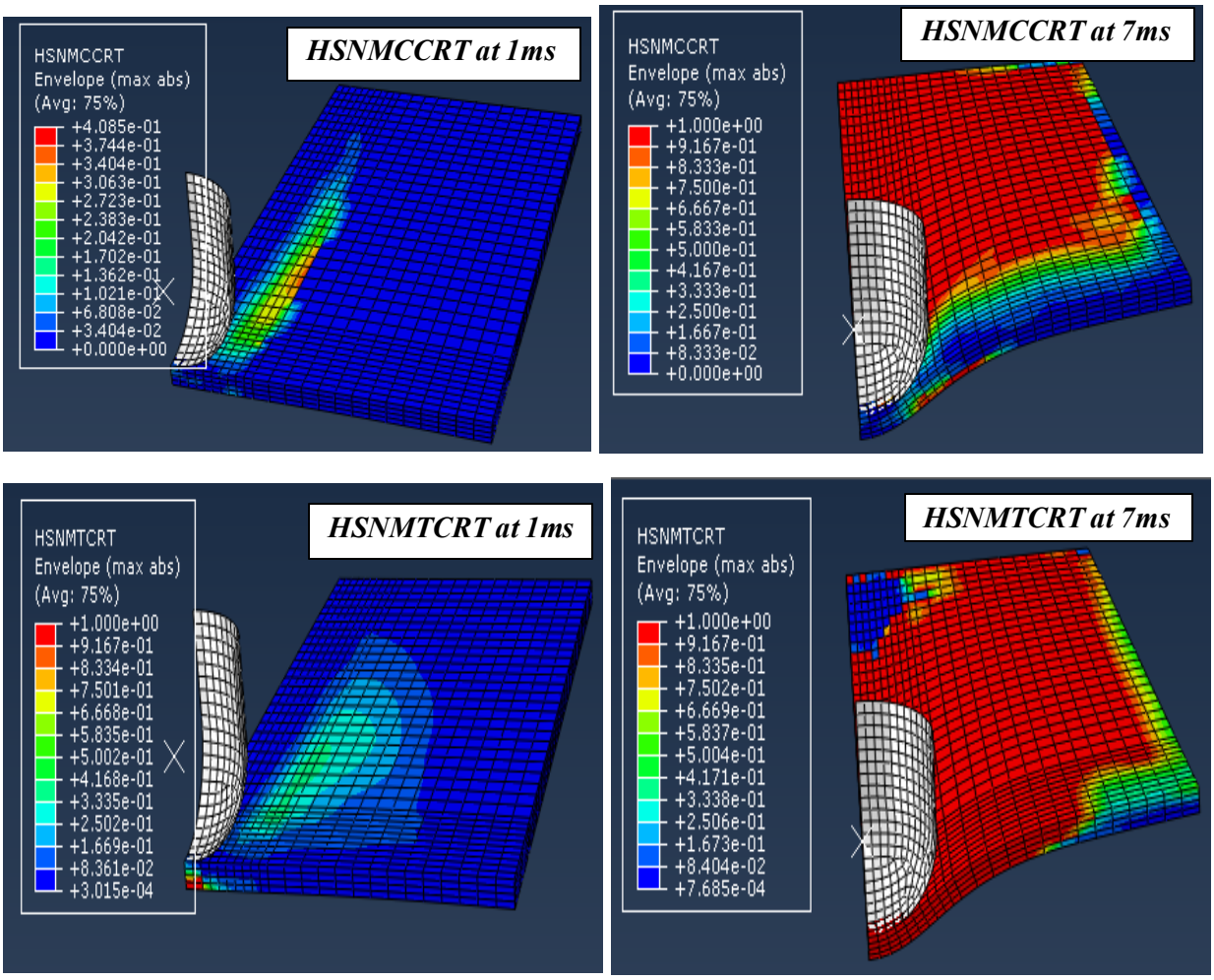

Figure 5.11. Typical matrix compression and tension damage for 0.5 kg of impactor at 1m/s.

From the simulation results, it observed that matrix compression damaged area was higher when compared to the area of matrix tension basically due to the nature of the impact force (compressive force).

When the impactor force increases (stress also increases), the composite fibre is starts to damage. As matrix damage, Hashin has two fibre failure modes, such as fibre tension (HSNFTCRT) and fibre compression (HSNFCCRT) mode.

According to the hashin damage criteria, when the criteria was fulfill, the fibre damage was occurred in the composite plate. Both the fibre tension and compression damage composite laminate are started from the projectile and composite plate contact point and then start spread to the composite plate during the impactor and plate contact period. As seen from the simulation

results, when the impactor mass and velocity increases, the damage area of the composite plate also linearly increases.

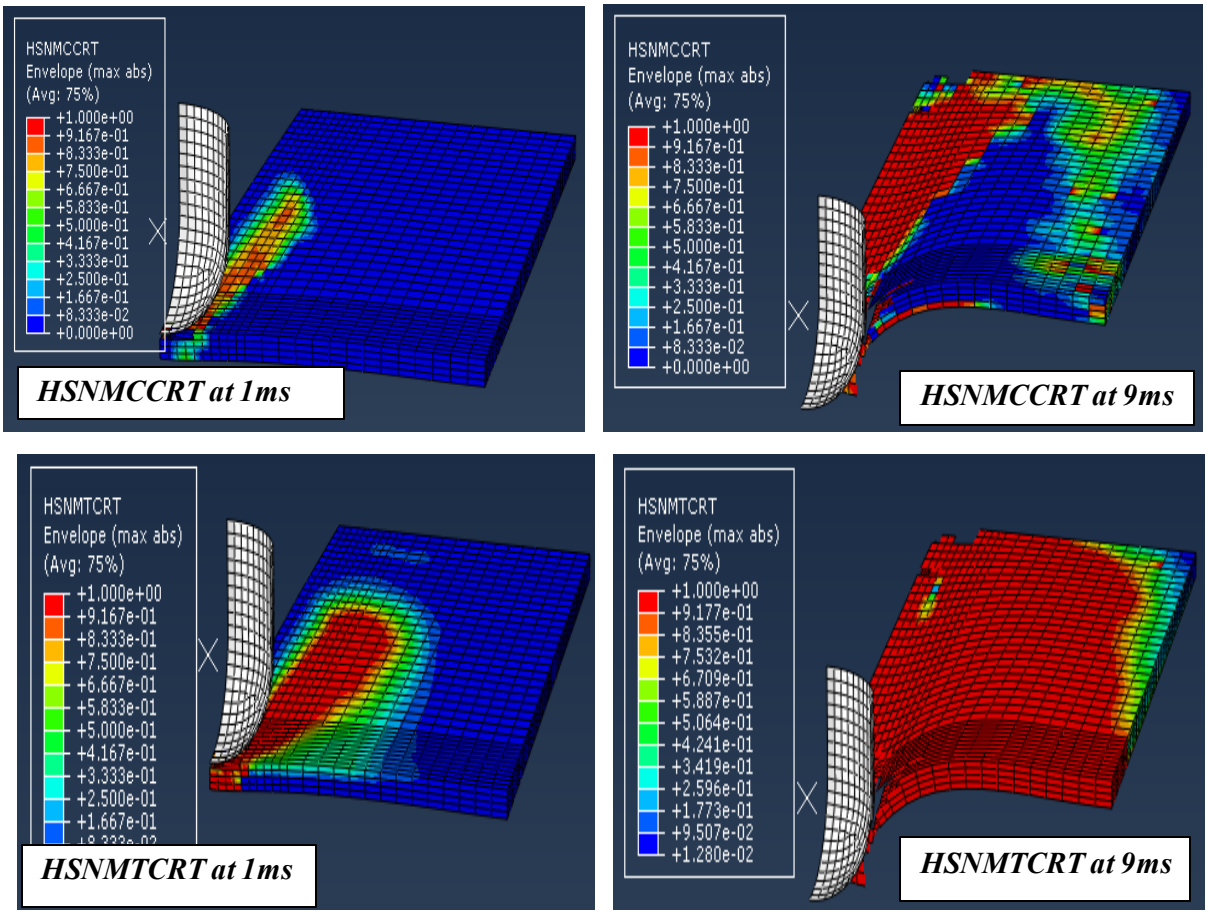

Figure 5.12. Typical matrix tension and compression damage for 3kg of impactor at 3m/s.

From the all simulation results, it observed that the area of the composite plate that damaged by fibre compression is higher when compared to the fibre tension damage. For example as depicted in the figure 5.13 and figure 5.14, the fibre tension damage is more localized around the contact and boundary region. However, for the fibre compression damage the damage is starts from the impact points and then spread in to the whole lamina during the impact time period. Also it's observed that the evolution of the damage for both damage mode was starts from the upper lamina and then goes down to all composite layers during the contact period.

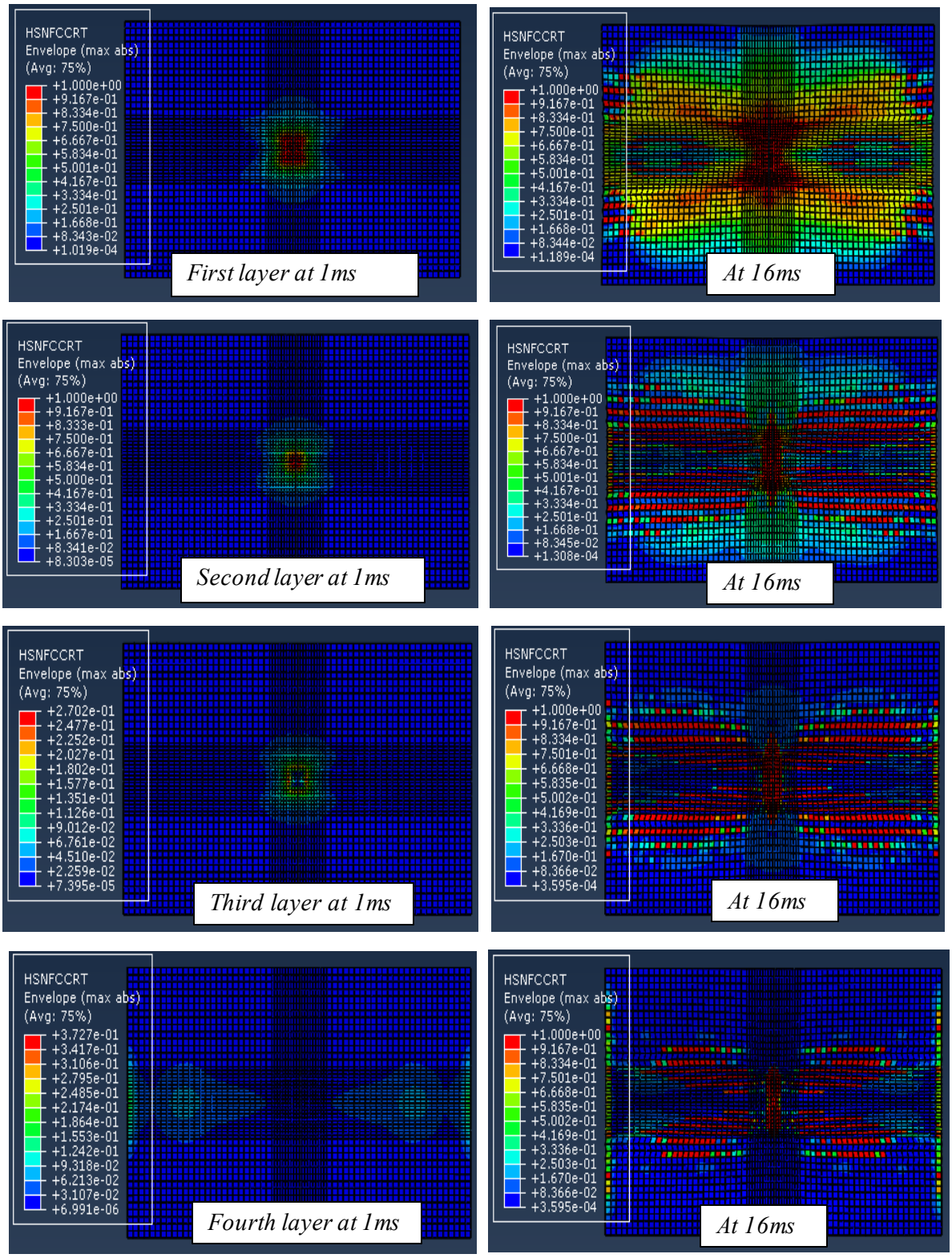

Figure 5.13. Fibre compression damage evolution in each full composite layer for 0.5 kg of impactor at 2m/s (from top view).

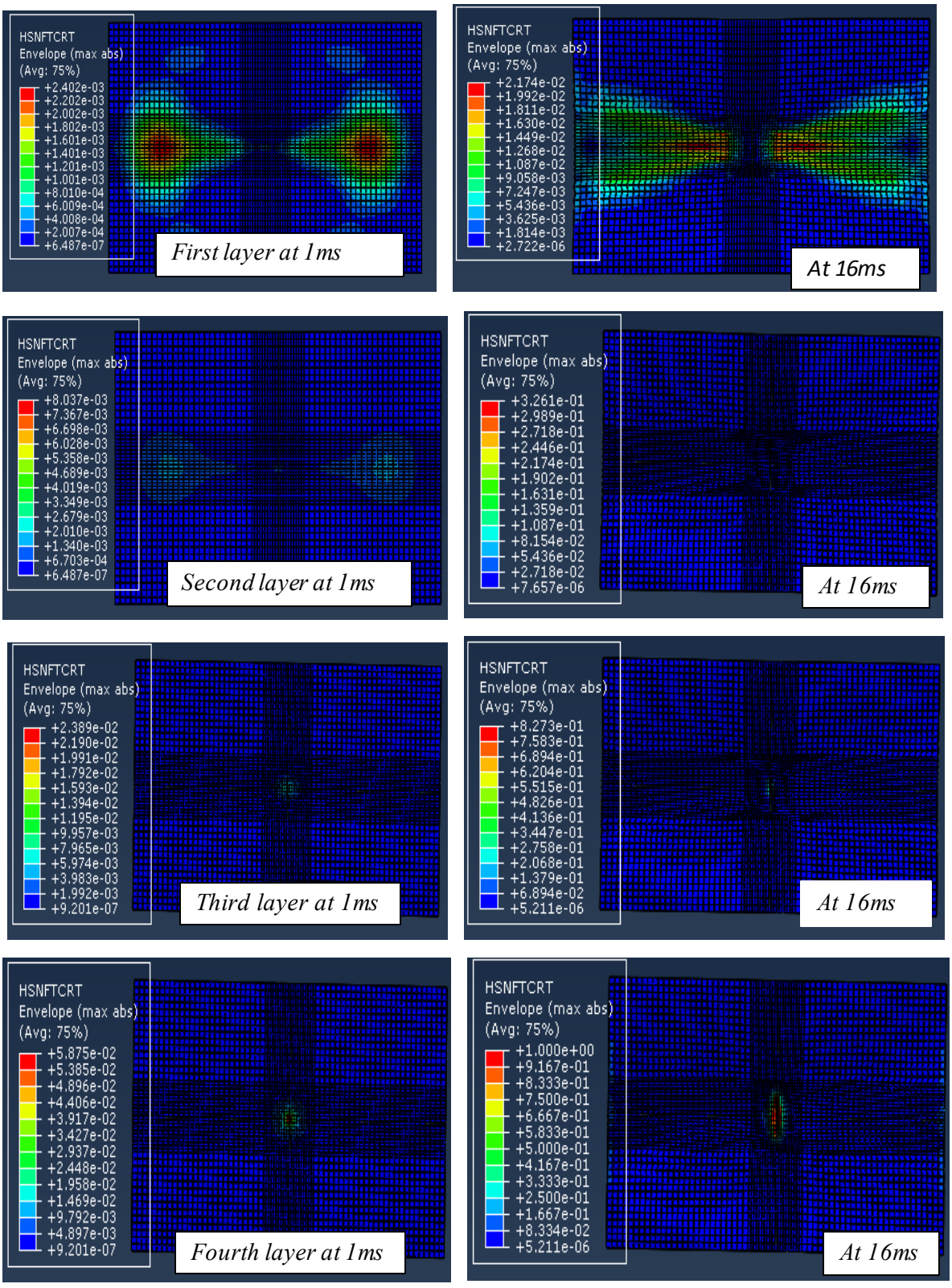

Figure 5.14. Fibre tension damage evolution in each full composite layer for 0.5 kg of impactor at 2m/s (from top view).

Furthermore, it is noticeable that for the impactor mass of 2kg and 3 kg with all velocities of 1m/s, 2m/s and 3m/s, due to excessive fibre breakage and fiber pull out, a full perforation of the composite laminate is happened. Also as shown in figure 5.16, due to the effects of boundary condition, some fiber breakages are occurs at the edges.

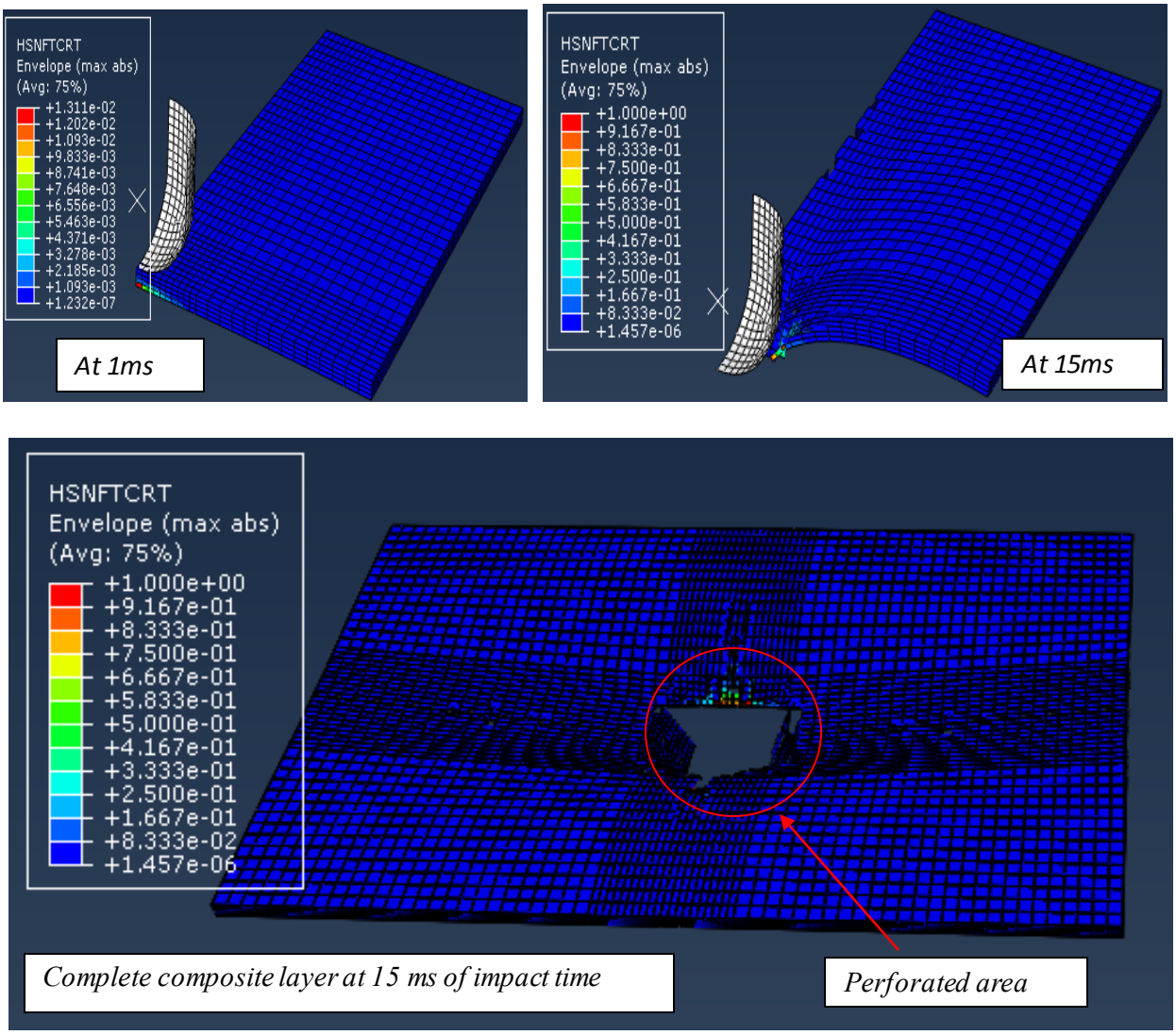

Figure 5.15. Perforation evolution of composite laminate for 2kg of impactor at 1m/s.

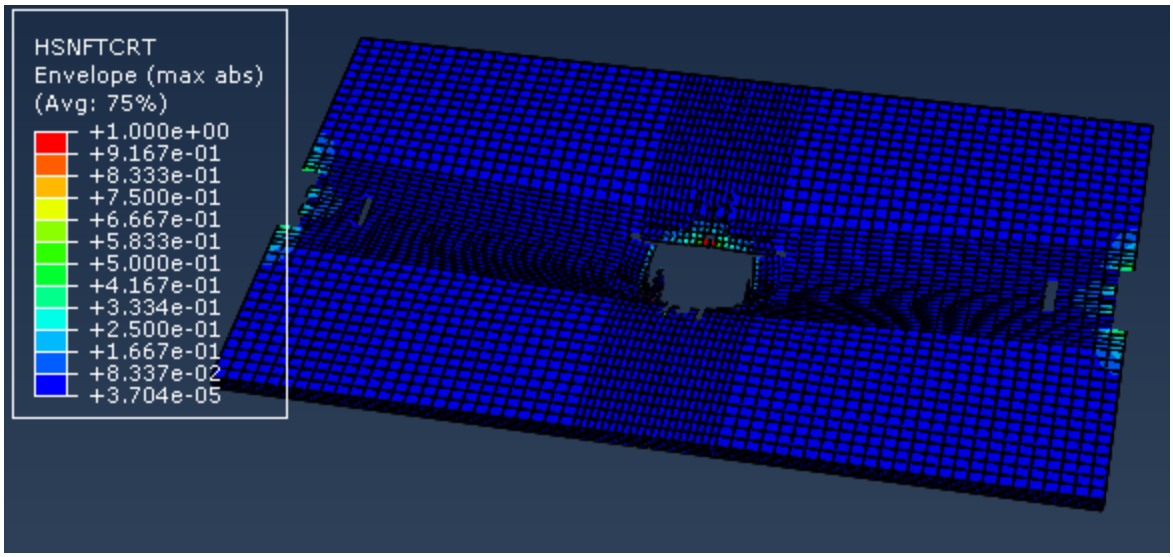

Figure 5.16. Perforation of composite layer for 3kg of impactor at 3m/s.

5.4. Energy absorption capacity

The kinetic energy of the projectile when impacted into the target is dissipated and absorbed in various ways by the target. For small mass of projectile and velocity impact, most of the kinetic energy of the impactor are absorbed by the composite material in the form of internal energy and very small energy was dissipated in other form such as frictional dissipation energy, damage dissipation energy, and etc.

As shown in below figure 5.17, from the simulation results it seen that, for low mass of impactor (0.5 kg, 1 kg) most of the kinetic energy is absorbed by the composite plate and very little are dissipated in the form of friction and etc. However for 2kg and 3kg of impactor, due to the complete perforation of the composite plate (also due to the contact period was decreased), only very small amount of energy is absorbed and most of the energy was goes with the impactor. For example for 0.5kg of impactor with 1m/s of velocity above 99.963% of the kinetic energy is absorbed by the composite plate. However for 3kg of impactor with 3m/s of velocity, only 1.482% of the kinetic energy is absorbed and the rest was dissipated in the damage and leave with the impactor. This comparison revealed that the sisal fibre reinforced epoxy resin composite resistance during the perforated process decreased when the impactor mass and velocities increases.

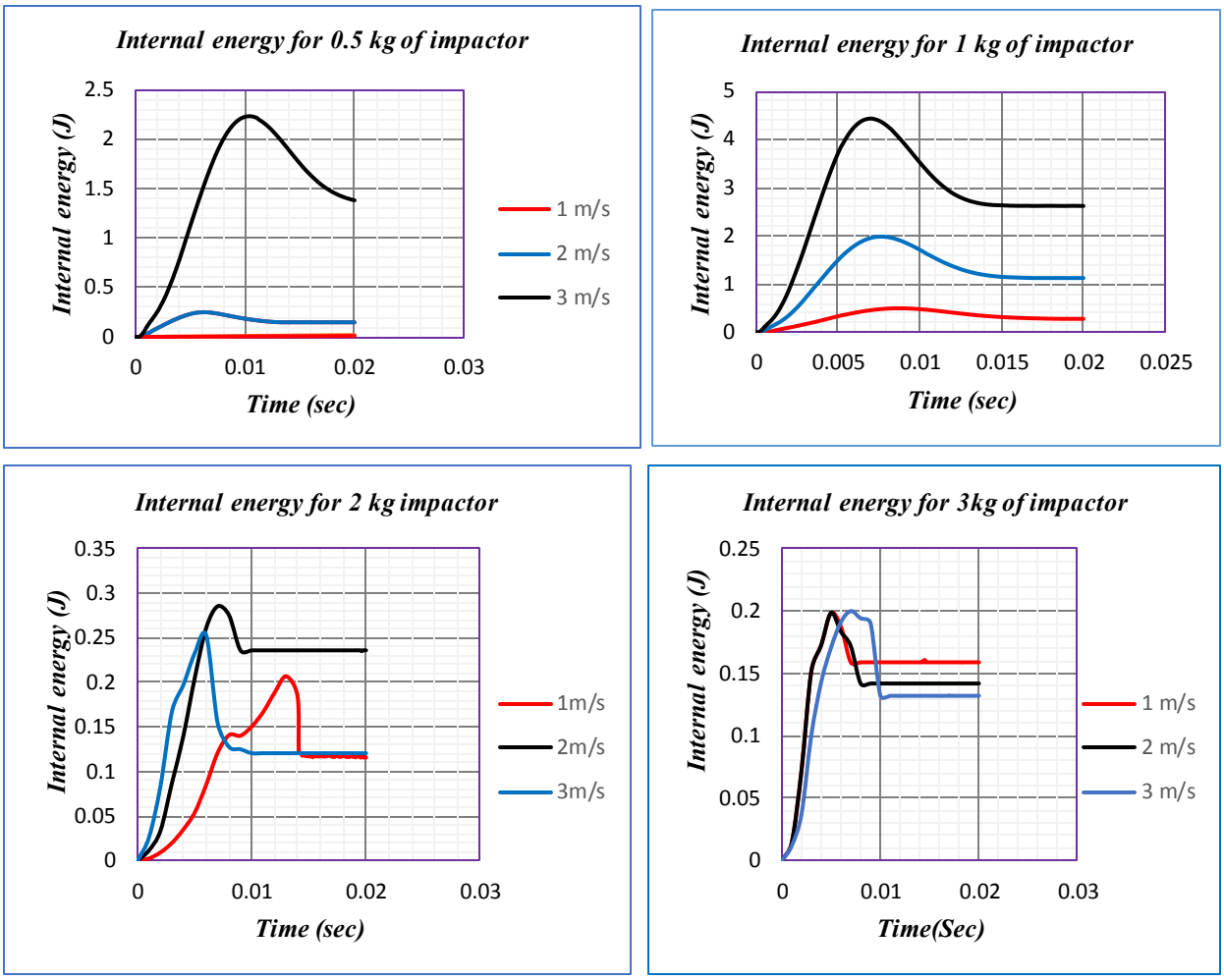

Figure 5.17. Absorbed energy vs time of the composite plate for different impactor mass and velocities.

Generally, the full comparisons such as out of plane deflection, contact force and internal energy simulation results was presented in below figures and table.

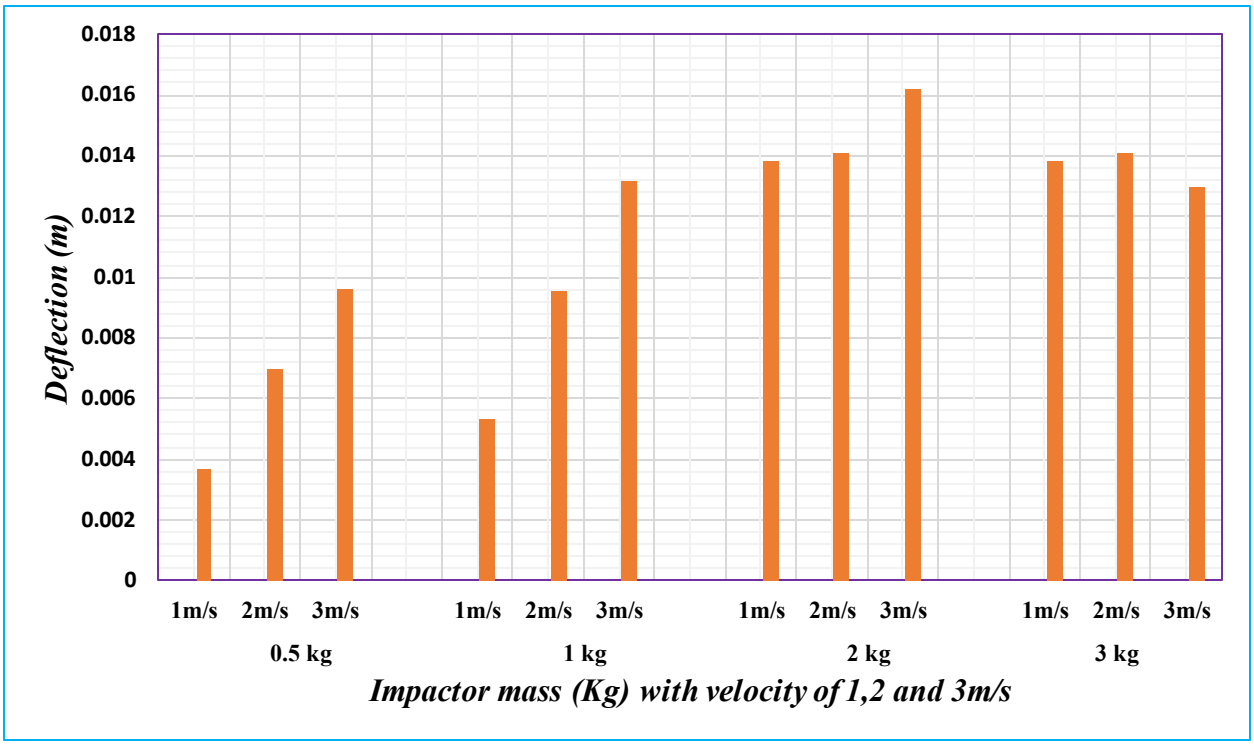

Figure 5.18. Deflection of composite laminate comparison for different impactor mass and velocity

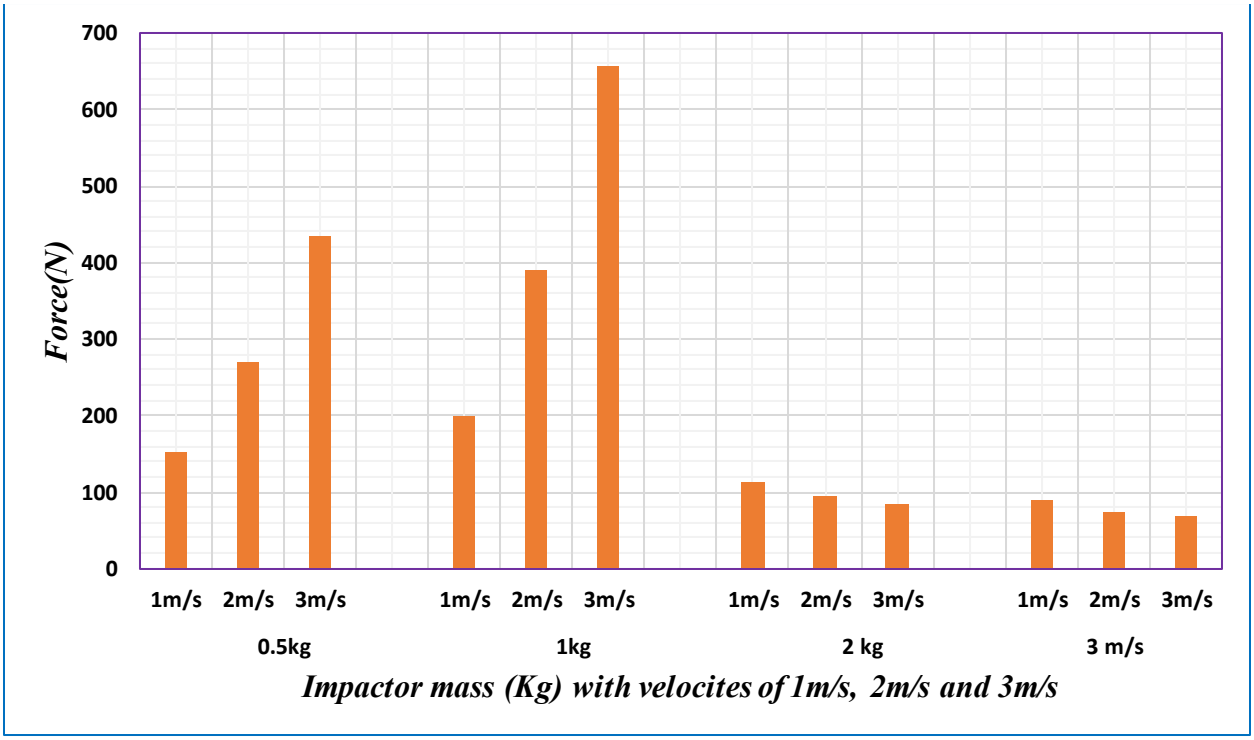

Figure 5.19. Contact force comparison for different impactor mass and velocity.

Mass(Kg)	***Velocity (m/s)***	***Impact energy (J)***	***Absorbed energy (J)***	***Main Characteristics***
0.5	1	0.25	0.24991	*matrix damage, fibre damage and shear damage*
	2	1	0.961841	
	3	2.25	2.234712	
1	1	0.5	0.4982	*matrix damage, fibre damage and shear damage*
	2	2	1.985	
	3	4.5	4.4338	
2	1	1	0.20694	*perforation*
	2	4	0.285448	
	3	9	0.2531	
3	1	1.5	0.198401	*perforation*
	2	6	0.198684	
	3	13.5	0.20007	

Table 5.1. Comparison of absorbed energy and damage mode for different impactor mass and velocities.

CHAPTER SIX
CONCLUSION AND RECOMMENDATION

6.1. Conclusion

In this study the impact analysis of sisal fibre reinforced epoxy resin composite material for automotive application was presented using Abaqus/Explicit software. Also starting from extraction process to fabrication, and mechanical characterization process was briefly presented and discussed. From the mechanical experimental test and simulation results, the following conclusion was drawn.

- The sisal fiber reinforced epoxy resin composite material was successfully manufactured using Vacuum bagging Assisted Hand Lay-up technique (VBAHT) and mechanical property characterization is done on it using universal testing machine. From the mechanical characterization results, it observed that the sisal fibre reinforced composite material has a good mechanical property basically in the longitudinal direction. However, it has moderate mechanical properties in the transverse direction and also have moderate shear strengths.
- From the simulation results it observed that when the impactor mass and velocity increases, the reaction forces of the composite plate was increase up to 1kg of the impactor with 3m/s. Apart from that the reaction forces of the composite plate was decreased and the full perforation of the plate was takes place. Also from all force-time history graph, it noticed that the $[0]_4$ unidirectional sisal fiber reinforced epoxy resin composite laminates has a capacity to withstand the transverse impact force up to 659.69 N without any perforation on the laminates.
- Sisal fiber reinforced epoxy resin composites has a good energy absorption capacity in the transverse direction up to the mass of 1kg of spherical impactor with 3 m/s (up to 4.5 J of energy). However, it's noticed that when the perforation or fibre dent indentation increased and perforation takes place, the absorption capacity was starts decreased.
- The damaged area of the sisal fiber reinforced epoxy resin composite laminate due to the fibre and matrix tension was higher when compared to the fibre and matrix compression.

- From all experimental mechanical test and impact simulation results, it can be concluded that the treated unidirectional sisal fiber reinforced epoxy resin composite materials has a capacity to be used in different automotive application specially which does not need a very high mechanical and impact performance in the transverse direction, but which needs light weight and recyclability.

6.2. Recommendation

The following recommendations for future work can be noted:

- Experimental impact test of sisal fibre reinforced epoxy resin composite using drop weight impact testing machine can be carried out to find the accuracy of the numerical simulation results.
- In this study, the mechanical experimental property characterization is done using only the universal testing machine. However the experimental testing should be done using appropriate universal testing machine that strain gauge was installed on it in order to attain a precise results.
- As shown in many literatures, the main disadvantage of natural fibres was their water absorption capacity. Therefore water absorption test and its improvement must need in order to use the sisal fibre reinforced epoxy resin composite for automotive application.
- 3D progressive impact simulation using user-defined material subroutine VUMAT/UMAT and using different failure criteria.
- This study was only limited to the transvers impact, therefore the full or part component front impact simulation of sisal fibre reinforced epoxy resin composite was recommended for future works.
- In this thesis the effects of the lamina thickness and orientation, and also the mesh size effect was not studied. Therefore the further study was recommended to deal the effects of this parameter on the load carrying and energy absorbing capacity of the sisal fibre reinforced composite laminates.
- Manufacturing and impact analysis of woven or cross-ply laminated sisal/epoxy composite laminate or by using different natural fiber composites in order to improve the energy absorption capacity during transverse impact.

REFERENCES

1. **Serge Abrate:** 'Modeling of impacts on composite structures', Composite structures, 2001, pp. 129-138.
2. **Zhidong Guan and Chihdra Tng:** 'Low velocity impact and damage process of composite laminates', journal of composite materials, Vol.36, No.07/2002.
3. **Mwaikambo, L.Y:** 'Review of the history, properties and application of plant fibres', African journal of science and technology(AJST), science and engineering series Vol.7, No.2, December 2006, pp. 120-133.
4. **Enrico Mangino, Joe Carruthers et al.:** 'The future use of structural composite materials in the automotive industry', International Journal of vehicle design, January 2007.
5. **Abaqus technology brief:** 'Projectile impact on a carbon fiber reinforced plate', April 2007.
6. **Pizhong Qiao, Mijia Yang et al. :** 'Impact mechanics and high-energy absorbing material review' , Journal of aerospace engineering, October 2008, pp.235-248.
7. **Ramazan Karakuzu , Emre Erbil et al.:** 'Damage prediction glass/epoxy laminates subjected to impact loading', Indinan journal of engineering and material sciences, Vol.17,June 2010, pp. 186-198.
8. **Avinash Ramsaroop and Krishnan Kanny:** 'Using Matlab to design and analyse composite laminates', 2010, pp.904-916.
9. **R.C. Batra, G. Gopinath et al.:** 'Damage and failure in low energy impact of fiber-reinforced polymeric composite laminates', composite structures 94, 2012, pp.540-547
10. **Dumitru Nicoara:** 'On the numerical analysis of laminate composite', Fascicle of management and technological engineering, May 2013.
11. **Dragan Kreculji and Basko Rasuo:** 'Review of impact damages modeling in laminated composite aircraft structures', Tehnički vjesnik 20, 3(2013), pp. 485-495.
12. **M.Sakthivel and S.Ramesh: '**Mechanical properties of natural fibre (banana, coir, sisal) polymer composites', Science Park ISSN: 2321-8045, Vol-1, July 2013.
13. **Sunith Babu L.H.K.Shivanand:** 'Impact analysis of laminated composite on glass fiber and carbon fiber', International Journal of emerging technology and advanced Engineering, Volume 4,Issue 6, June 2014.
14. **S.N.A.Safri, M.T.H.Sultan, Y.Yidris et al.:** 'Low velocity and High velocity test on

composite materials-A review', the international journal of engineering and science (IJES), Vol.3, 2014, pp.50-60.

15. **N.Razali, M.T.H.Sultan, F.Mustapha et al.:** 'Impact damage on composite structures- A review', International Journal of engineering and science (IJES), 2014, pp.8-20.
16. **Ramu Kolusu, Venkata Ramesh Mamilla:** 'Impact behavior on fiberglass reinforced laminates with the variation of composite core structure.' International journal of multidisciplinary research and development, 2014, pp.55-58.
17. **Rafi Ali Alqahtani:** 'Flexural Properties of sisal fibre/Epoxy composites', University of Southern Queensland, 2014.
18. **Azzam Ahmed and Li Wei:** 'The low-velocity impact damage resistance of the composite structures-A review, Rev. Adv. Mater. Sci.40(2015), pp.127-145.
19. **Rakesh Reghunath, Mahadevan Lakshmanan et al.**: 'Low velocity impact analysis on glass fiber reinforced composites with varied volume fractions', Materials Science and Engineering, 2015.
20. **Yehia Abdel-Nasser, Ninshu Ma et al.:** 'Impact Analysis of Aluminum-Fiber Composite Lamina', Quarterly journal of the Japan welding society, July 2015.
21. **Kuruvilla Joseph, Ramildo Dias Toledo Filho et al.: '**A review on sisal fiber reinforced polymer composites', Revista Brasileira de Engenharia Agrícola e Ambiental, v.3, n.3,1999, pp. 367-379.
22. **A.E.Ismail, M.A.Hassan, K.A.Kamaruddin:** 'Perforated Impact strength of woven Kenaf fiber reinforced composites'.
23. **Kumaresan. M, Sathish. S and Karthi. N:** 'Effect of Fiber Orientation on Mechanical Properties of Sisal Fiber Reinforced Epoxy Composites, Journal of Applied Science and Engineering, Vol. 18, No. 3, pp. 289-294 , 2015.
24. **Leonardo Jose da Silva, Tulio Hallak Panzera et al.:**' Numerical and experimental Analysis of Bio composites Reinforced with Natural Fibres', International Journal Materials Engineering, 2012, pp. 43-49.
25. **C.Chaithanyan, H.Venkatasubramanian et al.:** ' Evaluation of Mechanical properties of coir-sisal reinforced hybrid composite using Isophthalic Polyester Resin', International Journal of Innovative Research in Science, Engineering and Technology', Vol.2, Issue 12, December 2013.

26. **R.Tiberkak, S.Rechak and M. Bachene:** 'The dynamic Response of laminate composite plate under low-velocity impact', 25th international congress of the aeronautical sciences.
27. **W.H.Choong, K.B.Yeo and M.T.Fadzlita:** 'Impact damage behavior of woven glass fibre reinforced polymer composites', Journal of applied Sciences, 2011, pp. 2440-2443.
28. **P.Vieira, C.Romao, A.T.Marques et al.:** 'Mechanical characterization of Natural fibre reinforced plastics.
29. **Abiy Alene:** 'Design and Analysis of Bamboo and E-Glass Fiber Reinforced Epoxy Hybrid composite for wind turbine blade shell', Addis Ababa University, Master Thesis, October, 2013.
30. **Thi Thu Loan:** 'Investigation of Jute fibres and their composites based on polypropylene and epoxy matrices, 2005.
31. **D. Chandramohan and J. Bharanichandar:** 'Impact test on natural fiber reinforced polymer composite materials', Applied Science Innovations Pvt. Ltd., India, 2013, pp. 314-320.
32. **SeenivasaKumar M, Karthicks S:** 'Mechanical behaviour of sisal fiber and epoxy resin matrix composite', International journal of pure and applied research in engineering and technology, Volume 3(4), 2014, pp.325-332.
33. **Serge Abrate:** 'Impact engineering of composite structures', CISM courses and lectures.
34. **Autar K. Kaw:** 'Composite Materials', second edition, 2006.
35. **J.N.Reddy:**' Mechanics of laminated composite plates and shell and shell theory and analysis', Second edition, 2004.
36. **Prof. Allensom Herman V. Corey:** 'Composite Materials', Condensed Book Series.
37. **Vieira, L.M.G., Santos, J.C., Sousa et al:** 'The effects of chemical treatment and fiber orientation in sisal composites', Research gate conference paper, 2012.
38. **Ravi Kumar.M and Keerthiprasad. K.S:** ' Interlaminar Low-velocity Impact Resistance of Hemp and E-Glass Hybrid Composite Laminate', International Journal of Innovative Research in Science, Engineering and Technology, Vol. 3, Issue 7, July 2014.
39. **Tilahun Birhanu:** Finite element analysis of composite ballistic helmet subjected to impact load', Defense University College of Engineering, 2013.
40. **K.Pickering:** 'Properties and performance of natural-fibre composites'.
41. **P.K. Mallick:** 'Fiber reinforced composites', third edition, 2007.

42. **KinfeMichael Geressu Asfaw:** 'Investigation of the reasons for the Unique Growth and Development of Agave Species (Agave Sisalana and Agave Americana) crop plants at the Southern, Central, North Western and Eastern Parts of Tigray, Ethiopia', Current Research Journal of Biological Sciences, July 15, 2011.
43. **ASTM D3039:** 'Standard Test Method for Tensile properties of polymer matrix composite materials', ASTM international, USA, 2010.
44. **ASTM D3410:** 'Compressive properties of polymer Matrix composite materials with unsupported Gage section by shear loading', ASTM international, PA, USA, August 2003.
45. **ASTM D3518:** 'In-plane shear response of polymer matrix composite materials by Tensile test of a $+45^0$ laminate', ASTM International, PA, USA, July 2012.
46. **Abaqus theory manual.**
47. **Abaqus user manual 6.13.**
48. **Pradeep Kumar Uddandapu:** ' Impact analysis on car Bumper by varying speeds using materials ABS plastic and poly Ether Imide by Finite Element Analysis software Solid Works', International Journal of Modern Engineering Research(IJMER), Vol.3,Jan-Feb 2013,pp. 391-395.
49. **Haining Chen, Hao Chen, Liangjie Wang:** 'Analysis of vehicle seat and research on structure optimization in front and rear impact', World Journal of Engineering and Technology, 2014, pp.92-99
50. **Paul Du Bois, Clifford C. Chou et al.:**' Vehicle Crashworthiness and occupant Protection', American Iron and Steel Institute, 2004
51. **Jacob G.C., Fellers J.F., Simunovic S. et al.:** 'Energy Absorption in Polymer Composites for automotive crashworthiness', Journal of composite materials, 2002.
52. **George C. Jacob, John F. Fellers et al.:**' Crashworthiness of Automotive Composite Material Systems', Journal of Applied Polymer Science, Vol. 92, 2004, pp. 3218-3225.
53. **C.Lopes, Z.Giirdal, P.P.Camanho et al.:** 'Simulation of low-velocity impact damage on composite laminates', 50^{th} AIAA/ASME/ASCE/AHS/ASC structures, structural dynamics, and materials conference, California, May 2009.
54. **M.K.Gupta and R.K.Srivastava:** 'Tensile and flexural properties of sisal fibre reinforced epoxy composite: A comparison between unidirectional and mat form of fibres', International Conference on Advances in Manufacturing and Materials Engineering, 2014, pp. 2434-2439.

55. **Sudhir. A Madhukiran. J, Dr.S.Srinivasa Rao et al.:**' Tensile and Flexural Properties of Sisal/Jute Hybrid Natural Fiber Composites', International Journal of Modern Engineering Research(IJMER), Vol.4 , July 2014.
56. **Kotresh sardar, Dr.K. Veeresh et al.:** 'Characterization and Investigation of Tensile test on Sisal fiber reinforced Polyester Composite material', International Journal of Recent Development in Engineering and Technology, vol.3, October (2014).
57. **Beukers A. Lightness:** 'the inevitable renaissance of minimum energy structures', 2nd ed: Rotterdam, 010 publishers, 1999.

APPENDIX: A

Velocity –time history for different impactor mass

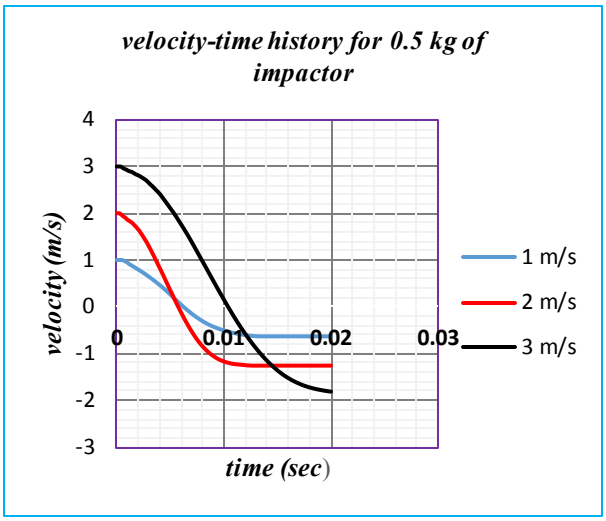

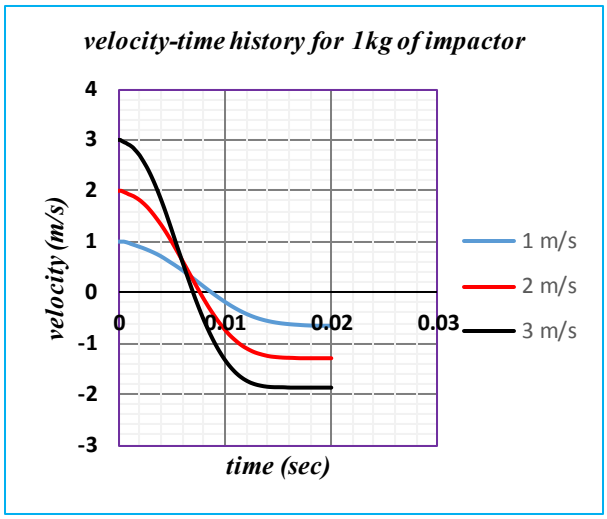

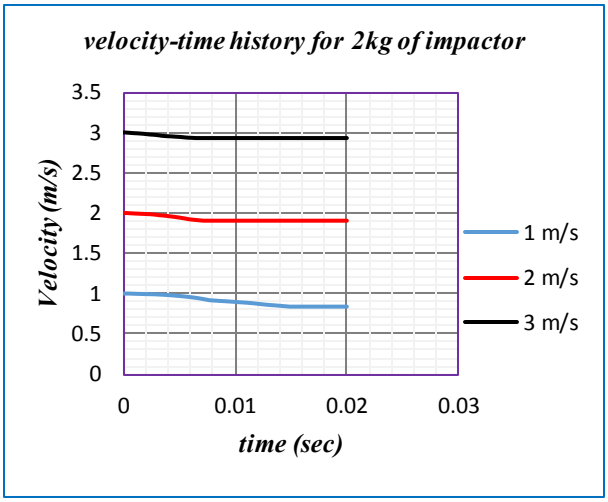

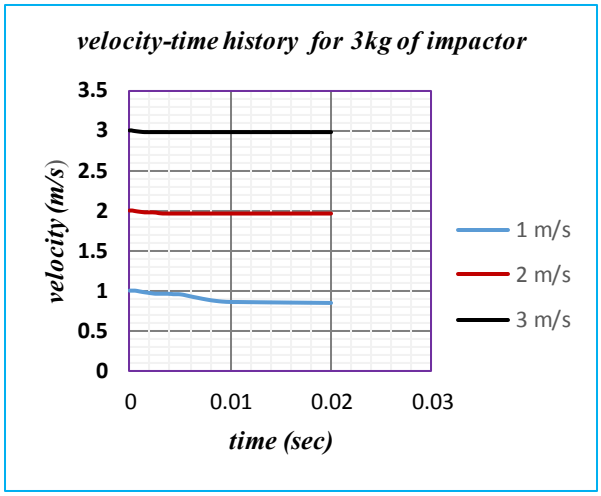

APPENDIX: B

Kinetic energy –time history for different impactor masses

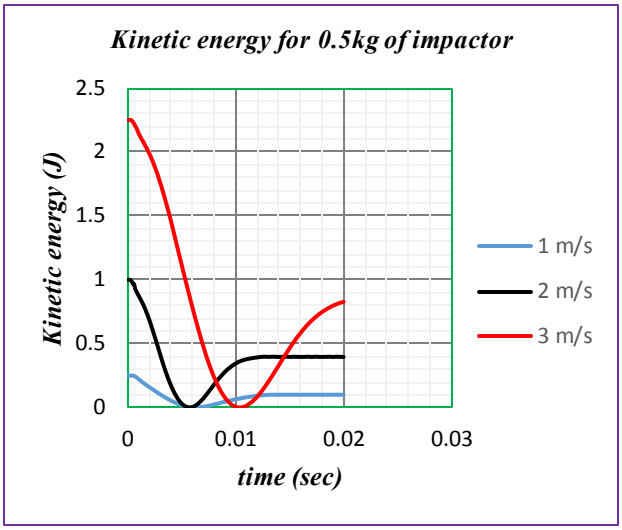

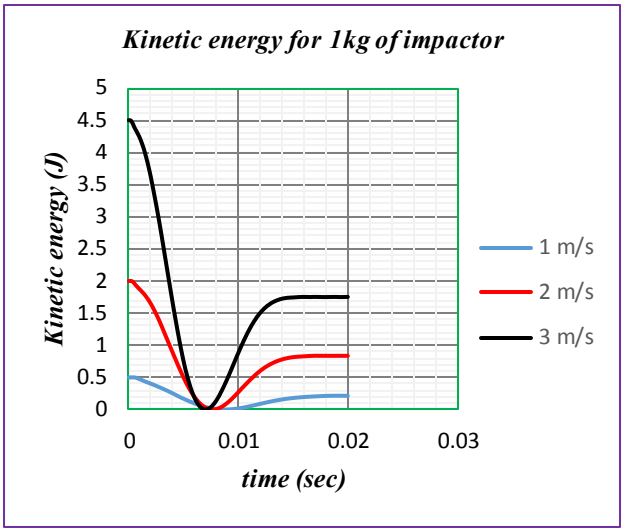

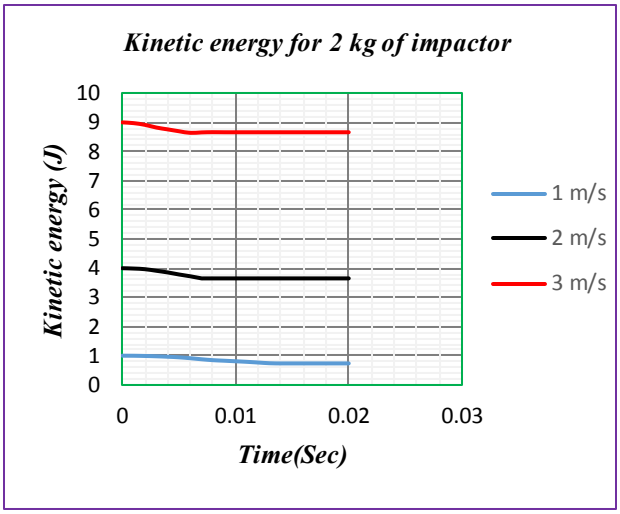

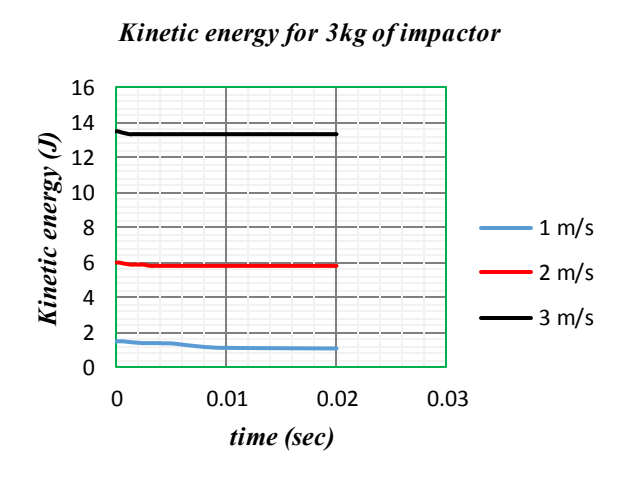

APPENDIX: C

Penetration mechanism for 2kg of impactor at different velocity

A. Penetration mechanism of composite plate for 2 kg of impactor at 1m/s

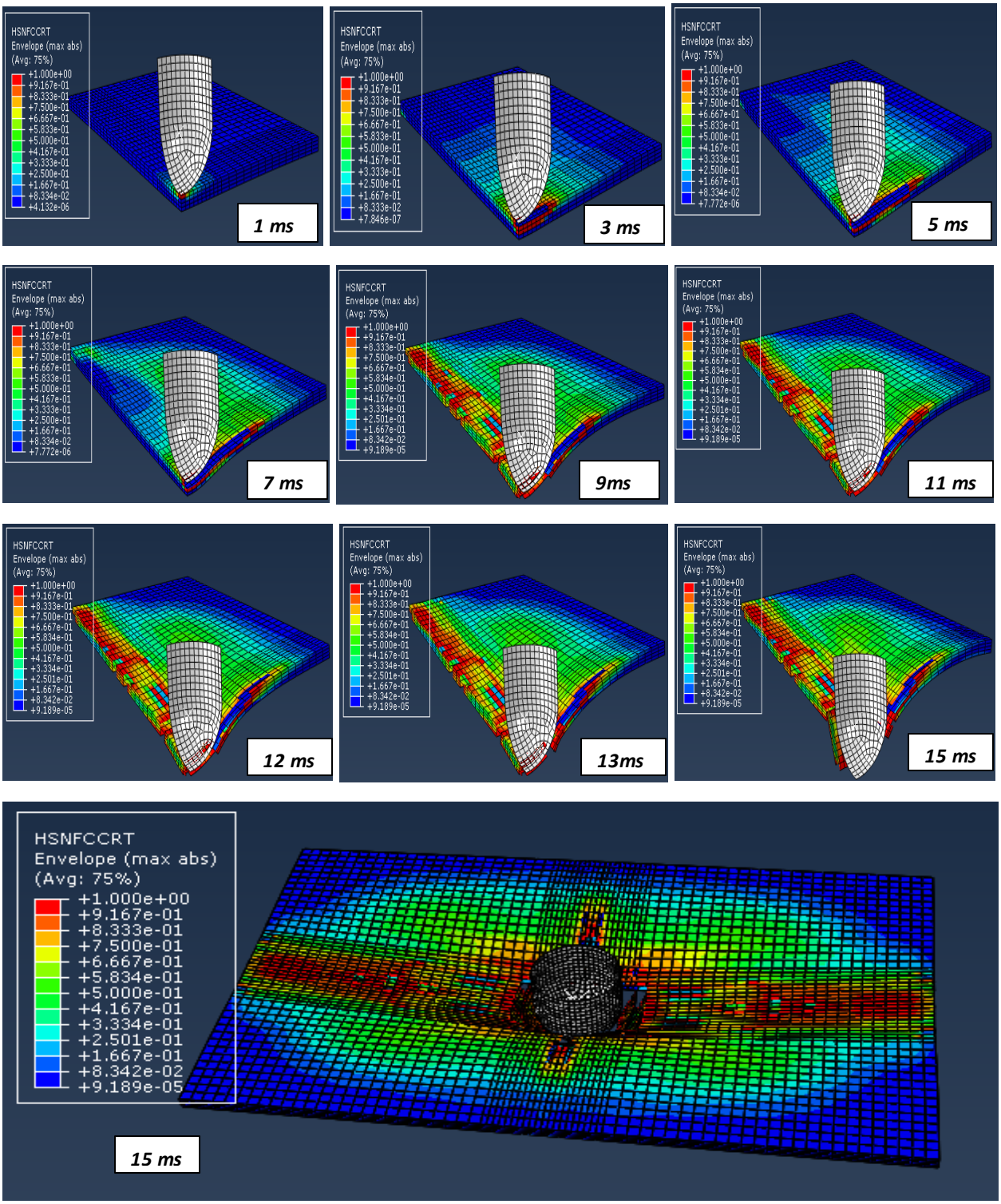

B. Penetration mechanism of composite plate for 2 kg of impactor at 2m/s

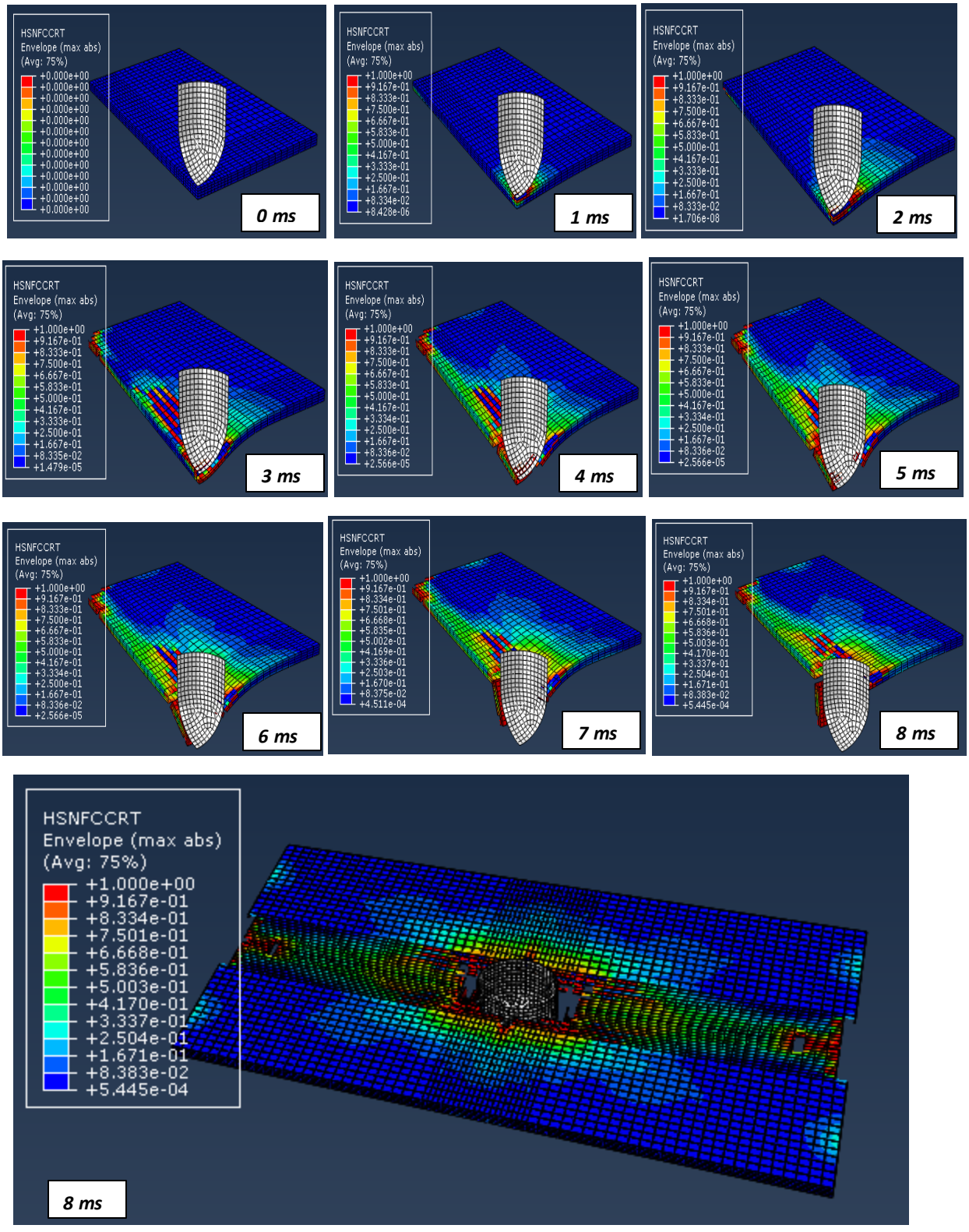

C. Penetration mechanism of composite plate for 2 kg of impactor at 3m/s

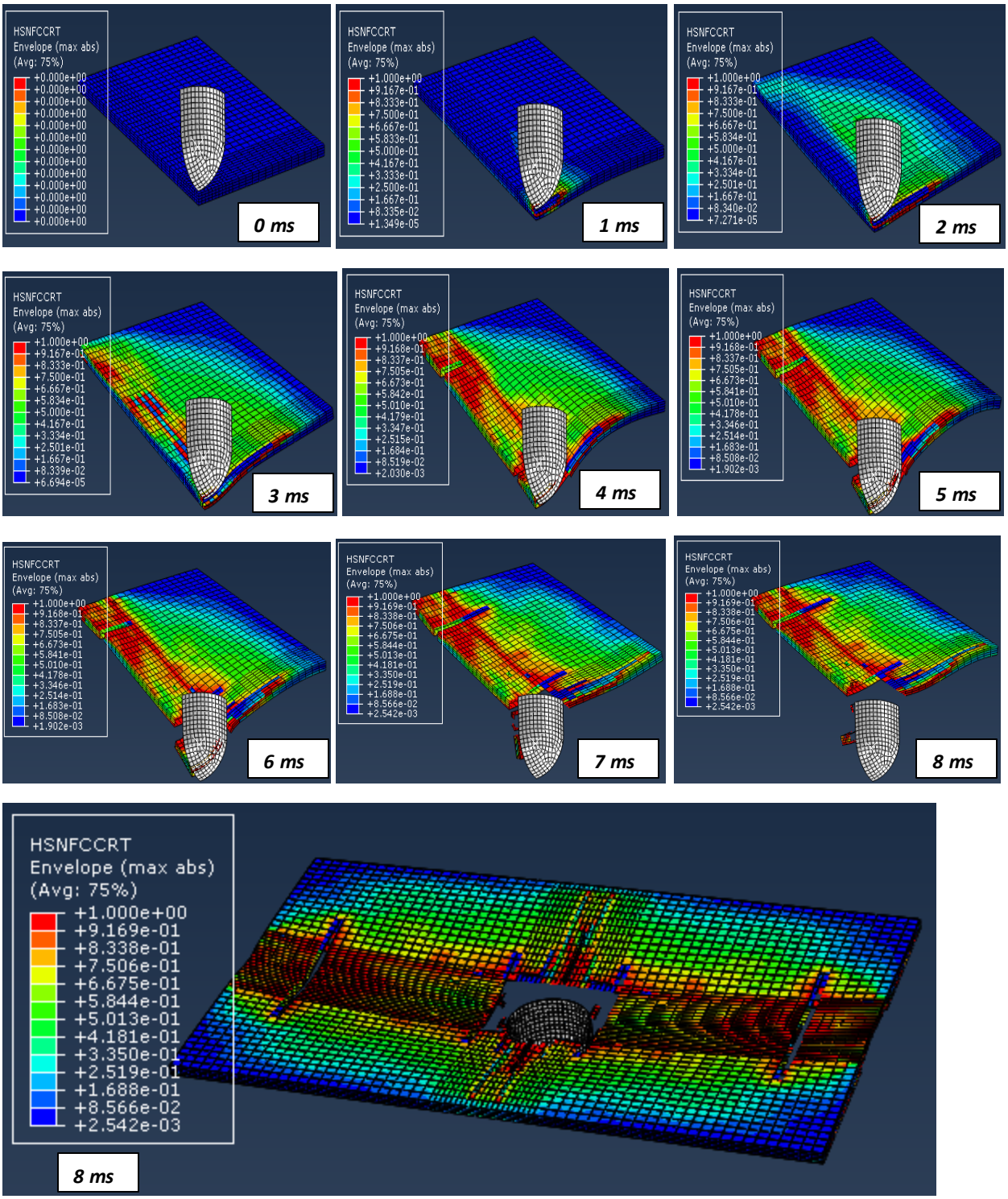

APPENDIX: D

Penetration mechanism for 3kg of impactor at different velocity

A. Penetration mechanism of composite plate for 3 kg of impactor at 1m/s

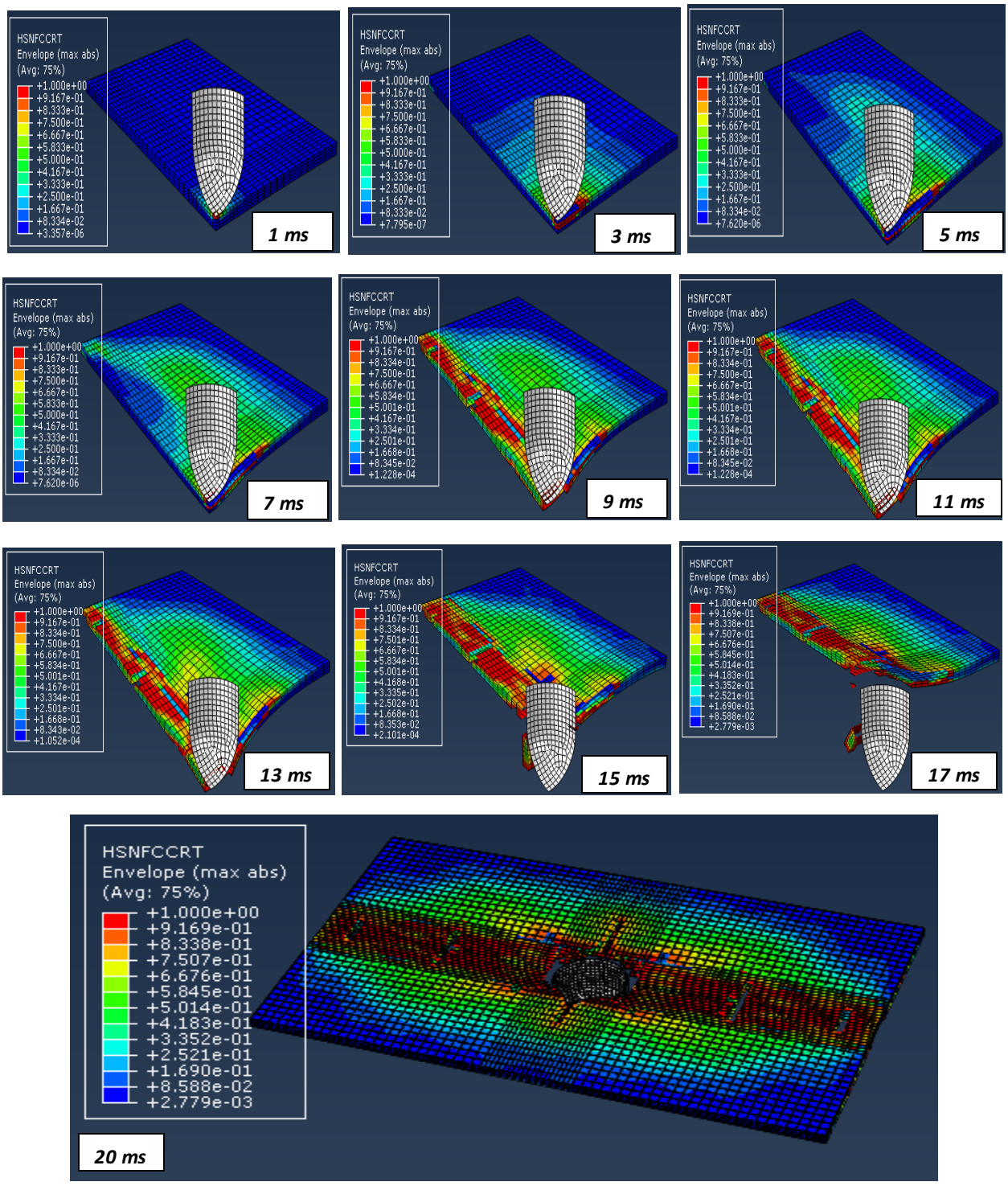

B. Penetration mechanism of composite plate for 3 kg of impactor at 2m/s

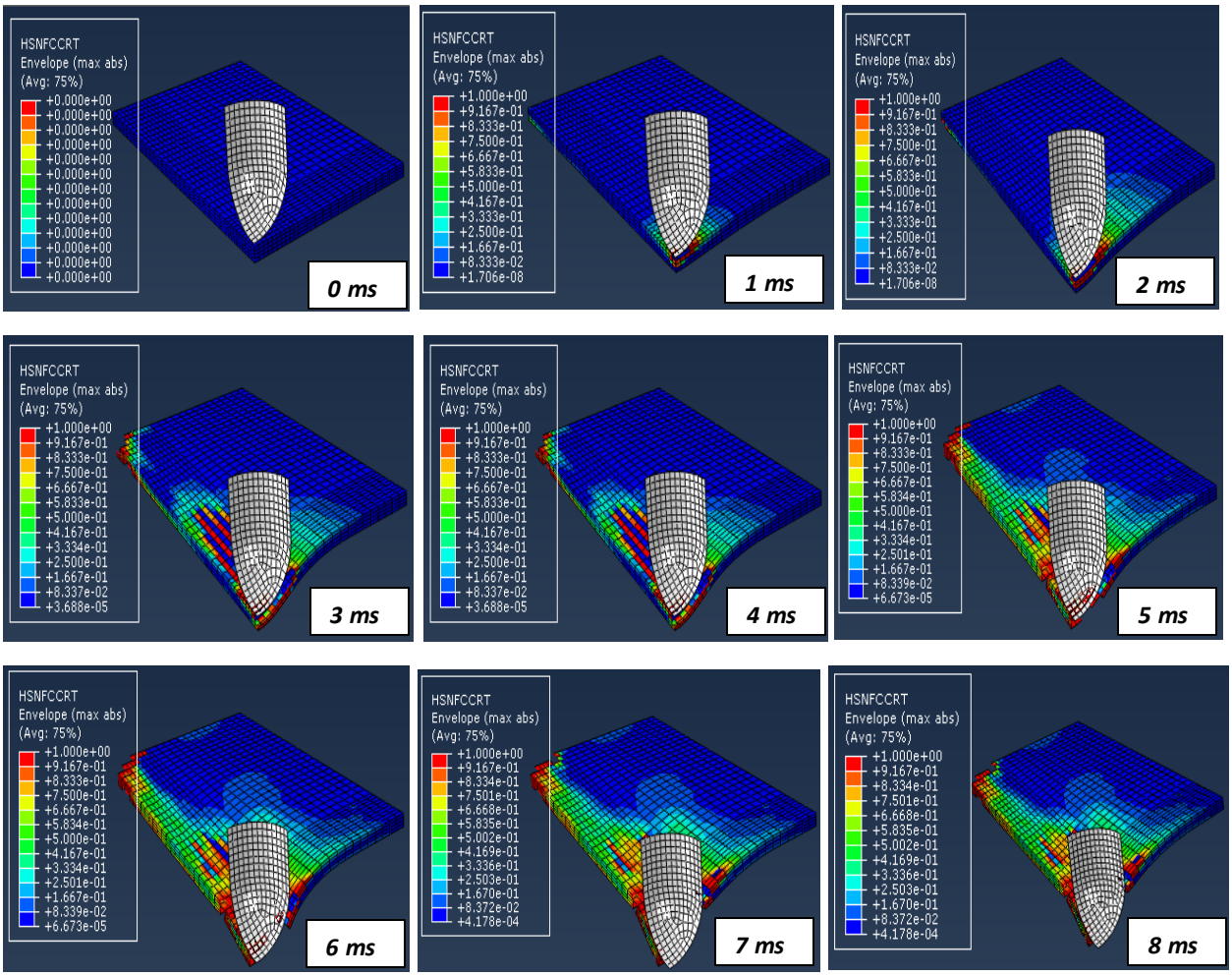

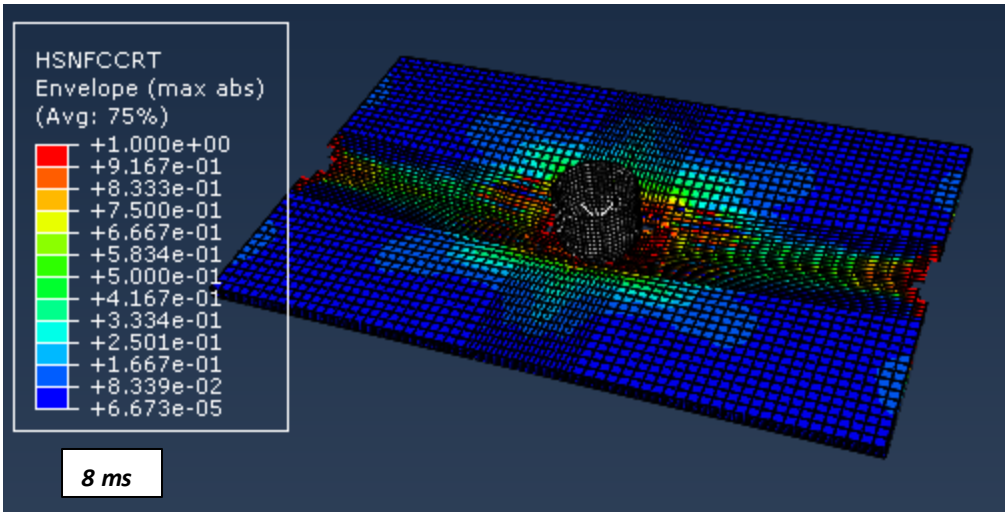

C. Penetration mechanism of composite plate for 3 kg of impactor at 3m/s

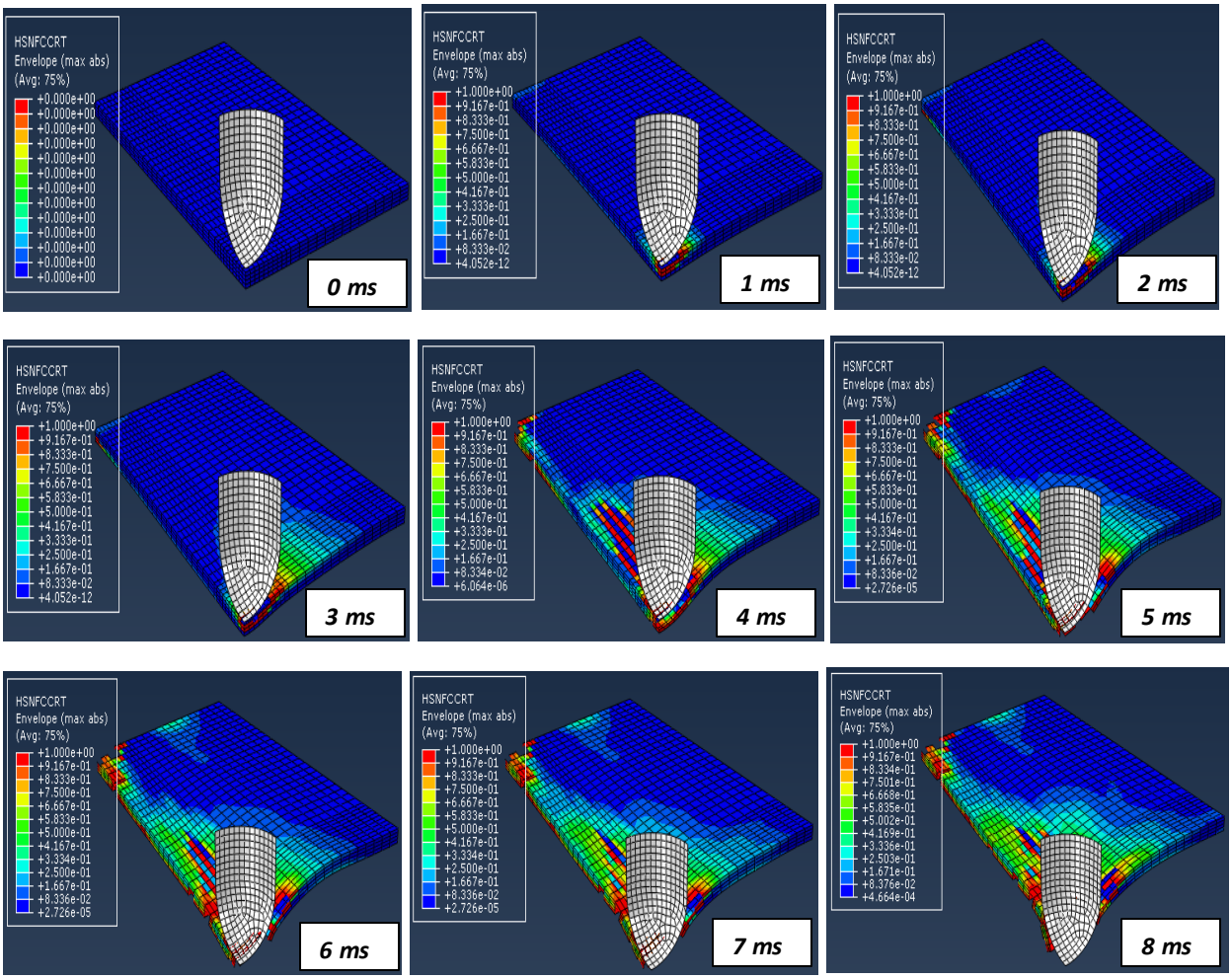

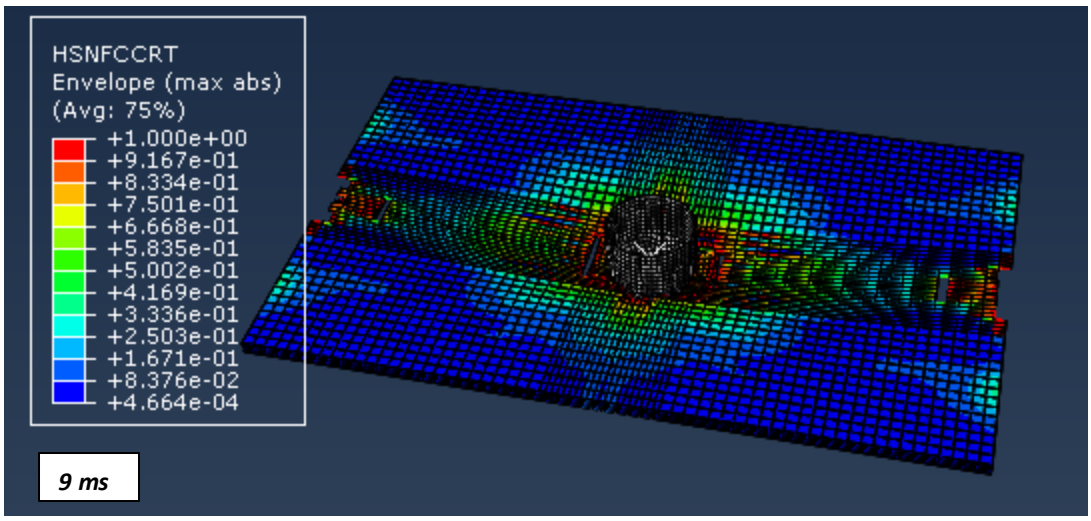

APPENDIX: E

Mechanical property Testing Specimens Three-Part Failure Identification Codes

A. Tensile and in-plane shear testing specimen failure codes and identification

Failure code/type	*Failure type*	*Failure area*	*Failure location*
AGM	**A**ngled	**G**age	**M**iddle
DGM	**E**dge Delamination	**A**t grip/tab	**T**op
GAT	**G**rip/tab	**A**t grip/tab	**T**op
LAT	**L**ateral	**A**t grip/tab	**T**op
LGM	**L**ateral	**G**age	**M**iddle
LIT	**L**ateral	**I**nside grip/tab	**T**op
SGM	**L**ong-Splitting	**G**age	**M**iddle
XGM	**E**xplosive	**G**age	**M**iddle

B. Compresion test specimens failure codes and identification

Failure code/type	*Failure type*	*Failure area*	*Failure location*
TAT	**T**ransverse shear	**I**nside grip/tab	**T**op
BGM	**B**rooming	**G**age	**M**iddle
HAT	**T**hrough-Thickness	**A**t grip/tab	**T**op
SGV	**L**ong-Splitting	**G**age	**V**arious
DTT	Delamination	**T**ab Adhesive	**T**op
HIT	t**H**rough-Thickness	**I**nside grip/tab	**T**op
CIT	End-**C**rushing	**I**nside grip/tab	**T**op
DIT	**D**elamination	**I**nside grip/tab	**T**op